UNIVERSITY OF CALIFORNIA, SAN DIEGO

Engineering tumor-specific oncolytic adenoviruses with small molecule-controlled expanded tropisms

A dissertation submitted in partial satisfaction of the requirements for the degree Doctor of Philosophy

in

Biology

by

Shigeki Joseph Miyake-Stoner

Committee in charge:

Professor Clodagh O'Shea, Chair
Professor Jeff Hasty
Professor Martin Hetzer
Professor Elizabeth Komives
Professor Stephen Mayfield

The Dissertation of Shigeki Miyake-Stoner is approved, and it is acceptable in quality and form for publication on microfilm and electronically:

_____

_____

_____

_____

_____

Chair

University of California, San Diego

2017

Table of Contents

List of Figures

List of Tables

Acknowledgements

I would like to thank Clodagh O'Shea for giving me the opportunity and providing the mentorship for me to be able to perform this research in her laboratory.

I would also like to acknowledge all members of the O'Shea Lab, current and past, who have provided support and conversation that contributed to the success of this work, and to members of the MCBL department at Salk.

A special thanks and acknowledgement to co-author Dr. Colin Powers, for his mentorship and guidance during the early stages of my time in the O'Shea Lab and thanks and acknowledgement to co-author Dr. Robert Svensson for his help and guidance on animal work and our *in vivo* models.

Chapters 2-4, in part are currently being prepared for submission for the publication of the material. O'Shea, Clodagh; Powers, Colin. The dissertation author was the primary investigator and author of this material.

Chapter 4, in part is currently being prepared for submission for the publication of the material. O'Shea, Clodagh; Powers, Colin; Svensson, Rob. The dissertation author was the primary investigator and author of this material.

I would also like to acknowledge the funding that supported this work; the UCSD Department of Biological Sciences, NIH CMG training grant 5T32GM0007240-35, The H. A. and Mary K. Chapman Charitable Trust and the laboratory of Clodagh O'Shea at the Salk Institute for Biological Studies.

Vita

2009 Senior Research Associate, Lab of Dr. Ryan Mehl, Franklin & Marshall College, Lancaster, PA

2009 Bachelor of Arts in Chemistry, Bachelor of Arts in Biochemistry and Molecular Biology, Franklin & Marshall College, Lancaster, PA

2010-2012 Teaching Assistant, Division of Biological Sciences, University of California, San Diego, CA

2017 Doctor of Philosophy in Biological Sciences, University of California, San Diego, CA

Publications

A Modular Platform for Rapid Assembly of Synthetic Viruses
In preparation
Authors: Colin Powers, Shigeki Miyake-Stoner, Clodagh O'Shea

Synthetic Virology: Highly Selective and Potent Rb/E2F-selective Oncolytic Viruses that Seek and Destroy Metastases
In preparation
Authors: Shigeki Miyake-Stoner, Colin Powers, Robert Svensson, Clodagh O'Shea

Metabolism goes viral
Cell Metabolism April 1, 2014
Authors: Shigeki Miyake-Stoner, Clodagh O'Shea

A Protein–Polymer Hybrid Mediated By DNA
Langmuir January 6, 2012
Authors: Shigeki Miyake-Stoner, Saadyah Averick, Eduardo Paredes, Debasish Grahacharya, Bradley Woodman, Ryan Mehl, Krzysztof Matyjaszewski, Subha Das

Genetically Encoded Initiator for Polymer Growth from Proteins
JACS September 14, 2010
Authors: Shigeki Miyake-Stoner, Jennifer Peeler, Bradley Woodman, Saadyah Averick, Audrey Stokes, Kenneth Hess, Krzysztof Matyjaszewski, Ryan Mehl

Micro-algae come of age as a platform for recombinant protein production
Biotechnology Letters June 17, 2010
Authors: Shigeki Miyake-Stoner, Liz Specht, Stephen Mayfield

Generating permissive site-specific unnatural aminoacyl-tRNA synthetases
Biochemistry January 18, 2010
Authors: Shigeki Miyake-Stoner, Christian Refakis, Jared T. Hammill, PhD, Hrvoje Lusic, Jennifer Hazen, Alexander Deiters, Ryan Mehl

Interpretation of p-Cyanophenylalanine Fluorescence in Proteins in Terms of Solvent Exposure and Contribution of Side-Chain Quenchers: A Combined Fluorescence, IR and Molecular Dynamics Study
Biochemistry August 6, 2009
Authors: Shigeki Miyake-Stoner, Humeyra Taskent-Sezgin, Juah Chung, Vadim Patsalo, Andrew Miller, Scott Brewer, Ryan Mehl, David Green, Daniel Raleigh, Isaac Carrico

Probing protein folding using site-specifically encoded unnatural amino acids as FRET donors with tryptophan
Biochemistry June 3, 2009
Authors: Shigeki Miyake-Stoner, Andrew Miller, Jared T. Hammill, PhD, Jennifer Peeler, Kenneth Hess, Ryan Mehl, Scott Brewer

Enhancing the utility of unnatural amino acid synthetases by manipulating broad substrate specificity
Molecular BioSystems May 28, 2009
Authors: Shigeki Miyake-Stoner, Audrey Stokes, Jennifer Peeler, Duy Nguyen, Robert Hammer, Ryan Mehl

Preparation of site-specifically labeled fluorinated proteins for 19F-NMR structural characterization
Nature Protocols October 18, 2007
Authors: Shigeki Miyake-Stoner, Jared T. Hammill, PhD, Jennifer Hazen, Jennifer Jackson, Ryan Mehl

SELECTIVE CELL TARGETING USING ADENOVIRUS AND CHEMICAL DIMERS
United States Patent Application PCT/US2013/031002
Inventors: Clodagh O'Shea, Shigeki Miyake-Stoner, Colin Powers

ONCOLYTIC TUMOR VIRUSES AND METHODS OF USE
United States Patent Application PCT/US2014/029587
Inventors: Clodagh O'Shea, Shigeki Miyake-Stoner

Abstract of the Dissertation

Engineering tumor-specific oncolytic adenoviruses with small molecule-controlled expanded tropisms

by

Shigeki Joseph Miyake-Stoner

Doctor of Philosophy in Biology

University of California, San Diego, 2016

Professor Clodagh O'Shea, Chair

A promising new strategy for cancer therapy is the use of engineered oncolytic viruses, adapted from their natural properties of seeking out and destroying cells to effectively find and specifically eliminate cancer cells. The overarching goal of the work presented here is to engineer powerful new adenoviruses that can preferentially infect cancer cells via disparate receptors, and replicate exclusively in cells that have lost tumor suppressor pathways.

Since the creation of adenoviruses with novel tropism is limited by the ability to build and test new genetic designs, we desired targetable oncolytic adenoviruses with a modular platform that would enable rapid identification of new and controllable targeting moieties. We employed the property of rapamycin-induced FRB/FKBP heterodimerization to construct adenoviruses with chemically-controlled tropism by inserting FRB into the adenovirus and genetically encoding a functionalized FKBP fusion protein. We validated the targeting of this new class of viruses in culture using a panel of NCI breast cancer cell lines, targeting the frequently-upregulated cancer marker EGFR. We demonstrate that our targeting components are compatible with other virus modifications and that new adenoviruses with these mutations are able to infect and destroy a model of intractable triple negative breast cancer. Based on our findings, rapid discovery of effective targeting moieties for oncolytic adenoviruses should be possible, and we should avoid limiting the potency of future vectors by disrupting the highly evolved adenovirus capsid structure.

While oncolytic adenoviruses have already shown to be safe in clinical trials, we have improved the replication specificity of an oncolytic virus based on the function of adenovirus genes that overlap with frequent tumor mutations. It has been shown that mutation in adenovirus E1A can prevent its inactivation of cell cycle-regulator retinoblastoma protein (Rb), and this mutation is the basis of selectivity for an oncolytic adenovirus in clinical trials. However, adenovirus also encodes E4orf6/7, which acts downstream of Rb by activating the cellular transcription factor E2F1 that also drives the cell cycle. We have combined

mutations in E1A and E4orf6/7 and discovered highly selective oncolytic adenoviruses that have the promise to be the basis for safe and potent oncolytic cancer therapies.

Chapter 1. Introduction

Cancer continues to be an intractable disease and accounts for more than half a million deaths each year in the US. There is a profound need for more effective, selective and safe treatments. In the last century, our knowledge about the origins of cancer and cancer biology has greatly advanced. However, despite our new understanding of cancer as a genetic disease, the standard of care for non-resectable, disseminated disease remains genotoxic therapies, such as chemotherapy and irradiation, which often exhibit deleterious side-effects such as intolerable and toxic side-effects that can outweigh therapeutic benefit.

1.1 The role of the retinoblastoma tumor suppressor pathway in cancer

The Rb tumor suppressor pathway is deregulated in almost every form of human cancer (1, 2) through either loss of function mutations in Rb, p16 point mutations or epigenetic silencing, mutations or amplification of cyclin dependent kinases (CDKs), mutations that down-regulate CDK inhibitors, or mutations that up-regulate E2F transcription factor activity (Figs. 1 & 2). Alterations in this pathway are prognostic markers for therapy (e.g. reviewed in (3)). Most current chemotherapies that inhibit E2F transcriptional targets are proliferative poisons that are also toxic to normal cells and frequently result in iatrogenic complications.

1.1.1 Retinoblastoma

Retinoblastoma (Rb) is a tumor suppressor protein that binds to and represses the activity of E2F1, the critical S-phase transcription factor that is also required for activation of Ad genes. The function of Rb tumor suppressor was first elucidated by the study of adenovirus and SV40 (reviewed in (4)). Rb is part of a protein family (Rb, p107, and p130) that have numerous cell binding partners, which include interaction and repression of E2F transcription factor family members (5). In normal, non-dividing cells, Rb remains hypophosphorylated and binds to transcription factor E2F at its target promoters, suppressing transcription by masking the E2F transactivation domain (6, 7) as well as recruiting chromatin-remodeling complexes and histone-modifying activities (8-14). During the G1-S transition of the cell cycle, CDKs phosphorylate Rb which releases E2F to induce cell cycle gene transcription (15) (Fig. 1). When Rb is misregulated, it leads to a loss of cell cycle control and allows aberrant E2F activity which leads to uncontrolled replication and can give rise to cancer. The role of Rb in cancer is reviewed in (2).

1.1.2 E2F/DP

E2F1 is a member of a family transcription family, and is the cell-cycle actuator controlled by the Rb tumor suppressor pathway. The E2F family of transcription factors play a diverse role in transcriptional regulation of the cell

(16). E2F1 was first described as an element that bound to the adenovirus E2a promoter (17). At active E2F promoters, E2F forms a heterodimer with transcription factors DP1 and DP2 to enhance DNA binding and transcriptional activation (18). In normal non-dividing cells, E2F1 is under tight regulation by Rb to arrest the cell cycle. When E2F1 is amplified or no longer regulated by Rb, as it is in almost every proliferating cancer, the cell has exited from cell cycle control and can lead to pathogenesis (reviewed in (19)). DP1 is also be amplified in many cancers (20-22), and may act as an oncogene downstream of Rb to drive cell proliferation through E2F target transcription.

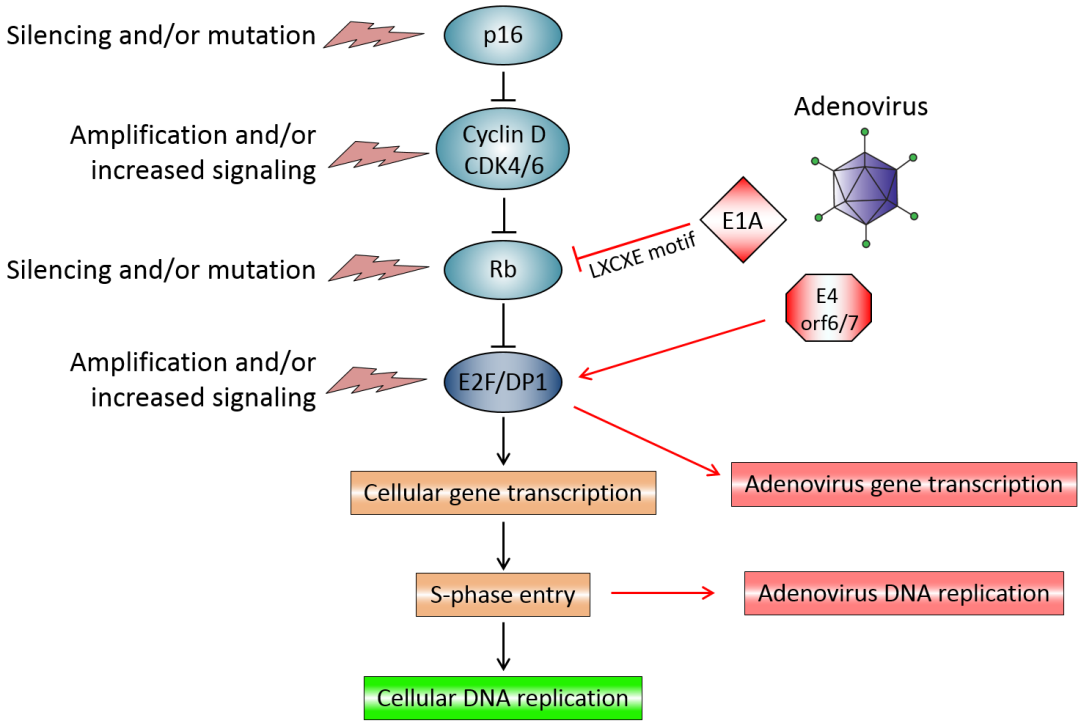

Figure 1. Tumor mutations and adenovirus early proteins converge to inactivate the Rb pathway to elicit uncontrolled replication.

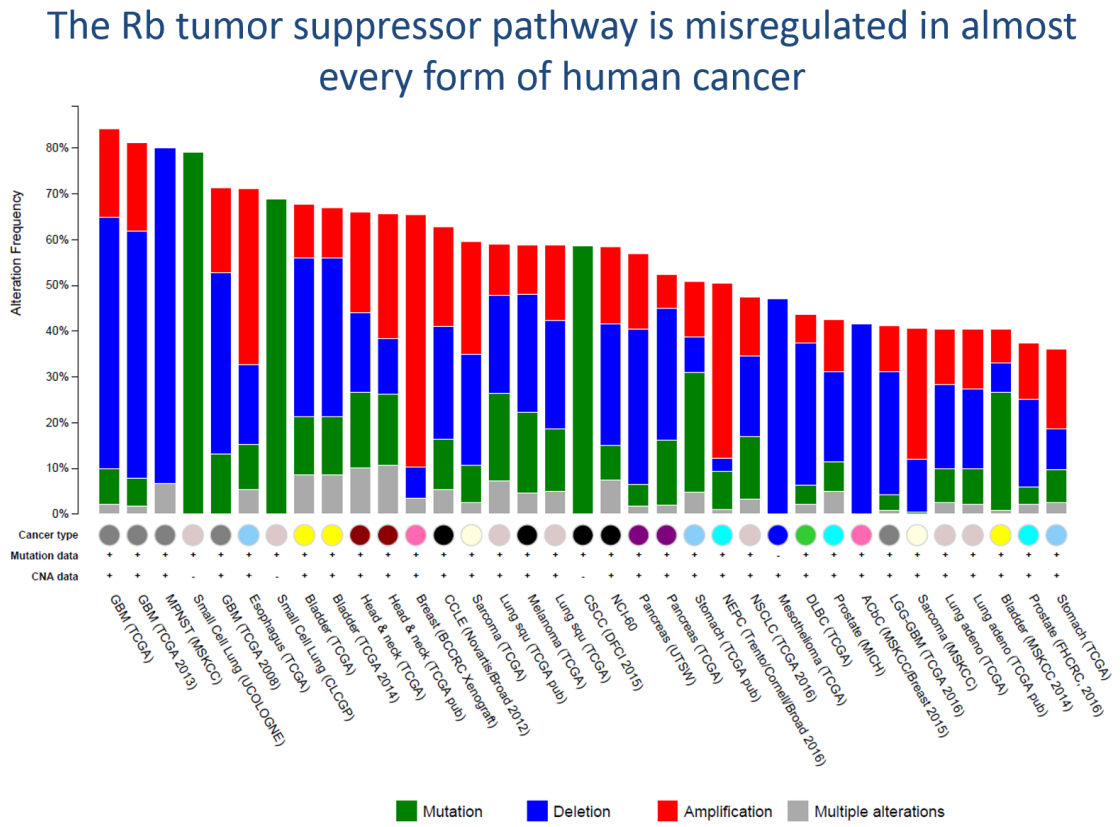

Figure 2. The Rb tumor suppressor pathway is misregulated in almost every form of human cancer. Alteration summary of top 35 frequency hits are shown for CCND1, CDK4, CDK6, CDKN2A, E2F1, and RB1 from the cancer genome portal (cbioportal.org). Notably almost all glioblastoma (GBM) and more than half of the NCI-60 cell lines contain alterations in this pathway.

1.2 Oncolytic Adenovirus

One approach that has the potential to address many of the shortcomings of current cancer treatments is oncolytic adenoviral therapy. Oncolytic viruses are designed to replicate specifically in cancer cells, but leave normal cells unharmed (Fig. 3) (reviewed in (23) and (24)). Most oncolytic viruses must be engineered to have tumor selectivity and while they are not limited to one order of viruses, adenovirus is an attractive oncolytic agent due to its extensive characterization, potential for genetic manipulation, and demonstration of safety and feasibility in ongoing and completed clinical trials for bladder cancer (25), glioma (26), melanoma (27), ovarian cancer (28), and other solid tumors (29-31). In October 2015, the U.S. Food and Drug Administration approved the first oncolytic virus Imlygic® (talimogene laherparepvec) for treatment of melanoma in the skin and lymph nodes, which demonstrates not only the future promise, but the practical application of oncolytic viruses to treat cancer (32).

Adenovirus (Ad) is a self-replicating biological machine. Ad consists of a linear double-stranded 36 kb DNA genome sheathed in a protein coat. Like all viruses, Ad requires a host cell to replicate. Ad invades the cell and hijacks the cellular replicative machinery with multiple encoded gene products that drive the cell cycle to enable efficient viral replication. Upon virus assembly, Ad induces lytic cell death to escape the cell and spread and invade surrounding cells (Fig. 4). No *ab initio* system has come close to mimicking the autonomy

and efficiency of Ad, so with the ability to manipulate the Ad genome, we can take the virus by the horns and redesign it to perform the oncolytic virus functions of tumor-specific infection and replication.

Tumor mutations and adenovirus proteins converge in inactivating retinoblastoma (Rb) (Fig. 1). Adenovirus expresses early viral oncoproteins that inactivate the Rb tumor suppressor pathway to force cells to replicate and concomitantly reproduce the viral genome.

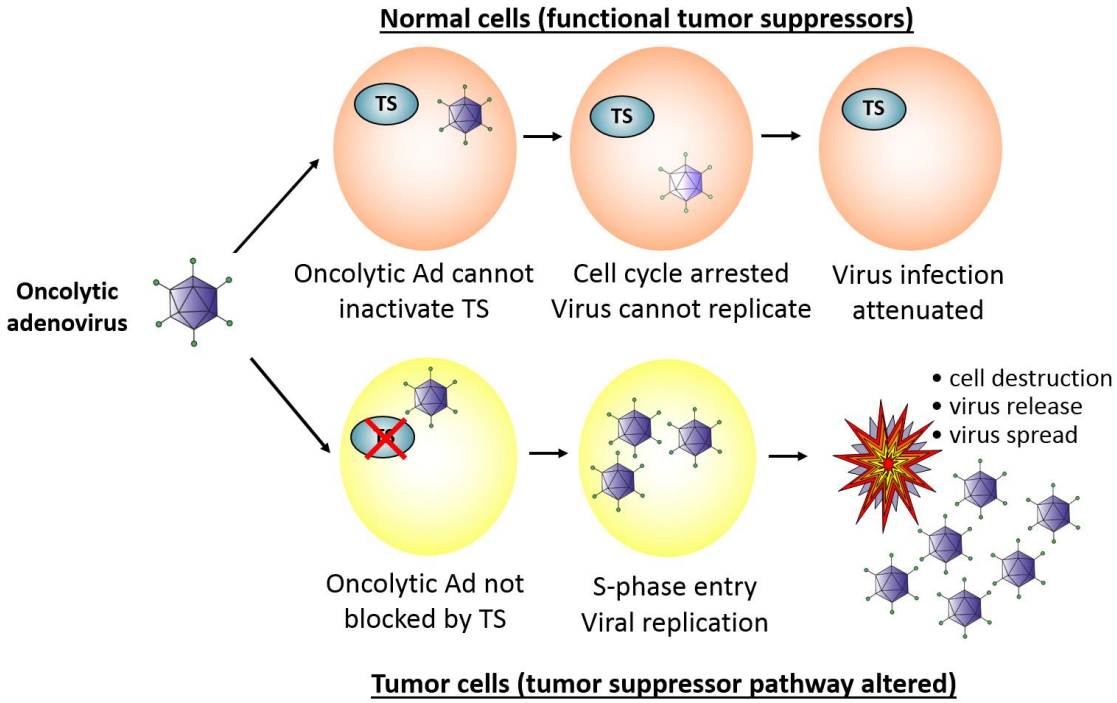

Figure 3. Model of the paradigm of selective oncolytic adenovirus replication. (Top) Oncolytic adenovirus infects normal cell with functional tumor suppressors and sensors that block cellular and consequently virus genomic replication. (Bottom) Oncolytic adenovirus infects cell with altered tumor suppressor pathway and continues to proliferate, consequently driving the virus lifecycle which results in lysis of the host cell and release of oncolytic adenovirus progeny.

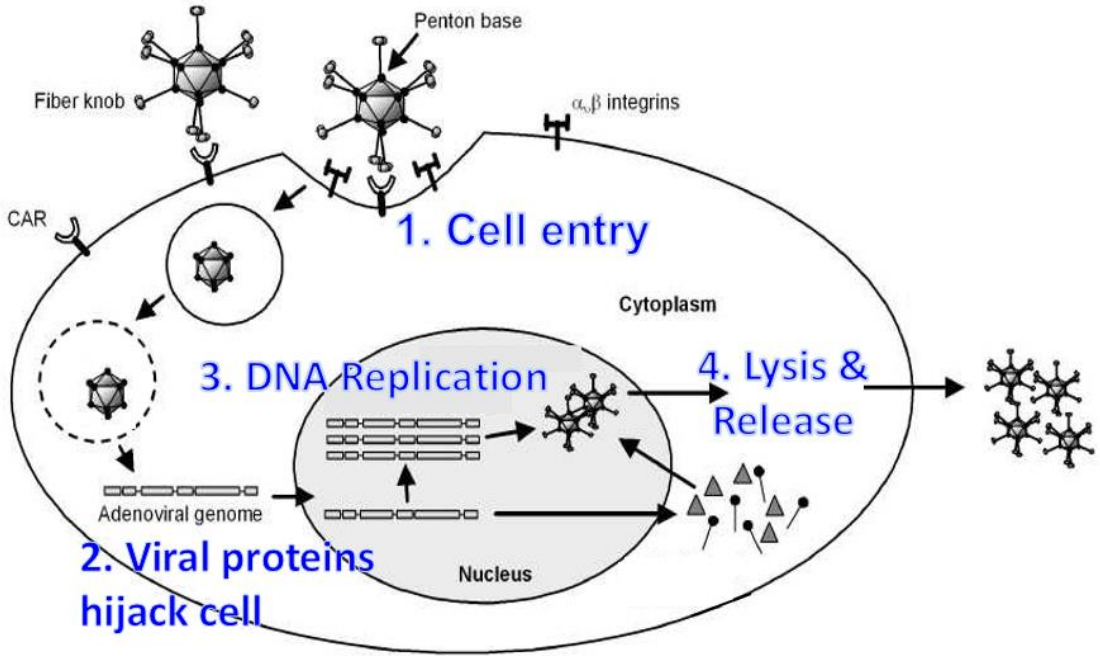

Figure 4. Diagram of the adenovirus lifecycle. 1. Adenovirus fiber knob binds to cellular receptor CAR. RGD peptides in adenovirus penton base interact with $\alpha_v\beta_3$ integrins and the virion is internalized via clathrin-mediated endocytosis. Adenovirus escapes the endosome and is released into the cytoplasm where it is trafficked to the nuclear pore by dynein motors where the adenovirus genome enters the nucleus. 2. Adenovirus gene transcription encodes for proteins that take over cell functions and drive the cell cycle. 3. The adenovirus genome is replicated to high copy concomitantly with cellular genome, and late structural adenovirus proteins are expressed and assemble into genome-packaged capsids in the nucleus. 4. The last stage of the lifecycle where adenovirus lyses the nuclear and plasma membrane, releasing progeny for subsequent rounds of infections.

1.2.1 E1A

Studies with adenovirus E1A led to early discovery and insights into Rb and E2F functions (reviewed in (5)). Ad E1A is the first gene transcribed and expressed during Ad infection, and the E1A isoforms activate cellular and viral gene expression by multiple mechanisms (reviewed in (33)). E1A binds and inactivates Rb through its conserved LXCXE motif (34), which releases the E2F transcription factor (35-37) (Fig. 5). This is considered to be the mechanism by which E1A activates E2F to drive expression of cellular and viral genes necessary for cellular and viral genome replication. It was thought that deletion of the LXCXE motif would be sufficient to generate an oncolytic Ad that would selectively replicate in cancer cells with defects in the Rb tumor suppressor pathway (38), but it is still able to activate E2F and replicate in primary cell culture (39).

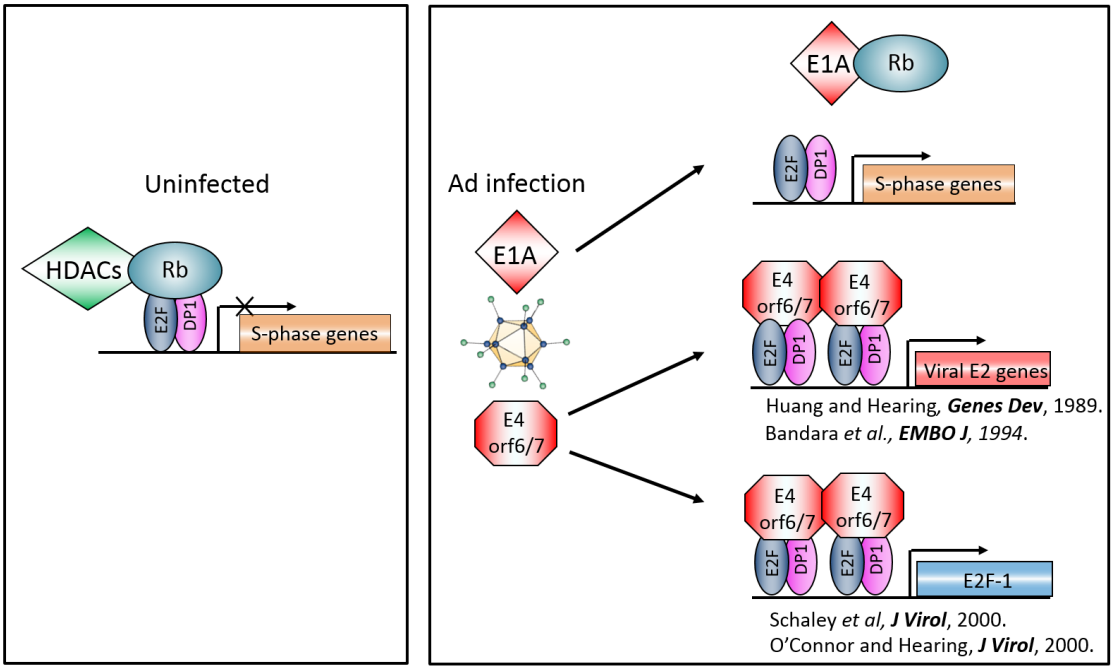

Figure 5. Adenovirus infection activates E2F and S-phase genes. (Left) In uninfected cells, Rb forms a repressive transcriptional state at E2F-binding sites, blocking the cell from entering the cell cycle. (Right) In adenovirus infection, E1A binds to Rb, releasing E2F, allowing for the activation of transcription at E2F targets. Independently, adenovirus E4orf6/7 binds to and stabilizes inverted repeats of E2F/DP1 heterodimer at viral gene promoters, and at cellular gene promoters, including the E2F1 promoter itself.

1.2.2 E4orf6/7

There is another Ad protein, E4orf6/7, that independently binds to active E2F1 transcription complexes at cell and Ad promoters (40-42), and can independently displace Rb from E2F (43) (Fig. 5). Adenovirus E4orf6/7 drives heterodimerization of E2F/DP1 to enhance Ad early E2a (40) and cellular E2F1 promoter transcription (41), and may also directly compete with suppressive Rb/DP1 interactions (44). Therefore, we hypothesized that an adenovirus bearing both E1A ΔLXCXE and lacking E4orf6/7 function would be a selective oncolytic viral therapy for cancer cells lacking Rb tumor suppressor function.

1.3 Expanding the limited tropism of Ad5

Oncolytic viral therapy has the potential to destroy a tumor mass of unlimited size, but only if the virus can cross through tumor vasculature, infect the cancer cells, and spread from one cell to another. Adenovirus (Ad) particles primarily interact with host cells through protein interactions between the knob-domain of fiber on the surface of the capsid and a cell surface molecule. Currently Ad vectors rely on a single cellular receptor for their uptake, and are primarily based on the most widely studied serotype 5 of Ad species C (Ad5). Ad5 primarily targets epithelial cells via interactions between the fiber protein on the outer viral capsid and the coxsackie and adenovirus receptor (CAR) (45, 46) (Fig. 4). Unfortunately, many cancer cells do not express CAR, such as mesenchymal and deadly metastatic cancer cells (47). Since viral replication

and cancer cell killing will be limited by the ability to infect cells, we need viruses that infect cancer cells via receptors other than CAR, ideally those specifically upregulated on cancer cells.

While myriad approaches to genetically modify and chemically coat adenovirus to target new receptors has been met with some success, there are systemic limitations of these approaches. The adenovirus capsid cannot tolerate large insertions, so it is risky and laborious to identify and confirm sequences that are both functional and do not disrupt capsid structural integrity. While chemical modifications to purified capsids are theoretically limitlessly customizable, a prepared virus delivered into a host will lose all of the modifications by the first round of replication, and will be reduced to genetically encoded tropism for subsequent rounds of infection.

To overcome these limitations of tropism manipulation, we employed the use of new genome engineering methodologies that enable rapid modification of the sequence with high precision to build and demonstrate a novel methodology that expands adenovirus tropism in an easily adaptable and highly controlled manner.

1.4 Generation of novel adenovirus mutants

For many years adenovirus genomes have been modified using standard molecular cloning techniques, which present many challenges due to the length and complexity of sequence. Consequentially, many oncolytic and vector adenoviruses are descendants of genomes bearing unwanted genetic

mutations along with the desired changes. While more precise methodologies have been developed, such as homologous recombination in bacteria (48-50) or CRISPR-Cas9-mediated modification (51), these approaches are still time consuming, frequently require multiple steps, and lack modularity.

Our lab sought to apply the principle of modularity to adenovirus genome engineering in order to break the sequence down into workable parts that could organized into libraries, selected and combined into whole genomes. Dr. Colin Powers split he adenovirus genome into four parts, representing an evolutionary modularity of the adenovirus gene architecture. He developed two strategies to assemble any of the parts to create full genomes. In a strategy termed “Adsembly,” we use Multisite Gateway technology to combine the four parts *in vitro* to reassemble a complete genome as quickly as 1 hour. A parallel approach to genome assembly termed “AdSLIC,” uses sequence and ligation-independent cloning (SLIC) is a hybrid restriction enzyme, PCR-based approach that reassembles the parts in a nearly seamless fashion.

These approaches enable rapid assembly of virus genomes that exclusively contain sequences of interest, increasing our ability to study viral genes, and enabling a rapid design, build, test lifecycle for the engineering of oncolytic viruses with compound modifications. This technology was crucial for the construction of all the adenoviruses described in this work. A list of viruses described in this work are listed in Table 1.

Table 1. List of viruses that were constructed and described in this work.

Virus	E1	Core (E2-L4)	E3	Fiber	E4	Construction
AdSyn-CO170	wt	wt	wt	wt	wt	Adsembly
AdSyn-CO205	GFP-E1A	wt	ΔE3B + EGFRVHH-FKBP	FRB-Fiber	wt	Adsembly
AdSyn-CO206	GFP-E1A	wt	ΔE3B + EGFRVHH-FKBP	wt	wt	Adsembly
AdSyn-CO207	GFP-E1A	wt	wt	FRB-Fiber	wt	Adsembly
AdSyn-CO220	GFP-E1A	wt	wt	FRB*-Fiber	wt	Adsembly
AdSyn-CO102	wt	wt	wt	wt	wt	AdSLIC
AdSyn-CO210	wt	wt	wt	wt	ΔE4orf6/7	AdSLIC
AdSyn-CO283	wt	wt	wt	wt	E4orf1 ΔPDZb, ΔE4orf6/7	AdSLIC
AdSyn-CO284	wt	wt	wt	wt	ΔE4orf1, ΔE4orf6/7	AdSLIC
AdSyn-CO236	E1A Δ2-11	wt	wt	wt	wt	AdSLIC
AdSyn-CO290	E1A Δ2-11	wt	wt	wt	ΔE4orf6/7	AdSLIC
AdSyn-CO291	E1A Δ2-11	wt	wt	wt	E4orf1 ΔPDZb, ΔE4orf6/7	AdSLIC
AdSyn-CO292	E1A Δ2-11	wt	wt	wt	ΔE4orf1, ΔE4orf6/7	AdSLIC
AdSyn-CO189	E1A ΔLXCXE	wt	wt	wt	wt	AdSLIC
AdSyn-CO181	E1A ΔLXCXE	wt	wt	wt	ΔE4orf6/7	AdSLIC
AdSyn-CO285	E1A ΔLXCXE	wt	wt	wt	E4orf1 ΔPDZb, ΔE4orf6/7	AdSLIC
AdSyn-CO286	E1A ΔLXCXE	wt	wt	wt	dE4orf1, dE4orf6/7	AdSLIC
AdSyn-CO235	E1A C124G	wt	wt	wt	wt	AdSLIC
AdSyn-CO287	E1A C124G	wt	wt	wt	ΔE4orf6/7	AdSLIC

Table 1. List of viruses that were constructed and described in this work, continued.

Virus	E1	Core (E2-L4)	E3	Fiber	E4	Construction
AdSyn-CO288	E1A C124G	wt	wt	wt	E4orf1 ΔPDZb, ΔE4orf6/7	AdSLIC
AdSyn-CO289	E1A C124G	wt	wt	wt	ΔE4orf1, ΔE4orf6/7	AdSLIC
AdSyn-CO238	E1A Y47H, C124G	wt	wt	wt	wt	AdSLIC
AdSyn-CO293	E1A Y47H, C124G	wt	wt	wt	ΔE4orf6/7	AdSLIC
AdSyn-CO294	E1A Y47H, C124G	wt	wt	wt	E4orf1 ΔPDZb, ΔE4orf6/7	AdSLIC
AdSyn-CO295	E1A Y47H, C124G	wt	wt	wt	ΔE4orf1, ΔE4orf6/7	AdSLIC
AdSyn-CO244	E1A Y47H, C124G, Δ2-11	wt	wt	wt	wt	AdSLIC
AdSyn-CO296	E1A Y47H, C124G, Δ2-11	wt	wt	wt	ΔE4orf6/7	AdSLIC
AdSyn-CO297	E1A Y47H, C124G, Δ2-11	wt	wt	wt	E4orf1 ΔPDZb, ΔE4orf6/7	AdSLIC
AdSyn-CO298	E1A Y47H, C124G, Δ2-11	wt	wt	wt	ΔE4orf1, ΔE4orf6/7	AdSLIC
AdSyn-CO312	E1A ΔLXCXE	wt	ΔE3B + EGFRVHH-FKBP	FRB*-Fiber	ΔE4orf6/7	AdSLIC
AdSyn-CO335	E1A ΔLXCXE	Hexon E451Q	ΔE3B + EGFRVHH-FKBP	FRB*-Fiber	ΔE4orf6/7	AdSLIC
AdSyn-CO442	E1A ΔLXCXE	Hexon E451Q	wt	FRB*-Fiber	ΔE4orf6/7	AdSLIC

Chapter 2. Engineering a modular and chemically-controlled mode of novel virus tropism

2.1 Introduction

Currently adenovirus (Ad) vectors rely on a single cellular receptor for their uptake, and are primarily based on the most widely studied Ad serotype 5 (Ad5). Ad5 is not a naturally blood-borne virus and does not actively target and cross the vasculature. Ad5 infects epithelial cells via interactions between the fiber protein on the outer viral capsid and the coxsackie and adenovirus receptor (CAR), primarily found at epithelial cell junctions (45, 46). Unfortunately, metastases are responsible for the death of most cancer patients, in which an epithelial to mesenchymal transition (EMT) results in downregulation of cadherin and CAR, instigating invasion and spread to distant sites (47). Thus, many malignant cells do not express CAR and are not susceptible to infection by Ad5 (47, 52, 53). Since oncolytic therapy is limited by the ability to infect cancer cells, we need viruses that infect cells via receptors other than CAR, ideally those specifically upregulated on cancer cells. To overcome this challenge, we developed a genetically-encoded switchable targeting moiety, enabling Ad to infect cancer cells independently of CAR-expression.

Myriad approaches have been attempted to control adenoviral targeting. One mode of adenoviral targeting includes the use of chemical adapters that link viral capsids to retargeting ligands (Fig. 6). For example, the capsid can be polymer coated or biotinylated to provide a chemical linker for high affinity binding to avidin-fused retargeting ligands (54) (other related methods reviewed in (55) and (56)). However, retargeting is only achieved with exogenously prepared virus, since the chemical modifications are lost upon viral replication. To overcome this drawback, genetically encoding retargeting adapter fusions to viral coat proteins is desirable, but also more challenging. Many studies have focused on the modification of the Ad fiber protein (57). Unfortunately, the incorporation of large ligands in capsid proteins frequently disrupts their folding/assembly. To avoid misfolding, smaller polypeptides can be inserted into the fiber HI loop (58) (also referred to as the H1 loop) (Fig. 7C). For example, insertion of some receptor-targeting peptides have shown some promise (59), and inserted RGD peptides have been shown to generally integrin-mediated uptake viral uptake (60, 61), but are not sufficient to alter viral tropism. Fiber fusions to single chain antibodies (scFVs) are attractive as well, but the former require processing in the endoplasmic reticulum (ER) or cytosol while fiber assembles in the nucleus (62). In an example of using fiber/receptor bridging molecules to control adenovirus tropism, Dreier *et al.* have explored the use of designed ankyrin repeat proteins (DARPins) (63). By using engineered bispecific trimeric DARPin adapters that bind both the adenovirus fiber and targeted receptors, they circumvent the problem with direct genetic modification

of fiber, however the original tropism of Ad is lost, and the DARPins have not been engineered in a fashion that is compatible with replicating virus. Thus, despite ongoing efforts to retarget infection, *in vivo* studies and gains have been modest (64).

An ideal virus would genetically encode an adapter that could be used to enhance viral tropism within the body via multiple retargeting moieties, without compromising viral replication and patient safety. Here I describe the development of a novel, inducible, genetically encoded chemical adapter system that targets infection to multiple cell types, and is not lost upon viral replication. This overcomes the limitations of current approaches and has several advantages. Any unanticipated toxicities associated with induced receptor-targeting could be stopped by drug withdrawal. Ultimately, this system could enable targeting of receptors in angiogenic tumor vasculature (e.g. TEMs, TVMs) to eliminate aggressive tumors, and upregulated markers in high-risk tumors (e.g. EGFR, HER2, TfR) such as breast cancer.

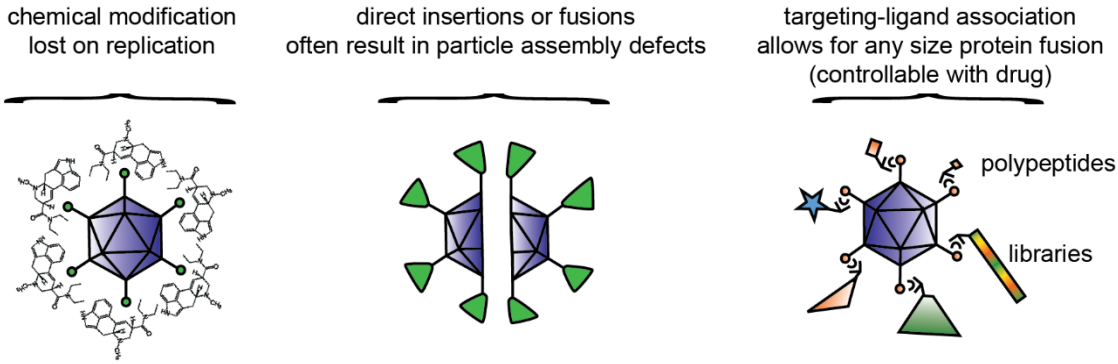

Figure 6. Limitations to conventional adenovirus modification and advancements for engineering tropism. Chemical modification of purified adenovirus particles can alter tropism of the initial infection, but progeny viruses will not bear the same properties. Systematic genetic modification of adenovirus is challenging since generation and testing of new sequences is slow and the capsid does not tolerate sequence modifications that disrupt particle assembly. An ideal system combines the strengths of the two previous strategies, where a stable genetic change to the virus provides a chemically-controllable handle for attaching new targeting polypeptides.

2.2 Rapamycin, FRB, and FKBP12

We modified the Ad capsid protein fiber to enable binding to alternate cellular receptors using a known property of the immunosuppressive and anti-tumor drug rapamycin (rap). Rapamycin (rap) is an approved macrolide antibiotic that inhibits the kinase activity of mechanistic target of rapamycin (mTOR), which is activated in many cancer cells. Unlike many kinase inhibitors, rap is not an ATP structural homolog, and instead blocks mTOR kinase activity by forming a stable heterodimer between the FK506-binding protein (FRB) domain of mTOR and cellular FKBP12 (65). Rap can be used to induce heterodimers of heterologous proteins if one is fused to an FKBP12 domain and the other contains the FRB domain (65). The high affinity and stability of rap-induced heterodimerization has been used with great success in several applications including phage display of receptor-ligand complexes (66), transcriptional activation (67), and reconstitution of bi-functional proteins (68). Importantly, heterodimerization of FRB and FKBP12 by rapamycin has been shown to function *in vivo (69)*.

Here we show a novel application of this system, which also takes advantage of our previous studies of rap as a rational combination with oncolytic viruses (70). Since rap already has anti-tumor properties (71, 72), and can induce the dimerization of heterologous proteins with the FKBP12 and FRB domains, I engineered the fiber protein of Ad5 to incorporate a minimal FRB domain in the fiber knob HI loop. Unlike other insertions, such as ligands that

directly bind transferrin (73), α_V integrin, or heparan sulfate (74), the Ad5 with fiber bearing inserted FRB replicates to wild type levels. In principle, any protein or polypeptide fused to FKBP12 that can bind to a cell surface molecule should direct the virus to infect the targeted cell by increasing affinity of the virus particle to the surface of the cell (Fig. 4). Since the FKBP-fusion protein is not part of the assembly of the base adenovirus particle, it should not inhibit the replication of engineered Ads with this mechanism of expanded tropism. The rap-dependent FRB-FKBP heterodimerization-controlled Ad tropism is highly modular and should enable rapid identification of new targeting moieties while retaining control and safety of viruses with novel tropisms by controlling rap administration.

2.3 Epidermal Growth Factor Receptor

Epidermal growth factor receptor (EGFR) is a transmembrane protein that is activated by the extracellular mitogen epidermal growth factor (EGF). Alterations in EGFR much as mutation or overexpression that result in elevated or constitutive signaling can drive cell proliferation. EGFR is upregulated in many cancers of epithelial origin such as breast (75), head and neck (76), prostate (77), lung (78), skin (79), and bladder carcinomas (80). Upregulation of EGFR is also associated with the progression of metastatic disease due to upregulation of caveolin-1 function (81) that results in the loss of cell-cell adhesion protein E-cadherin (E-cad), a hallmark of the epithelial to mesenchymal transition (EMT) (reviewed in (82)). The importance of this cancer

target is corroborated by its routine assessment in preliminary cancer diagnosis and the growing list of approved drugs such as the EGFR agonist Tarceva® (erlotinib), the EGFR-inhibiting antibodies Erbitux® (cetuximab) and Vectibix® (panitumemab), and the development of an EGFRvIII-targeted oncolytic adenovirus (83).

As a proof of concept, we fused FKBP to a single-domain camelid antibody with specificity for EGFR (84). Upon rap treatment, this virus is induced to infect cells via EGFR. This is a rational and powerful synergy of chemical and viral weapons that can be combined with the enhanced replication specificity of E1A/E4orf6/7 mutants (described in Chapter 3) to create a new safe form of effective, self-amplifying therapy that breaks the paradigm of systemic genotoxic treatments for cancer.

2.4 Adenovirus fiber tolerates FRB insertion in the HI loop

The fiber protein which infers tropism to Ad has been extensively targeted for modification in attempts to control Ad tropism. We wished to exploit the use of the known heterodimerizing properties of rapamycin with the FRB domain from mTOR and its cellular partner FKBP12 (Fig. 7A). Polypeptides can be fused to the N-terminus of FKBP to further functionalize protein complex assembly. By inserting the FRB domain into fiber, we sought to expand the tropism of adenovirus beyond its native receptor CAR by using rapamycin to bring FKBP12 fused to a targeting ligand to the surface of the virus particle,

therefore directing the virus to attach to the alternatively targeted receptor (Fig. 7B).

Fiber is generally not permissible to large insertions or modifications, because the correct folding and assembly of fiber trimers into Ad particles are critical to produce viable progeny. Despite defects in replication due to large inserted ligands that directly bind their targets such as transferrin (73) or heparan sulfate (74), and reported loss in infectivities of Ads with >50 aa insertions in the HI loop (85), we were able to insert the 90 aa FRB domain of mTOR (Glu2025-Gln2114) into the fiber HI loop between residues Thr546 and Pro567 (FRB-Fiber) (Fig. 7C). We constructed a virus bearing this insertion as well as a genetically encoded GFP-reporter (AdSyn-CO207) using a multi-site gateway reaction method we have termed Adsembly (Fig. 7D). The insertion of FRB did not inhibit viral replication or infection as evidenced by GFP reporter fluorescence, observed cytopathic effect of virally induced cell lysis, and by expression of late adenovirus proteins (Fig. 7E). We confirmed the FRB insertion by immunoblot to detect fiber expressed during infection, and observed the expected ~11 kDa change in migration of FRB-fiber (72.4 kDa) versus wt fiber (61.6 kDa) in SDS-PAGE (Fig. 7E).

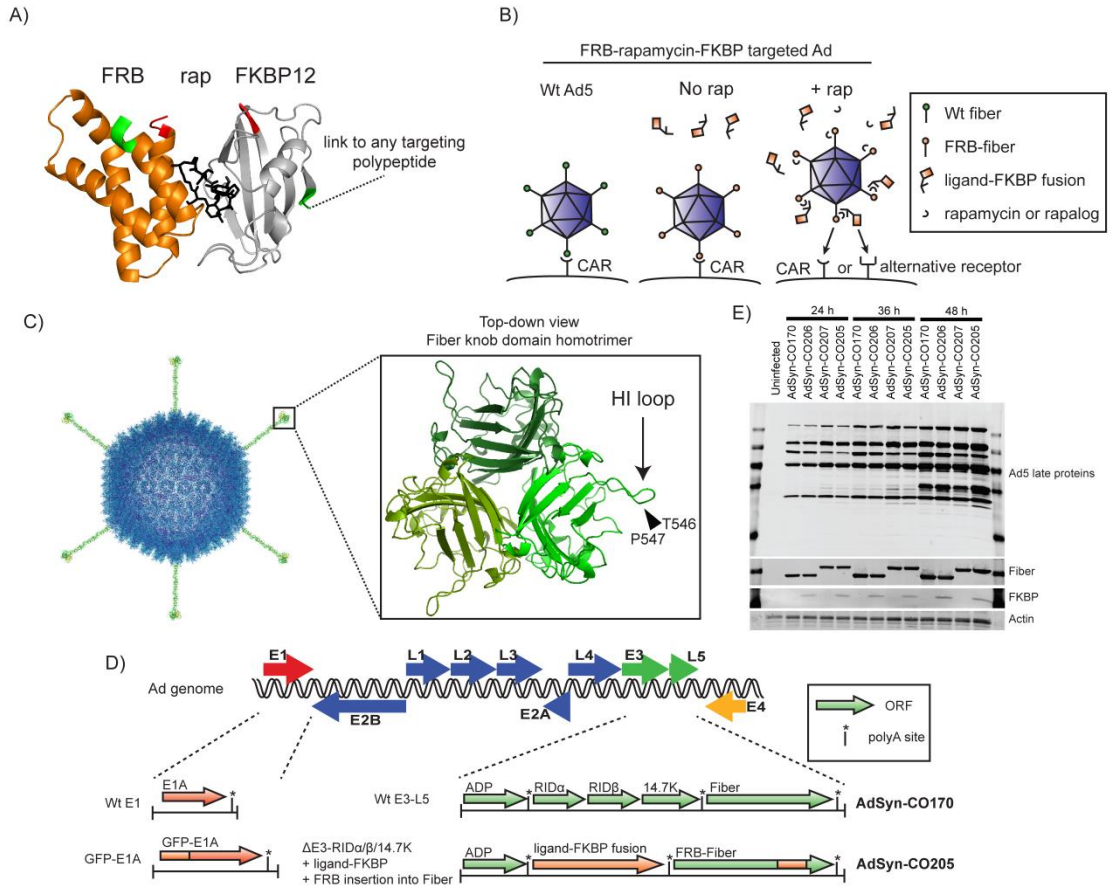

Figure 7. Our strategy using the chemical-induced heterodimer FRB-rapamycin-FKBP to create a modular platform to target adenovirus. A) Crystal structure of FRB/rap/FKBP12 complex (PDB ID: 1NSG). FKBP12 shown as gray ribbon with N-terminus in green, C-terminus in red. Rap shown as black sticks. FRB domain shown as orange ribbon with N-terminus in green, C-terminus in red. B) Diagram illustrating strategy of how to employ rapamycin to expand engineered adenovirus tropism to new receptor targets. C) Site of FRB domain insertion into Ad5 fiber. (Left) Structure of adenovirus modeled from capsid structure (PDB ID: 3IYN), shaft (PDB ID: 1V1H), and knob (PDB ID: 1KNB). (Right) Site of insertion of FRB domain. D) Map of Ad genome and sites of modification to create engineered-tropism viruses by Adsembly. E) Immunoblot of protein expression in infected 293-E4 from synthetic adenoviruses bearing rapamycin-dependent EGFR-targeting components.

2.5 FRB-containing AdSyn-CO207 can be targeted with ectopically co-expressed FKBP-fusion protein

An ideal targeting protein for virus infection is a stable molecule with strong affinity for an upregulated cancer cell surface molecule. A class of proteins that best fits the ideal criteria for targeting are the heavy chain domains (VHH) from single-domain antibodies (sdAbs). Camelids and sharks encode sdAbs which have specificity for their target from one variable chain domain, instead of the conventional two found in most other mammals (e.g. rodents, humans) (62). The application of sdAbs for targeting adenovirus infection has been tested in a fiber-mutant Ad (86).

Although small single-chain variable fragments (scFVs) have been more widely used, the smaller and more stable VHHs have the distinct advantage of not requiring post-translational disulfide bond formation to function. Notably, since virion assembly occurs in the nucleus, the formation of disulfide bonds is not available to Ad capsid proteins.

As a proof of principle, I fused FKBP to a VHH (7C12) with specificity for epidermal growth factor receptor (EGFR) identified by Gainkam *et al* (84). The gene sequence encoding EGFRVHH was human codon optimized for expression and synthesized by Blue Heron Biotechnologies based on the protein sequences identified by Gainkam *et al.* (84). Based on our structural modeling using PyMol, the EGFRVHH domain was fused to the N-terminus of

FKBP with a GSGSGST linker sequence for the least steric hindrance for VHH/target interactions and the FKBP/rap/FRB dimerization interface.

To test the hypothesis that an FKBP-fusion protein would change the tropism of an adenovirus containing an FRB domain in the capsid in the presence of rapamycin, we ectopically expressed EGFRVHH-FKBP in cells infected with AdSyn-CO207. We cloned the EGFRVHH-FKBP fusion protein into a mammalian expression plasmid, and transfected 293 E4 cells with this vector 24 h prior to infection with AdSyn-CO207. 24 h following infection, rapamycin or solvent control was added to the cells.

We anticipated that progeny virus assembling in the presence of EGFRVHH-FKBP and rapamycin would gain the ability to infect cells via EGFR. We harvested viruses assembled in the presence and absence of rapamycin 48 h after infection and tested their ability to infect breast cancer cells. We found that indeed, AdSyn-CO207 prepared with EGFRVHH-FKBP and rapamycin had an enhanced ability to infect cultured MDA MB 453 breast cancer cells (Fig. 8).

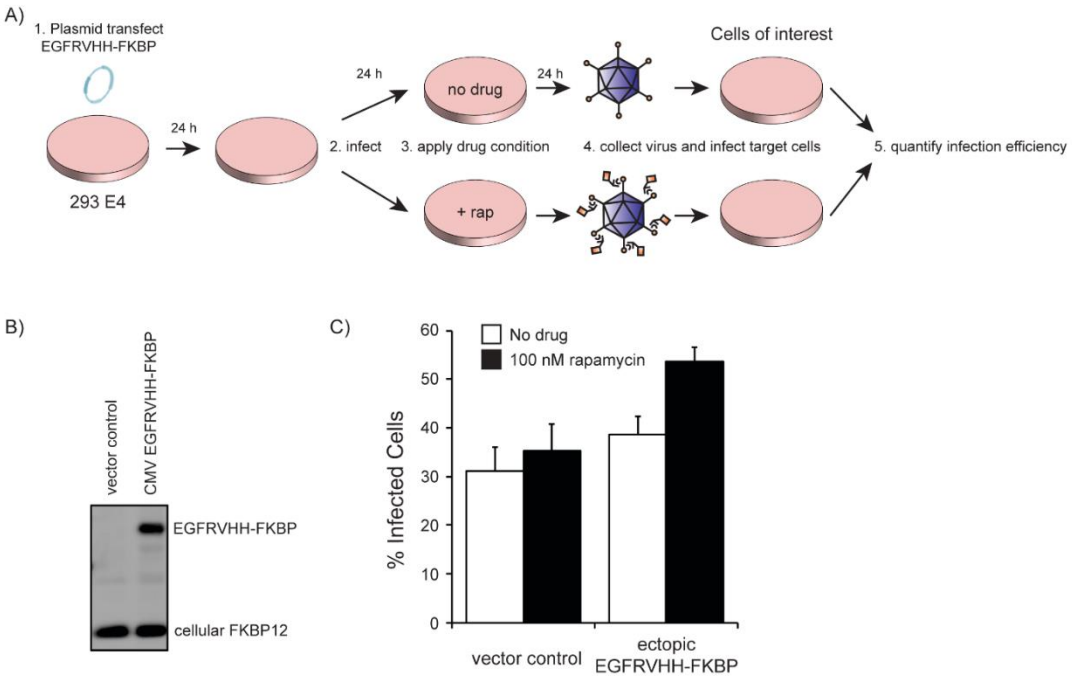

Figure 8. Infection can be targeted with ectopically expressed FKBP-fusion protein. A) Scheme of strategy to prepare targeted Ad using ectopically expressed FKBP-fusion protein. B) Immunoblot of ectopically expressed EGFRVHH-FKBP, in 294 E4 cells, 24 h post-transfection. The ligand-FKBP fusion (or GFP as a control) was transiently expressed in 293 E4 cells, then infected with AdSyn-CO207. C) FACS analysis of MDA MB 453 infection by virus prepared in the presence of absence of 100 nM rapamycin.

2.5.1 Importance of VHH-FKBP fusion orientation

We also attempted fusing EGFRVHH to the C-terminus of FKBP using the GSGSGST linker, but we were unable to detect improved targeting functionality with this construct, suggesting that the orientation of the domains is important for protein-protein interactions.

2.5.2 Direct fusion of VHH to FKBP does not allow for viable virus replication

We tested if we could fuse EGFRVHH directly to fiber, with the objective to generate a “constitutively” EGFR-targeted adenovirus, however a virus genome with direct C-terminal fusion of EGFRVHH to fiber was unable to generate productive virus in 293E4 (data not shown). This failure underscores the importance of the modular design using the chemically controlled heterodimerization strategy to control adenovirus targeting, since the direct fusion likely caused a defect in protein folding and adenovirus particle assembly.

2.6 FKBP retargeting moiety can be expressed from adenovirus E3 promoter

While ectopic expression of a targeting FBKP-fusion protein can yield progeny with expanded tropism, the virus would not carry this property through multiple rounds of replication in cancer cells unless it encoded the FKBP-fusion protein.

We attempted a variety of strategies to encode FKBP expression in the adenovirus genome. Our first attempt was to link FKBP expression with fiber expression by using a Furin-2A autocleavage site at the C-terminus of fiber (87).

While this strategy could have afforded a potentially ideal 1:1 stoichiometry between fiber and FKBP, the virus exhibited practically no replication. Our second strategy was to transcriptionally link FKBP expression with the fiber protein by adding an internal ribosome entry site (IRES) following the fiber ORF on the adenovirus L5 transcript. These viruses were able to replicate, however we were unable to detect accumulation of FKBP expression by immunoblot.

When engineering the Ad genome, the size of the genome must be taken under consideration, because genomes that are significantly larger than the wild type sequence result in decreased particle stability (88). Other work in our lab has also revealed that extra promoter and terminator sequences can disrupt the virus lifecycle. To avoid inserting additional exogenous promoter and terminator sequences, we ultimately attempted to use the natural architecture of the Ad E3 region to express the FKBP-fusion retargeting protein. The E3 region contains genes that are involved in host immune response evasion, and they have been shown to be dispensable for viral replication in tissue culture. Other groups have also described use of this Ad genomic region to express transgenes (89), and many Ad vectors have deletions or modifications of the E3 region, and in the context of replicating oncolytic adenovirus therapy, it may actually be beneficial to avoid suppressing or even recruit a host immune response at the site of the tumor.

We removed the sequence of the *E3B* transcript encoding *RIDα*, *RIDβ*, and *14.7k* and replaced it with EGFRVHH fused to FKBP12 (EGFRVHH-FKBP)

as the targeting gene (Fig. 7D). The VHH sequence was inserted at the N-terminus of FKBP with a GSGSGST linker sequence. We constructed the virus AdSyn-CO205 using Adsembly, containing the FRB-fiber insertion, the EGFRVHH-FKBP gene, as well as the genetically encoded GFP reporter fused to the N-terminus of E1A (Fig. 7D). The expression of the fusion protein was verified by immunoblot by probing for FKBP12 (Fig. 7E). A control virus is shown that expresses EGFRVHH-FKBP, but retains the wt fiber (AdSyn-CO206). A timecourse of late protein expression shows that there is no obvious defect in replication of the fiber-mutant, or EGFRVHH-FKBP expressing viruses compared to our wild type Ad5 (AdSyn-CO170) (Fig. 7E).

2.7 Retargeting with EGFRVHH-FKBP and rapamycin

As a first test to evaluate AdSyn-CO205 targeting, we infected the breast cancer cell line MDA MB 453. Although reports consistently identify that MDA MB 453 lacks expression of estrogen-receptor and progesterone-receptor, there is conflicting evidence of EGFR expression levels. However, we and others have detected EGFR by immunoblot and by immunofluorescence in agreement with expression (Fig. 11A) (90).

AdSyn-CO205 was prepared by first infecting two plates of 293 E4 cells with MOI 10 AdSyn-CO205. In one plate, the media was replaced 24 h post-infection (hpi) with fresh media containing 500 nM rapamycin. The other plate served as the solvent control. The media was collected 48 hpi and passed

through a 0.22 μm filter to remove 293 E4 cells, then used directly to infect the target cancer cell lines with equal volumes of infectious media. We avoided freezing/thawing the 293 E4s to simulate a more representative passage of progeny virus from a lysed host cell to infect new cells. Infection efficiency of the MDA MB 453 was quantified by FACS using an LSRII® (BD) (Fig. 9A), and the results were corroborated using high-content imaging on an ImageXpress® (Molecular Devices) (Fig. 9B).

We compared the AdSyn-CO205 and control viruses AdSyn-CO206 and AdSyn-CO207 for their rapamycin-induced infection of MDA MB 453 cells. The luminal MDA MB 453 cells were moderately transduced by non-targeted AdSyn-CO205, while we observed a 1.5 fold improvement in infection with the rap-treated virus (Fig. 9A). We did not observe an effect on infection with rapamycin alone with the control viruses AdSyn-CO206 or AdSyn-CO207

We did not anticipate that the insertion of the FRB domain into fiber would eliminate CAR-binding by fiber. Supporting this prediction, we did not observe a reduction of infection of MDA MB 453 by AdSyn-CO205 or AdSyn-CO207 in the absence of rapamycin when compared to AdSyn-CO206 (Fig. 9A). In this experiment with MDA MB 453, we actually see an increased baseline level of infection, suggesting that the FRB insertion alone may enhance the tropism of Ad to this cell line.

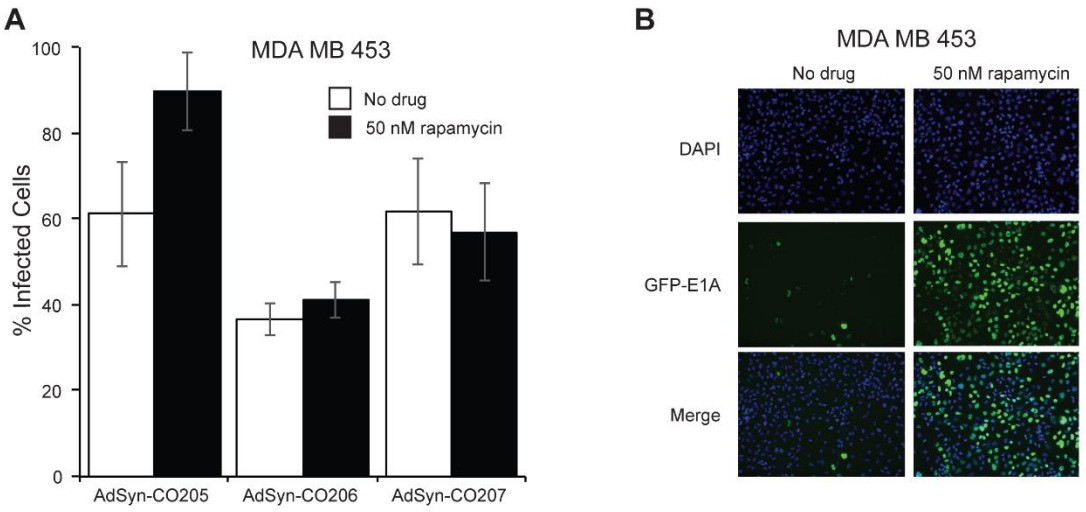

Figure 9. Rapamycin targeting of synthetic adenovirus AdSyn-CO205 infection of MDA MB 453. A) MDA MB 453 cells were seeded at equal density in 12-well plates, and infected with equal volumes of viruses in the presence or absence of 50 nM rapamycin. 24 hours following infection, FACS for GFP-positive cells was used to quantify infection with EGFR-targeted AdSyn-CO205, and control viruses AdSyn-CO206 (no FRB domain) and AdSyn-CO207 (no EGFRVHH-FKBP). B) Representative high-content fluorescence microscopy pictographs of MDA MB 453 infected with AdSyn-CO205 in the presence or absence of 50 nM rapamycin.

2.8 Retargeting AdSyn-CO205 with rapamycin is dose responsive

A range of concentrations of rapamycin were tested for targeting MDA MB 453 infection by AdSyn-CO205. We observed a peak efficiency of infection at low concentrations of rapamycin (25-50 nM), while at higher concentrations there was a diminished targeting, potentially due to a saturation effect of excess rapamycin (Fig. 10).

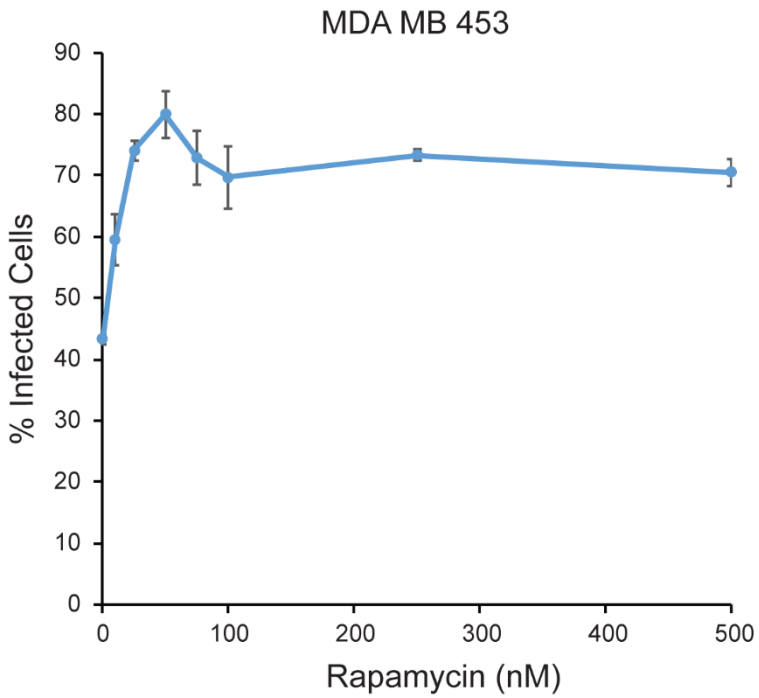

Figure 10. AdSyn-CO205 targeting of MDA MB 453 infection by rapamycin is dose-dependent. Infection of MDA MB 453 with AdSyn-CO205 and a range of rapamycin concentrations was quantified by FACS.

2.9 Retargeting with EGFRVHH-FKBP is EGFR-dependent

To test the specificity of AdSyn-CO205 to infect via EGFR upon rapamycin treatment, we knocked down EGFR expression in MDA MB 453 by short hairpin RNA (shRNA). We used the validated EGFR shRNA B sequence from Engelman *et al.* (91) and cloned it into the pLentiX2 puro backbone with two different hairpin linkers.

These vectors were used to generate lentivirus, which were used to transduce MDA MB 453 cells. We selected for a population of cells to generate cell lines with stable EGFR knockdown. EGFR knockdown was verified by immunoblot and immunofluorescence microscopy (Fig 11A & B). We tested the rapamycin targeting of AdSyn-CO205 in the context of the loss of EGFR expression.

The loss of targeting in the EGFR knockdown cells, but not in luciferase shRNA control cells suggests that the targeting is relies on the presence of cell surface EGFR and is EGFR-dependent (Fig 11C).

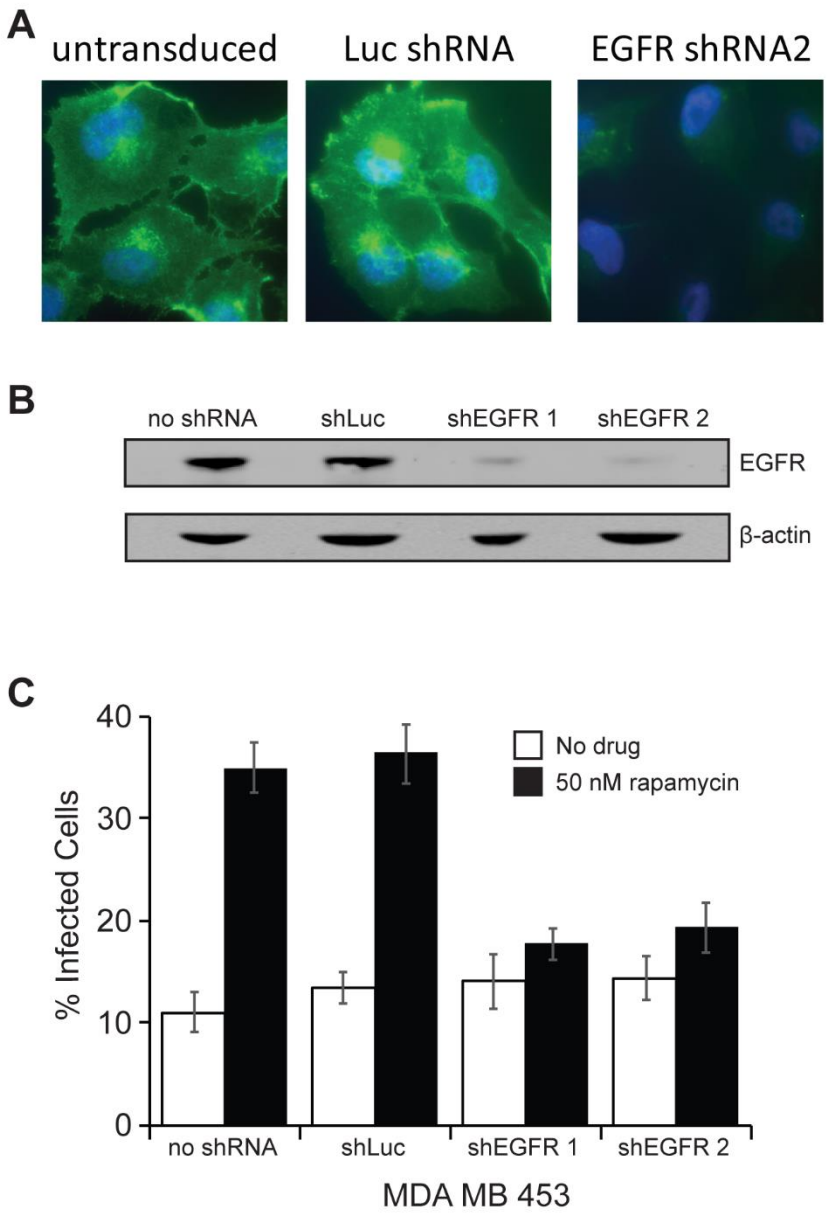

Figure 11. The targeting of AdSyn-CO205 is EGFR-dependent. MDA MB 453 cells were transduced with lentiviruses expressing short hairpin RNAs (shRNA) to knock down EGFR expression. A) Knock down efficiency shown by immunostaining of EGFR in photomicrographs of MDA MB 453. EGFR staining (anti-EGFR ab2430, Abcam) shown in green, nuclei staining (Hoechst 33258, Molecular Probes) shown in blue. B) Knock down efficiency shown by immunoblot for EGFR expression (anti-EGFR ab2430, Abcam). B-actin used as loading control (A5441, Sigma). C) Results of MDA MB 453 infection by AdSyn-CO205 in the presence of absence of 50 nM rapamycin quantified by FACS.

2.10 Rapamycin induces improved infection of breast cancer cell lines by AdSyn-CO205

To explore the general efficacy of the EGFR targeting of AdSyn-CO205 with rapamycin, we queried a panel of clinically validated breast cancer cell lines, including MDA MB 453 (92, 93). These cell lines are classified by cancer subtype by gene clustering and morphology (basal A, B, or luminal), and by status of receptor expression (ER, PR, HER2). Luminal cells appear more differentiated and form tight cell-cell junctions like epithelial cells, while Basal B cells have a mesenchymal appearance, and Basal A cells have intermediate appearances. In general, Basal B cells are more frequently highly invasive in Boyden chamber assays than luminal or Basal A cells. We selected a subset of these cell lines to cover the different subtypes and clinical prognoses (Table 2).

We predicted efficient Ad5 infection of the basal and luminal epithelial-like cells which express CAR, but a much lower level of infection of invasive cells that have undergone epithelial-to-mesenchymal transition (EMT) with decreased CAR expression. As predicted, basal MDA MB 468 and luminal MDA MB 415 were transduced with high efficiency, and infection was not enhanced with rapamycin-induced targeting (Fig. 12). The cell lines that were characterized to have undergone EMT were poorly transduced by non-targeted AdSyn-CO205, and as predicted they all were more efficiently infected by rap-targeted virus.

Table 2. Breast cancer cell lines used in this study. Table adapted from Neve *et al*. 2006 (92).

Cell line	**Gene Cluster**	**ER**	**PR**	**HER2**	**Tumor Type**
MDA MB 468	Basal A	-	-	normal	Acantholytic squamous carcinoma
MDA MB 415	Luminal	+	-	normal	Acantholytic squamous carcinoma
MDA MB 453	Luminal	-	-	normal	Acantholytic squamous carcinoma
MDA MB 231	Basal B	-	-	normal	Acantholytic squamous carcinoma
BT549	Basal B	-	-	normal	Invasive ductal carcinoma
HS578T	Basal B	-	-	normal	Invasive ductal carcinoma

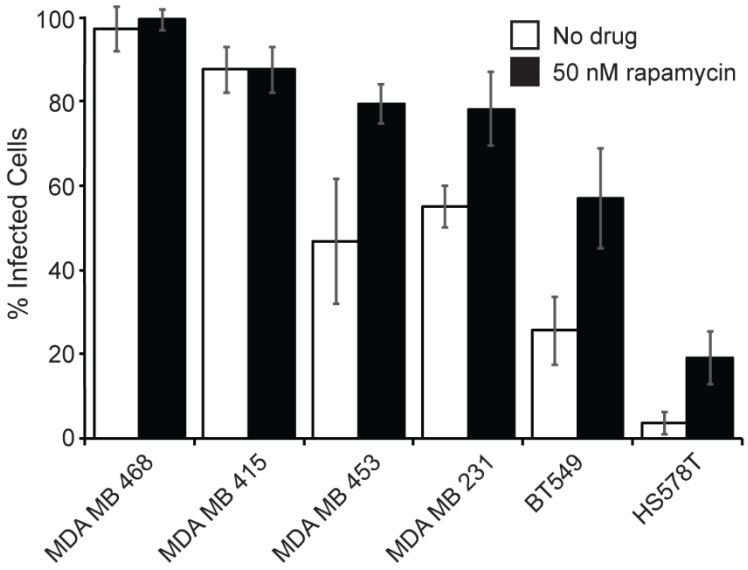

Figure 12. Rapamycin-targeted AdSyn-CO205 infection efficiency of a panel of breast cancer cell lines. Infected cells were fixed and quantified by FACS. Cancer cell lines of epithelial origin (basal, luminal) were generally infected well by non-targeted Ad. The infection of luminal MDA MB 453 was modest with non-targeted Ad, but was substantially improved in the presence of 50 nM rapamycin. The invasive breast cancer cell lines, which have undergone EMT and lost CAR expression, are able to be more effectively infected with the rapamycin induced AdSyn-CO205.

2.11 Engineered adenovirus can be targeted with biologically orthogonal rapalog AP21967

Although rapamycin is a rational combination with oncolytic therapy, there are cases where it may be desirable to avoid the cellular and organismal effects of rapamycin. To further improve the targeted adenovirus tool, we explored the use of a rapamycin structural homolog AP21967. AP21967 is able to form stable heterodimers with FKBP12 and a mutant FRB* domain (mTOR mutation T2098L), but not with the wt FRB domain (94). Below the targeting-concentration of rapamycin (50 nM), phosphorylation of S6K1 is blocked, while higher concentrations of AP21967 (100 nM) does not inhibit mTOR (Fig. 13A). AP21967 does not affect Ad replication, and at the functional concentration of rapamycin (50 nM), there is no effect on virus replication despite the inhibition of mTOR (Fig. 13B). The mutation of FRB in the adenovirus (AdSyn-CO220) results in the ability to induce targeting with either rapamycin or AP21967 (Fig. 13C). The effect of EGFR-targeting with AP21967 is dose-responsive (Fig. 13D), and interestingly does not exhibit a decrease in effectiveness at high concentrations like rapamycin (Fig. 10).

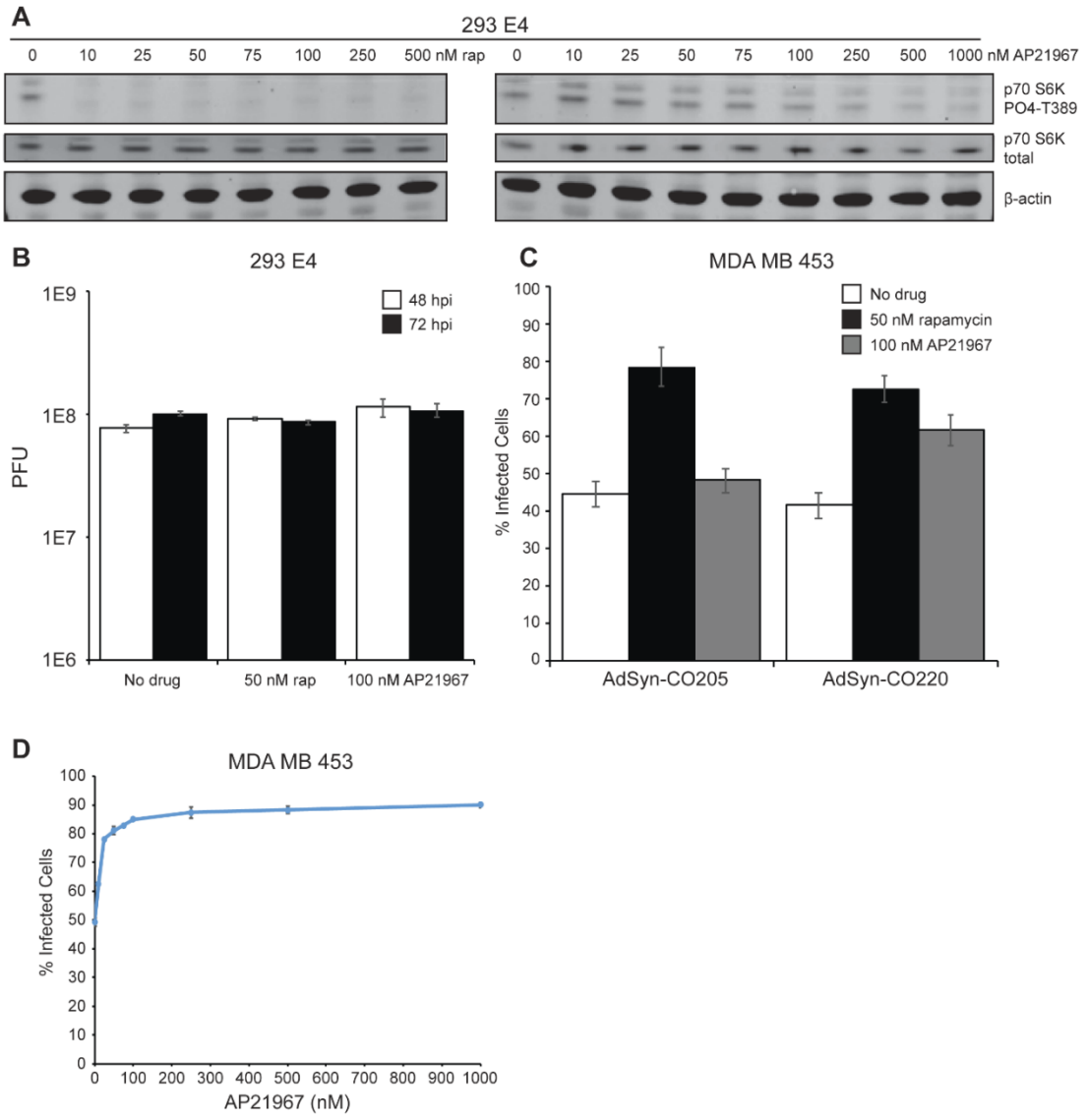

Figure 13. Targeted infection of MDA MB 453 using AP21967 and FRB-mutant fiber adenovirus AdSyn-CO220. A) Immunoblot showing the activity of the kinase mTOR to phosphorylate its target S6K1 under a range of rapamycin and rapalog AP21967 concentrations. B) Quantification of adenovirus replication when grown in the presence of rapamycin or AP21967. C) FACS quantification of MDA MB 453 infection with AdSyn-CO205 and AdSyn-CO220 prepared with either 50 nM rapamycin or 100 nM AP21967. D) Dose-dependent targeting of MDA MB 453 with AP21967-treated AdSyn-CO220.

Chapter acknowledgements

Chapter 2, in part is currently being prepared for submission for the publication of the material. O’Shea, Clodagh; Powers, Colin. The dissertation author was the primary investigator and author of this material.

Chapter 3. Mutation of both E1A and E4orf6/7 is necessary to create a replication-specific oncolytic virus

3.1 Introduction

We currently have no approved therapies that rationally target loss of tumor suppressor functions specifically. The tumor suppressor p53 is inactivated in many human cancers. In Ad infected cells, the Ad E1B-55K targets p53 for proteosomal degradation. Thus, it was proposed that an E1B-55K deleted Ad5 (ONYX-015) would replicate specifically in cancer cells lacking p53. While clinical trials with ONYX-015 demonstrated the safety of oncolytic Ad therapy (95), ONYX-015 was not p53 selective (96). Contrary to expectations, despite the induction of high p53 levels in ONYX-015 infected cells, p53 fails to activate transcription of downstream targets. Hence, its replication in cancer cells is not dependent on loss of p53. Our lab discovered that there is a another Ad protein, E4orf3, that prevents high p53 levels activating transcription of downstream targets by inducing heterochromatin silencing of p53 targets (97), which our lab is now exploiting to develop true p53 selective viral cancer therapies. In addition to developing new p53-selective viruses, it is also of utmost importance to pursue other routes for replication-selectivity.

Adenovirus E1A binds Rb via an LXCXE motif in its conserved region 2 (CR2) domain, deregulating its tumor suppressor activities (35, 36) (Fig. 1). It was proposed that deleting the LXCXE motif in E1A would eliminate Rb inactivation, and make a selectively replicating virus (ONYX-838). However, in our hands, this mutation alone was found to not be sufficient for selective replication. Johnson *et al.* (39) also provide evidence that Ad E1A LXCXE mutation is not sufficient to prevent S-phase entry, viral DNA replication, and late adenovirus protein expression. Even though the Rb-selectivity of the E1A CR2 mutant is controversial, this mutation has been carried forward as the basis for an oncolytic virus (DNX-2401, DNAtrix) that has completed a phase 1 clinical trial and is entering a phase 2 clinical trial for glioma. To address this shortcoming and achieve Rb-selectivity, Johnson *et al.* replaced the promoters for the Ad E1 and E4 regions with E2F promoters, and combined it with the E1A LXCXE deletion to generate a selective virus ONYX-411 (39, 98). However, the homologous E2F sequences precluded use in clinical trials due to the risk of recombination within the virus.

We have identified another Ad protein, E4orf6/7, that also deregulates the Rb pathway to drive cell and adenovirus gene transcription (40, 41). Given that the E1A LXCXE mutant still activates E2F and replicates in primary cells, it was hypothesized that E4orf6/7 activates E2F-dependent cellular targets to drive S phase entry and viral replication, independently from E1A. Therefore to design viruses that selectively replicate in tumor versus normal cells, we engineered adenoviruses with compound mutations in both E1A and E4orf6/7.

The functional mutations for specific oncolytic replication we discovered can be combined with other mutations or new genetic sequences to enhance the infection and potency of a therapeutic oncolytic adenoviruses.

3.2 Generation of adenovirus mutants

To generate the E1A ΔLXCXE mutation, the codons encoding LXCXE were removed from the E1A gene on the wild type E1 module by sequence and ligation-independent cloning (SLIC) to generate a new E1 module bearing the E1A ΔLXCXE mutation.

To generate the ΔE4orf6/7 mutation, the sequence between the stop codon of E4orf6 and the stop codon of the E4orf6/7 second exon was removed from the wild type E4 module by SLIC to generate the E4 module bearing the ΔE4orf6/7 mutation (Fig. 14).

AdSLIC was used to seamlessly combine either wild type or mutant modules to generate complete virus genomes (see Table 1).

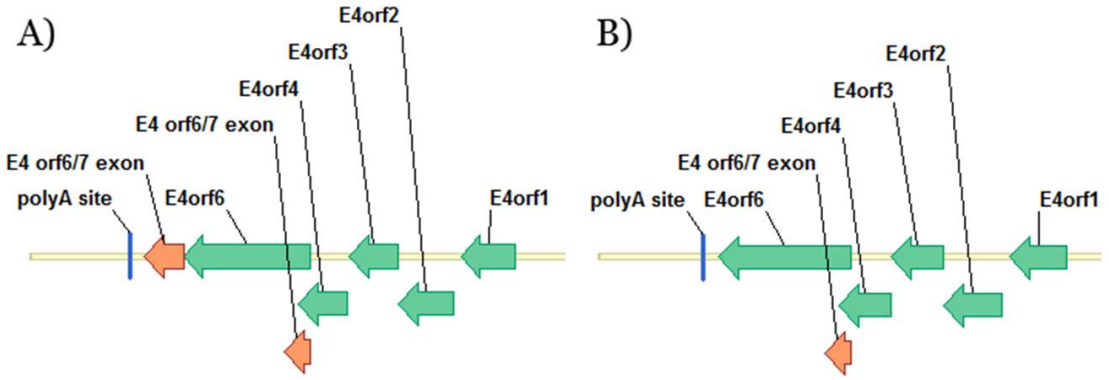

Figure 14. Deletion of E4orf6/7 exon to generate ΔE4orf6/7 mutant Ads. E4 gene expression is controlled by alternative splicing of mRNA from the E4 promoter. Coding sequences are denoted by arrows. A) Ad5 wild type E4 region. B) Ad5 ΔE4orf6/7 region lacking second E4of6/7 exon used in this study.

3.3 E1A ΔLXCXE/ΔE4orf6/7 double mutant AdSyn-CO181 has defective late adenovirus protein expression and fails to induce cyclin A and B expression in small airway epithelial cells

Since Ad E1A has been found to block Rb-tumor suppressor function via LXCXE binding, and E4orf6/7 has been shown to enhance E2F transcription factor activity, we hypothesized that the E1A ΔLXCXE/E4orf6/7 double mutant virus AdSyn-CO181 should be defective in inducing S-phase relative to wild type adenovirus in infected normal cells. Additionally, there should be a defect in Ad late protein expression, which is linked to Ad genome replication, and has a profound effect on production of infectious virus progeny (99). Conversely, in cells lacking functional Rb, we hypothesize that the functions of E1A and E4orf6/7 would not be necessary to lead to S-phase entry and late protein expression. To test these hypotheses we infected quiescent primary human small airway epithelial cells (SAEC, ATCC) and A549 lung adenocarcinoma cells and evaluated S-phase-associated cyclin expression, as well as Ad late protein expression by western blot.

As hypothesized, AdSyn-CO181 showed reduced levels of late protein expression in SAEC infection relative to wild type, and fails to induce accumulation of cyclin A or B (Fig. 15). In mammalian somatic cells, cyclin A is a transcriptional target of E2F and is required for S-phase (100). While viruses bearing either mutation alone (AdSyn-CO189 E1A ΔLXCXE and AdSyn-CO210 ΔE4orf6/7) appear to have lower levels of late protein expression relative to wild type, neither mutation alone appears to be sufficient to prevent cyclin induction.

These data suggest a defect in the ability of AdSyn-CO181 to efficiently induce S-phase due to reduced cyclin expression relative to wild type. The lower levels of Ad late protein expression also suggest a defect in Ad genome replication, which is required for late protein expression.

Even if a virus has reduced replication in normal cells, it should be able to effectively replicate in cancer cells to be a useful and effective oncolytic virus. A549 cells have been characterized to bear a mutation in p16, which causes the deregulation of Rb (Fig. 1). Accordingly, we observed a rescue of cyclin and late protein expression in infected A549, regardless of Ad mutation (Fig. 16). These data suggests that the loss of Rb function in A549 compliments the S-phase induction defect in AdSyn-CO181.

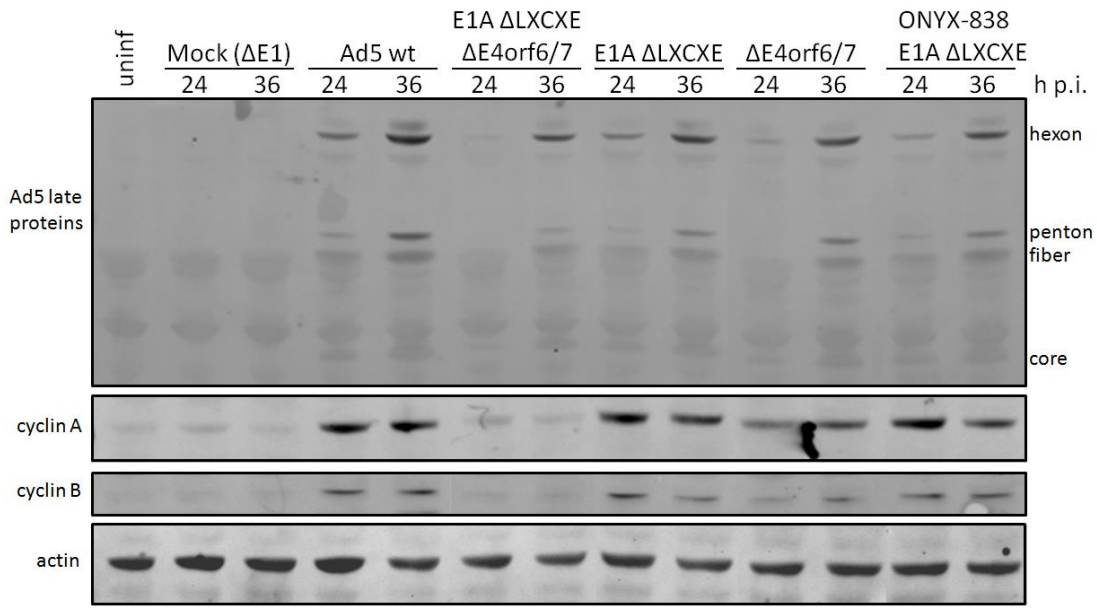

Figure 15: Ad5 E1A ΔLXCXE/ΔE4orf6/7 double mutant AdSyn-CO181 has protein expression defects in SAEC. Quiescent SAEC were infected (MOI 10) with adenoviruses bearing the E1A and E4orf6/7 mutations alone or together. Onyx-838 infection was included to compare with an existing proposed oncolytic adenovirus model. Late protein expression in AdSyn-CO181 infection is delayed and reduced relative to wild type infection. AdSyn-CO181 fails to induce expression of cyclin A and B, markers of S-phase initiation.

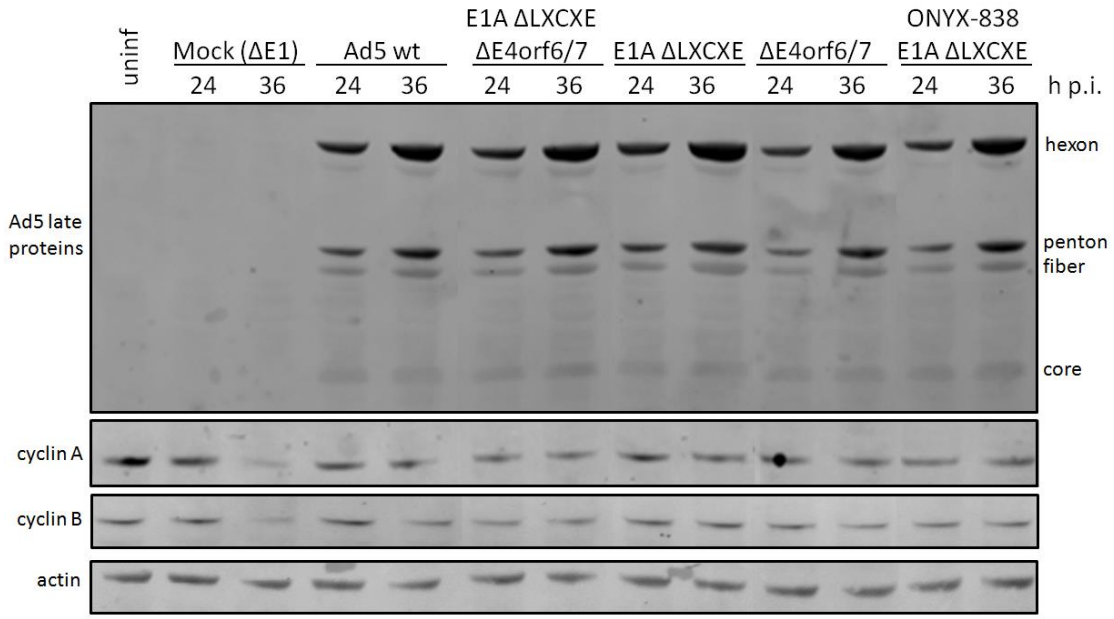

Figure 16: Ad5 E1A ΔLXCXE/ΔE4orf6/7 double mutant AdSyn-CO181 has no protein expression defects in A549 infection. Confluent A549 were infected (MOI 30) with adenoviruses bearing the E1A and E4orf6/7 mutations alone or together. Onyx-838 infection was included to compare with an existing proposed oncolytic adenovirus model. Late protein and cyclin expression in AdSyn-CO181 infection matches wild type infection levels.

3.4 AdSyn-CO181 fails to induce efficient DNA replication in SAEC

Adenovirus requires the cell to enter the S-phase to enable efficient replication of the Ad DNA genome. We hypothesized that there would be a decreased amount of DNA synthesis in AdSyn-CO181 infected SAEC, since it should be defective at initiating S-phase transition via Rb/E2F deregulation. To evaluate DNA replication, we directly quantified the amount of DNA in infected cells 48 hpi by propidium iodide (PI) staining and analyzed by FACS. Indeed, while a wild type (AdSyn-CO102) infection strongly induces DNA replication as evidenced by the dramatic peak shift to the right, AdSyn-CO181 has a dramatically decreased amount of DNA replication with a DNA content profile similar to mock infected SAEC (Fig. 17A). These data show that the cells infected with viruses bearing single mutations show no obvious defect in DNA replication relative to wild type infected cells, suggesting that E1A and E4orf6/7 have some redundant function to enhance DNA replication. Since we saw no defect in cyclin expression in infected A549 by the single mutant Ads, we did not expect to see a DNA replication defect in these infected cells, and accordingly observed a similar increase in DNA content following A549 infection with all of the viruses tested (Fig. 17B).

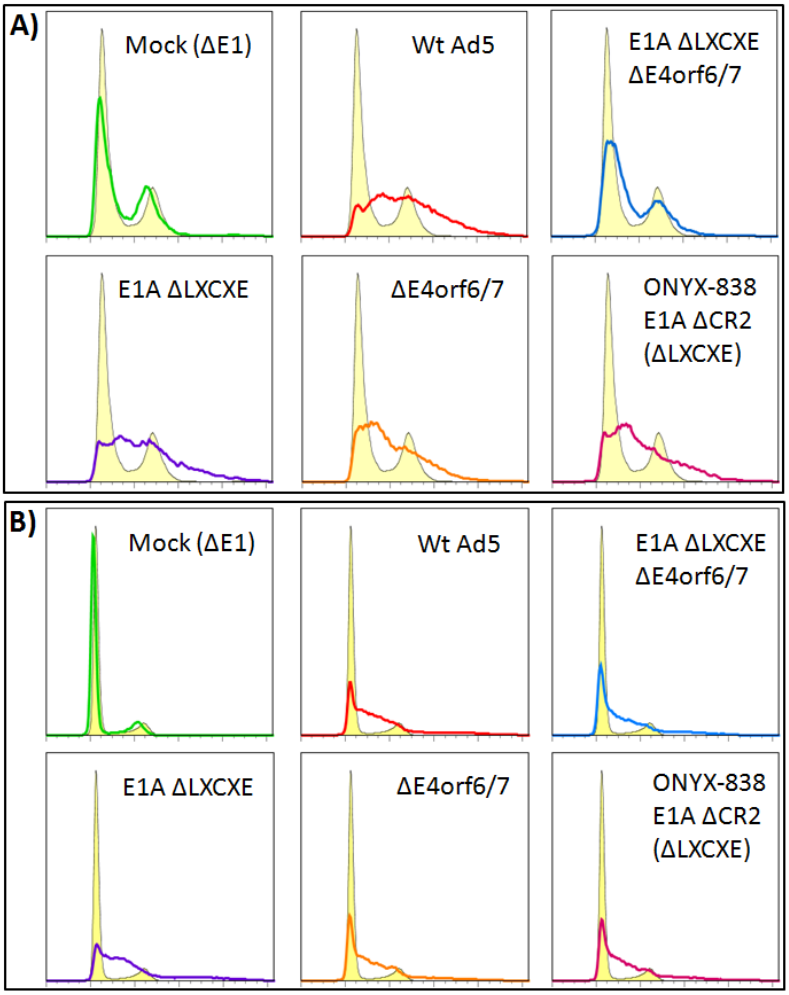

Figure 17. DNA replication quantified 48 h p.i. by PI FACS shows a defect in E1A ΔLXCXE/ΔE4orf6/7 double mutant AdSyn-CO181 infection in SAEC, but not in A549 infection. DNA content of uninfected cells shown in background yellow profile. The Y-axis is the relative abundance of cells, and the X-axis is the PI fluorescence of the cell which is proportional to the amount of nucleic acid. A) Quiescent SAEC-hTERT infected MOI 10. B) Confluent A549 infected MOI 30.

3.5 AdSyn-CO181 has defective replication in SAEC, but replicates to wt Ad5 levels in A549

We expected a decreased number of virus progeny for AdSyn-CO181, due to the observed defects in late protein expression and decreased DNA synthesis. To evaluate replication, we collected and titered virus by ELISA 48 hours following infection. There was a clear defect at with more than a 15-fold defect in AdSyn-CO181 replication relative to wild type (Fig. 18). Notably, there was a similar defect seen with AdSyn-CO210 (ΔE4orf6/7) infection, which exhibited wild type DNA replication levels despite having slightly lower cyclin levels relative to wild type (Fig. 15). Since there was a rescue of late protein expression and DNA synthesis in A549 infected cells, we expected to see similar amounts of virus progeny from mutant virus infections.

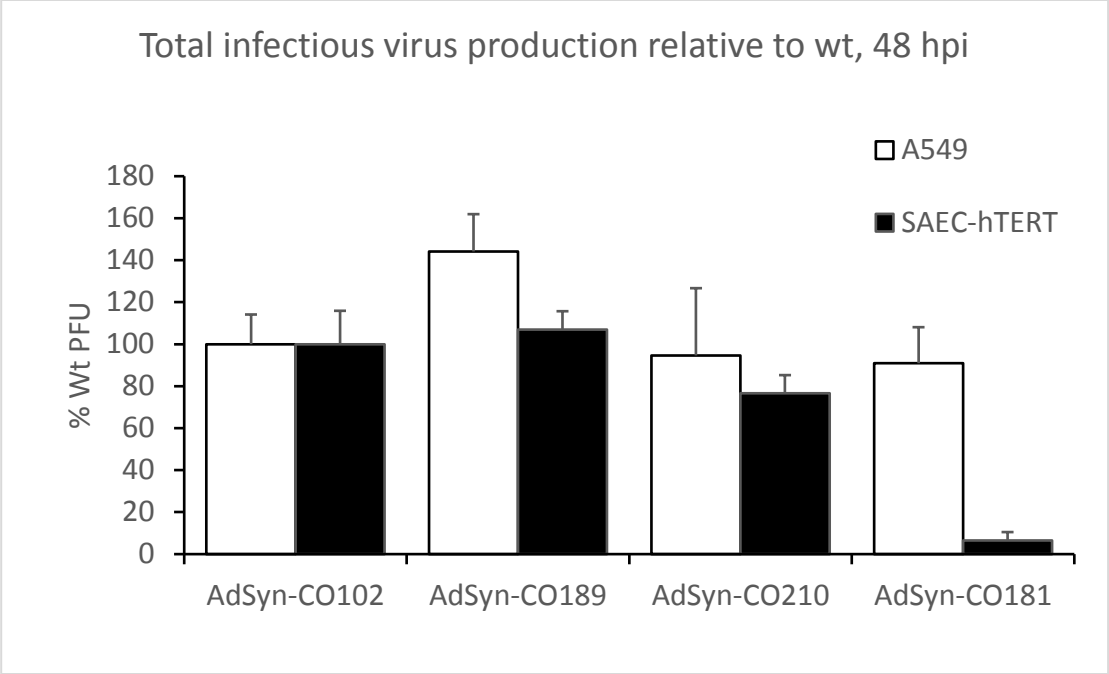

Figure 18. The replication defect of the E1A ΔLXCXE/ΔE4orf6/7 double mutant AdSyn-CO181 infection in normal SAEC-hTERT is rescued in A549 adenocarcinoma cells. Total adenovirus was harvested at 48 hpi and titered by ELISA (see methods). Each total mutant virus quantified was normalized to the amount of wild type virus produced in that respective cell line.

3.6 CDK4/6 inhibitor PD0332991 (PD) strongly inhibits AdSyn-CO181 replication in normal cells

Adenovirus requires the host cell to support the replication of its genome, achieved primarily by Rb inactivation by E1A, and activation of E2F by E4orf6/7 (Fig. 1). To test the dependence of E1A, E4orf6/7 double mutant AdSyn-CO181's dependence on the cell cycle, we used a pharmacological approach to inhibit the cell cycle.

PD0332991 (PD), also known as Palbociclib, trade name Ibrance (Pfizer®) is a drug used to treat ER-positive and HER2-negative breast cancer, and is currently being evaluated as a combination therapy for other indications. PD is a selective inhibitor of CDK4 and CDK6, which phosphorylate and inactivate Rb, and by this mechanism is thought to slow the progression of advanced cancers (101). In agreement with its mechanism of action, it was reported that ovarian cancer cell lines that were Rb-proficient with low p16 expression were the most responsive to PD (102).

It has been shown that CDK4/6 inhibition by PD can be partially relieved by E1A expression, which requires the LXCXE motif of E1A (103). PD has been shown to limit cell killing by *dl922-947*, an E1A ΔCR2 virus, which lacks the LXCXE motif (104). We hypothesized that inhibition of CDK4/6 would limit wild type adenovirus replication in normal cells that are sensitive to PD, would inhibit AdSyn-CO189 (E1A ΔLXCXE) replication, and would block replication of

AdSyn-CO181 with both the Rb-binding mutation E1A ΔLXCXE and the ΔE4orf6/7 mutation.

In low-passage normal small airway epithelial cells immortalized with hTERT (SAEC-hTERT), treatment with PD results in a 50% loss in infectious virus production at 48 hours after wild type (AdSyn-CO102) infection relative to no drug treatment (Fig. 19A). This result agrees with the partial rescue of the CDK4/6 inhibition with E1A seen by Rivadeneira *et al (103)*. Strikingly, the ΔE4orf6/7 mutant AdSyn-CO210 has a 65% reduction in infectious virus production at 48 hpi relative to no CDK inhibition, suggesting that the contribution of E2F activation alone plays its own significant role in adenovirus replication in the context of repressive tumor suppressor Rb. Infectious virus production is even more severely inhibited in PD-treated cells for the E1A ΔLXCXE mutant AdSyn-CO189 which has an 80% reduction in infectious virus production at 48 hpi. Infectious virus production for the double mutant AdSyn-CO181 is reduced 99% when CDK4/6 are inhibited, demonstrating that this virus cannot overcome an active and repressive Rb.

We tested the ability of these viruses to replicate in cancer cells that are insensitive to CDK inhibition, to determine if there was any unanticipated interaction between PD and the virus mutants and to see if the oncolytic mutations of AdSyn-CO181 were compatible with this clinical therapeutic. In the non-small cell cancer (NSCLC) model A549 cells, which lack p16 and express high levels of CDK4 (105), we did not observe a significant inhibition of wild type

or mutant virus replication in the presence of 1 μM PD (Fig. 19B). This demonstrates that the oncolytic AdSyn-CO181 can retain its potency even in the presence of a drug that acts in opposition to its mechanism of selective replication.

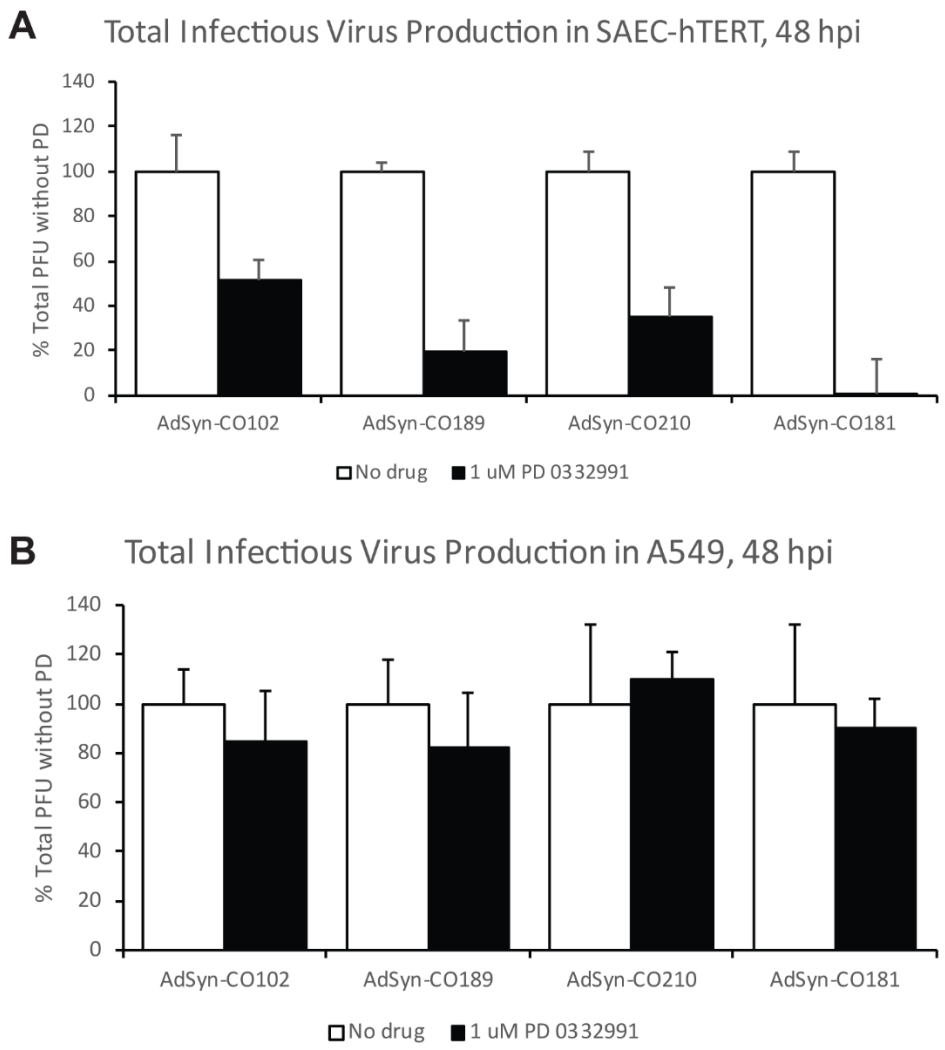

Figure 19. The CDK4/6 inhibitor PD0332991 (PD) potently blocks mutant adenovirus replication. The total plaque forming units (PFU) quantified by ELISA (96) were normalized for each virus to their replication without PD treatment in each cell line. A) In low-passage normal lung cells immortalized with hTERT (SAEC-hTERT), when CDK4/6 is inhibited by PD, Rb blocks E2F activation and the cells cannot enter S-phase. The double mutant AdSyn-CO181 (E1A ΔLXCXE, ΔE4orf6/7) has the greatest loss of viral replication in the presence of PD relative to no treatment when compared to the either of the single mutants AdSyn-CO189 (E1A ΔLXCXE), AdSyn-CO210 (ΔE4orf6/7) or AdSyn-CO102 (wt). B) In A549 lung cancer cells, which express Rb but have aberrantly high expression of CDK4, the tumor suppressor Rb is inactivated by CDK4. PD has no significant effect on the replication of any viruses compared to no drug treatment, since this concentration of PD is not sufficient to restore normal Rb activity.

3.7 RNA-Seq shows AdSyn-CO181 is defective for inducing G1/S cell cycle transition pathway in normal cells

One of the hallmarks of adenovirus infection is the transcriptional control over the cellular program of proliferation (106). A large number of cell cycle genes are induced, including E2F targets, which leads to the induction of the G1/S phase transition. Since we observed a defect with the double mutant AdSyn-CO181 in the induction of E2F targets cyclin A and cyclin B (Fig. 15), and a defect in the induction of DNA synthesis (Fig. 17), we sought to gain a more detailed view in the differences in cellular gene transcription regulation between the Ad mutants and wild type virus infection.

We performed an RNA-Seq experiment in normal small airway epithelial cells (SAEC), collecting total RNA at 12 and 24 hours post-infection. Our data agrees with results from previous studies of adenovirus-infected human foreskin fibroblasts (HFF) (106) and primary lung fibroblasts (IMR-90) (107, 108). Using pathway enrichment analysis, we compared the “cell cycle G1/S phase transition” between SAEC infected with our mutant viruses. This biological process (GO:0044843) contains 259 different gene products, and is defined as "The cell cycle process by which a cell in G1 phase commits to S phase.”

Notably, at 24 hpi AdSyn-CO181 and 335 do not significantly differ from mock infection for the G1/S transition pathway genes (Table 3). However, AdSyn-CO102 (wild type) is significantly enriched for G1/S transition pathway genes relative to AdSyn-CO181, 335, and mock. This data suggests that

AdSyn-CO189 (and AdSyn-CO210) is not selective on the basis of G1/S phase transition, since it is also enriched for this biological process relative to mock and AdSyn-CO181 and AdSyn-CO335. Interestingly, AdSyn-CO335 skirts an edge with AdSyn-CO210, where there is a trend ($P = 0.0545$) of difference in the G1/S transition pathway expression.

Table 3. Adjusted P-values comparing the cell cycle G1/S phase transition (GO:0044843) in infected SAEC at 24 hours post infection by mutant viruses.

24 hpi	vs AdSyn-CO102	vs AdSyn-CO189	vs AdSyn-CO210	vs AdSyn-CO181	vs AdSyn-CO335	vs Mock
Up in AdSyn-CO102		not enriched	not enriched	7.89E-06	4.45E-12	1.12E-06
Up in AdSyn-CO189	not enriched		not enriched	1.44E-05	4.89E-13	7.63E-06
Up in AdSyn-CO210	not enriched	not enriched		0.0031	0.055	2.72E-05
Up in AdSyn-CO181	not enriched	not enriched	not enriched		not enriched	not enriched
Up in AdSyn-CO335	not enriched	not enriched	not enriched	not enriched		not enriched
Up in Mock	not enriched	not enriched	not enriched	not enriched	not enriched	

3.8 Deletion of p16 in normal cells partially rescues double mutant AdSyn-CO181 replication

We hypothesized that in cells that were specifically defective in the regulation of the Rb tumor suppressor pathway, the double mutant AdSyn-CO181 virus would exhibit a rescue in replication. p16 is an important regulator of the Rb tumor suppressor pathway, acting upstream of the CDKs to regulate Rb (Fig. 1). P16 inhibits the activity of CDK4 and CDK6 to regulate the phosphorylation of Rb and consequentially the control of progression into S phase (109, 110). Loss of p16 is frequently an early event in tumor progression (reviewed in (111)). We used CRISPR/Cas9 gene editing technology (112) to target p16 for indel mutation in low passage telomerase-immortalized normal small airway epithelial cells (SAEC-hTERT).

Although $p16^{INK4A}$ shares exons 2 and 3 with a different gene $p14^{ARF}$, we were able to specifically target the p16-specific exon 1 using a pair of guide RNAs and the Cas9 nickase (113) (Fig. 20A). After transfection of CRISPR/Cas9 constructs with guide RNAs directed towards the first exon of $p16^{INK4A}$, the SAEC-hTERT were diluted to single cells to select for clonal populations. Clones were evaluated by sequencing both alleles of p16 to identify indel mutants. One of the clones (#13) exhibited a 5 bp deletion on one allele, and a 32 bp insertion on the other allele. Both of these mutations resulted in a frame shift and early termination of the p16 coding sequence (Fig. 20C) which resulted in undetectable p16 expression in confluent cells (Fig. 20D).

When we quantify the DNA content of confluent ∆p16-SAEC-hTERT, we see a clear increase in DNA content per cell, demonstrating that these cells do not undergo contact inhibition and have misregulated cell cycle control (Fig. 20E). While the DNA content appears to increase in AdSyn-CO181 infected cells over mock infection of ∆p16-SAEC-hTERT, it does not appear to rescue to wild type levels of induction (Fig. 21).

We quantified and compared the amount of productive viral replication in SAEC-hTERT and ∆p16-SAEC-hTERT. Total virus from media and from cells was harvested, and virus production was measured against a known standard Ad5 by infecting the complementing cell line 293E4 which expresses E1 and E4 proteins in trans. The standard was serially diluted to generate a curve to calculate the number of infectious viruses in our samples. Adenovirus infection was quantified 48 hours after infection *in situ* by ELISA using a polyclonal antibody that recognizes adenovirus late proteins.

There was a modest increase (2-3 fold) in replication of wild type and single mutant viruses, but strikingly there was nearly a 15-fold increase in AdSyn-CO181 replication, showing that the misregulation of the Rb tumor suppressor pathway by deletion of p16 specifically overcame the replication defect engineered into oncolytic AdSyn-CO181 (Fig. 22). This partial rescue due to the deletion of p16 alone is consistent with the fact that adenovirus targets this pathway. It is interesting we did not observe a complete rescue like we see in p16-null A549 cancer cell line infection (Fig. 18), suggesting that the

additional accumulated mitogenic mutations that occur during oncogenesis further enhance the proliferative phenotype that supports AdSyn-CO181 replication. Taken together, this data demonstrate that the mechanism of oncolytic replication specificity is due to the overlapping functions of Rb tumor suppressor pathway misregulation by adenovirus genes and cellular cell cycle regulatory genes.

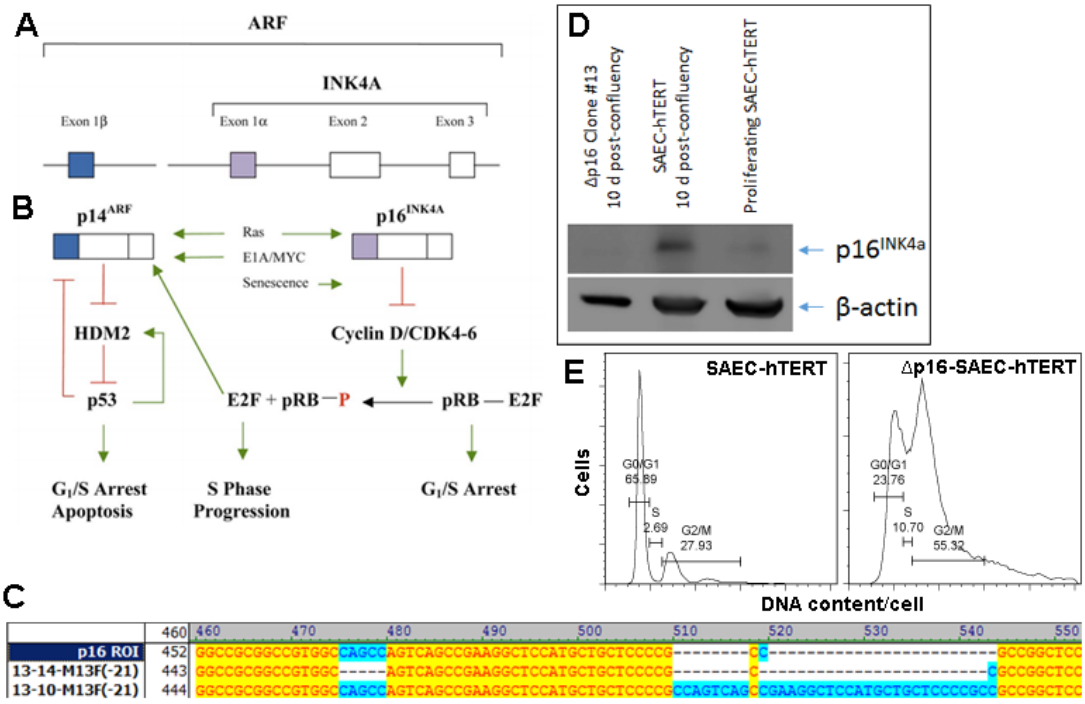

Figure 20. Generation of Δp16-SAEC-hTERT by CRISPR/Cas9. A) Structure of the $p14^{ARF}$/$p16^{INK4A}$ locus. The $p14^{ARF}$ unique exon is shown in blue, the $p16^{INK4A}$ unique exon is shown in purple. B) The tumor-suppressor pathways of $p14^{ARF}$ and $p16^{INK4A}$. Stimulatory pathways are indicated by green arrows, inhibitory pathways are shown in red. Panels A and B adapted from *Rocco and Sidransky 2001 (111)*. C) Wild type sequence of p16 exon 1 region of interest, followed by 5 bp deletion allele and 32 bp insertion allele of Δp16 SAEC-hTERT clone #13. D) Immunoblot for p16 expression (ab81278, Abcam). P16 is detected in quiescent SAEC-hTERT, but is at very low levels in proliferating SAEC-hTERT. P16 is undetectable in Δp16 SAEC-hTERT clone #13. E) Histograms of FACS quantified PI staining for DNA content in cells grown to confluence. The cell cycle is misregulated in Δp16-SAEC-hTERT cells shown by a dramatic increase in the percentage of cells in S, G2, and M phase.

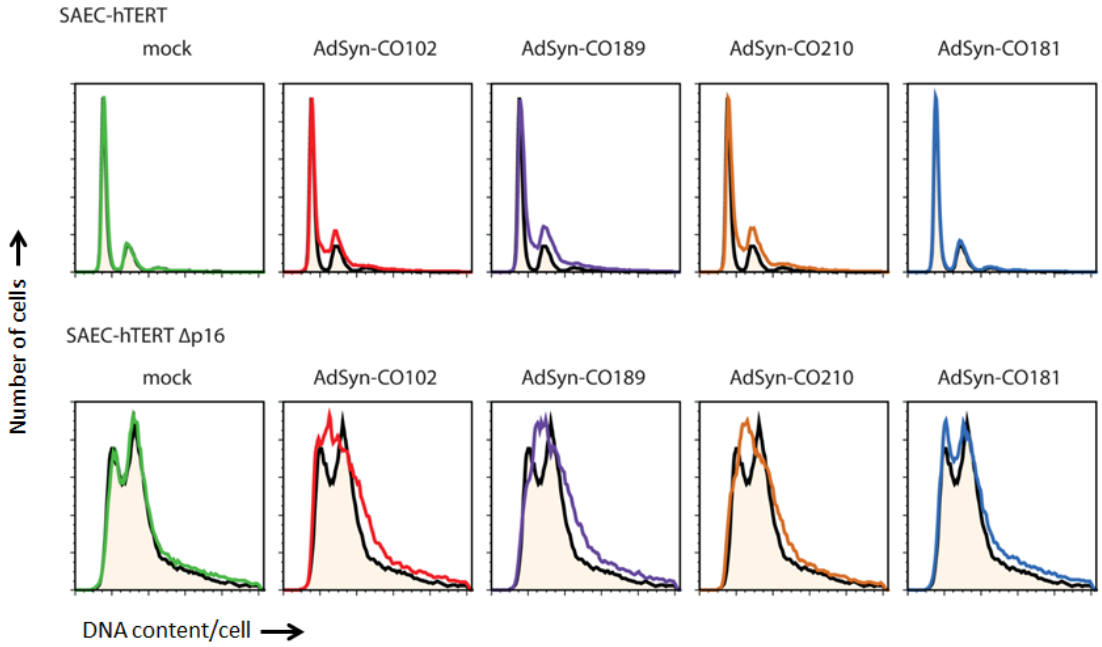

Figure 21. FACS quantification of DNA content per cell by propidium iodide staining of adenovirus-infected SAEC-hTERT or Δp16-SAEC-hTERT. Cells infected with MOI 10 adenovirus, and collected at 48 hpi to quantify DNA. DNA content of infected cells under colored curve overlaid on uninfected cells in yellow. DNA synthesis is induced in SAEC-hTERT infected with wild type (AdSyn-CO102), or single mutant AdSyn-CO189 (E1A ΔLXCXE) or AdSyn-CO210 (ΔE4orf6/7), but is not induced by mock infection or double mutant AdSyn-CO181 infection.

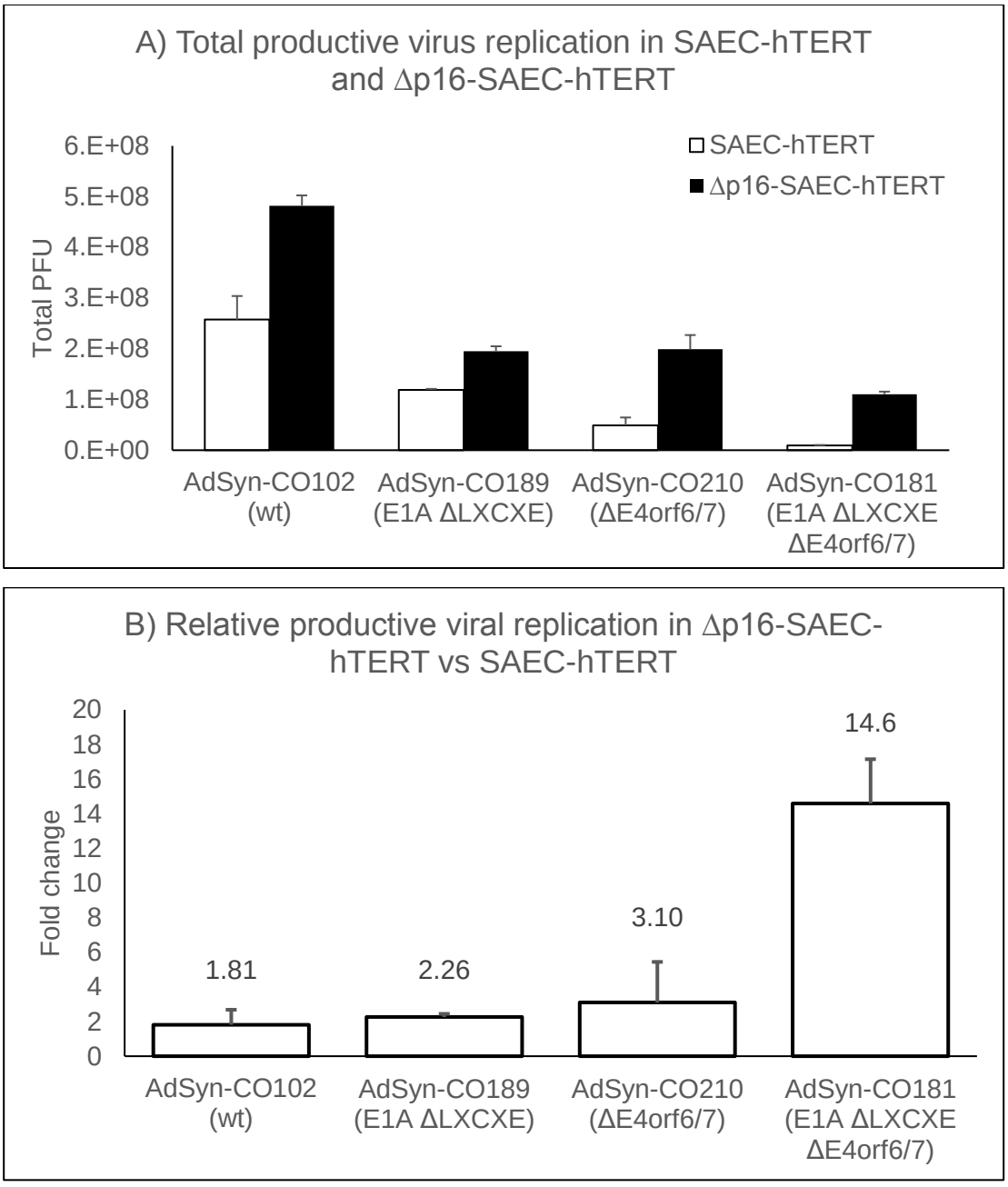

Figure 22. Rescue of AdSyn-CO181 replication by deletion of p16. A) Total productive virus replication from infected SAEC-hTERT and Δp16-SAEC-hTERT, 72 hours post-infection (hpi). B) Productive viral replication of each adenovirus at 72 hpi in infected Δp16-SAEC-hTERT relative to its productive viral replication in infected SAEC-hTERT.

3.9 Further evaluation of E1A and E4 mutations to enhance oncolytic specificity

E1A contains multiple regions that regulate host gene expression. Although the LXCXE domain in the CR2 region of E1A is thought to be the primary interaction site with pocket proteins and Rb, a double mutation of E1A C124G (the C of LXCXE) and Y47H has been shown to abrogate all E1A interaction with Rb (114). Wang *et al.* describes mutations in the N-terminus of E1A that block its interaction with transcriptional activator p300 (114). E1A has also been reported to antagonize the anti-viral cGAS-STRING DNA-sensing pathway through its LXCXE motif (115). Other features and binding-partners of the multi-functional E1A are reviewed in (116).

The E4 region encodes a protein E4orf1 that is thought to induce a metabolic signaling cascade that is representative of one of the hallmarks of cancer (117). E4orf1 contains a PDZ binding motif at its C-terminus through which it upregulates PI3K signaling and prevents negative regulation of cellular proliferation. We have reviewed this pathway as a preview to an article on this subject (118). We hypothesized that abrogating the metabolic stimulation by E4orf1 might yield this additional aspect of cancer cell-specific replication due to the Warburg effect found in many cancer cells.

Our continuing goal is to continue developing increased levels of replication specificity in cancer cells, but also to maintain the tumor-killing potency of adenovirus. To explore this possibility of further increasing the replication specificity of an oncolytic adenovirus, we combined deletion of the

N-terminus of E1A (d2-11) with point mutations, as well as the combination of mutation or deletion of E4orf1 with ∆E4orf6/7 (Table 1).

We infected quiescent and proliferating normal small airway epithelial cells (SAEC), normal human astrocytes (NHA), and a small panel of cancer cell lines and evaluated cell viability to compare the potency and safety of our matrix of virus mutations. In a serial dilution experiment, cell viability was determined 7 days following infection. While all the adenoviruses in this series replicate robustly in the A549 adenocarcinoma cell line, two sub-classes of viruses clearly emerged from the cell viability assay of infected SAEC (Fig. 23). The “lower” group that exhibited more cell killing (or non-oncolytic selectivity) included viruses that either had a wild type E1A or E1A d2-11, or had a wild type E4. The “upper” group that exhibited less cell killing of SAEC included our double mutant AdSyn-CO181, viruses that had E1A Rb-binding mutations and ∆E4orf6/7. Interestingly the one acceptation in the “upper” group was AdSyn-CO244, which had E1A Y47H C124G d2-11 mutations with a wt E4, although it was the least selective of this group.

We visualized the metabolic activity in the panel of cell lines and viruses over three of the initial MOIs (10, 3.33, and 1.11) in a heat map (Fig. 24). All of the viruses in this panel robustly replicated in the A549 adenocarcinoma cell line. The double mutation of E1A ∆LXCXE and ∆E4orf6/7 (AdSyn-CO181) appeared to maintain an ideal balance between cancer-specificity (high metabolic activity in normal cells), while retaining potency (low metabolic activity

in cancer cells). While AdSyn-CO293 had more targeted E1A mutations Y47H C124G compared to AdSyn-CO181 (deletion of LXCXE residues), it exhibited a similar phenotype, so we moved forward with the better characterized AdSyn-CO181. The additional E4orf1 mutations may increase replication selectivity in some cases, such as in highly proliferative tumor tissue environments such as colon cancer, but the general decreased potency we observed in cancer cells will not be desirable as a therapeutic in most cases.

We have published the use of these mutations as compositions of oncolytic adenoviruses in a US patent entitled, “Oncolytic adenovirus compositions,” PCT/US2014/029587.

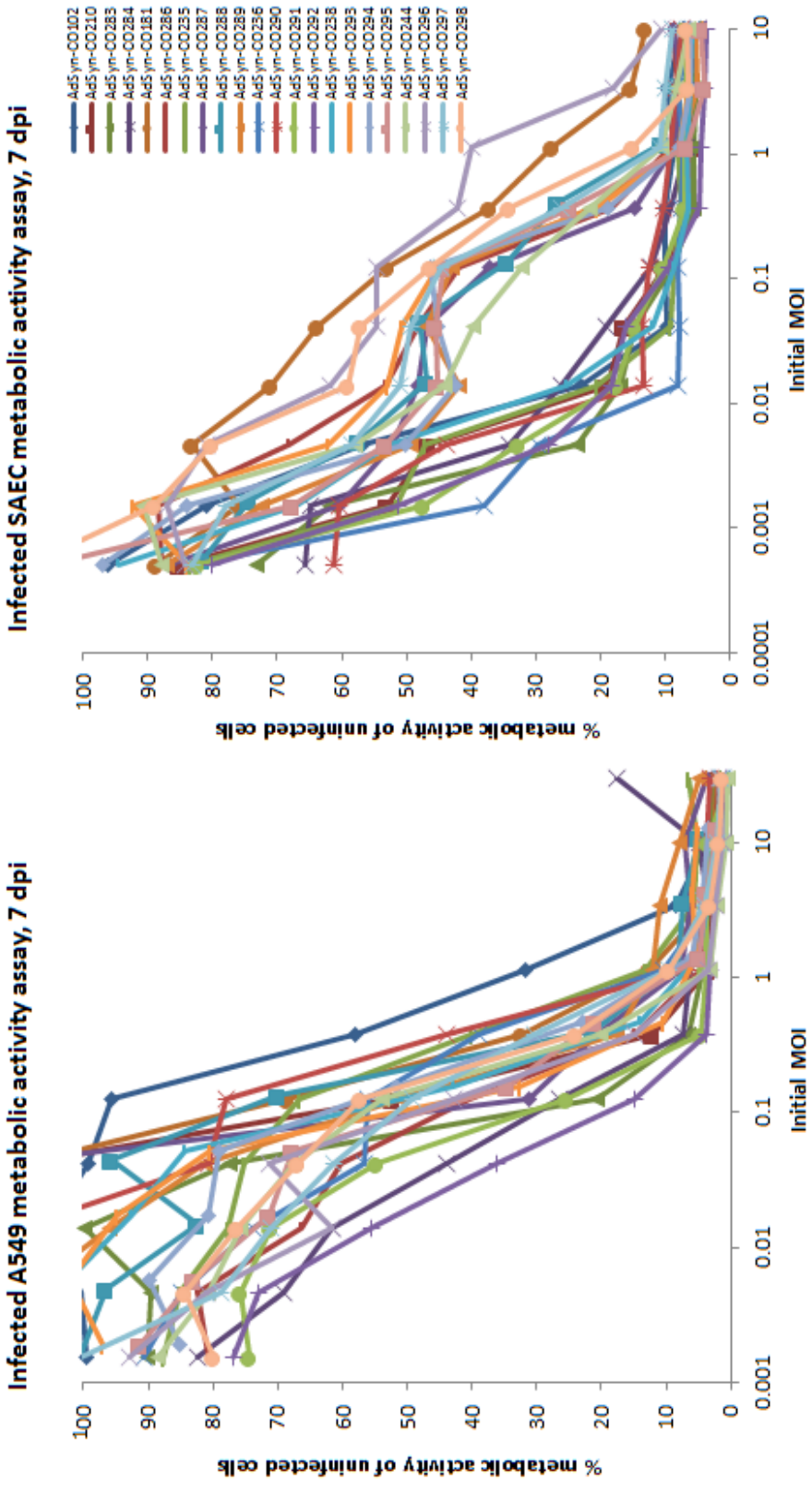

Figure 23. WST-1 metabolic activity assay on infected A549 adenocarcinoma or normal SAEC with panel of oncolytic adenoviruses.

			NHA			Quiescent SAEC-hTERT			Proliferating SAEC-hTERT			A549			MDA MB 231			U87		
E1	E4	Initial MOI	10	3.33	1.11	10	3.33	1.11	10	3.33	1.11	10	3.33	1.11	10	3.33	1.11	10	3.33	1.11
wt	wt	AdSyn-CO102	27	31	40	8	14	20	4	6	6	3	3	5	6	8	24	34	23	31
wt	dE4orf6/7	AdSyn-CO210	19	25	32	11	30	50	22	37	59	3	3	4	5	7	30	18	11	16
wt	E4orf1 dPDZb, dE4orf6/7	AdSyn-CO283	11	17	32	7	19	37	21	47	67	1	1	1	1	4	46	10	14	29
wt	dE4orf1, dE4orf6/7	AdSyn-CO284	14	18	29	57	84	82	13	15	24	0	1	1	1	5	34	16	8	33
E1A d2-11	wt	AdSyn-CO236	5	6	32	15	29	59	9	30	50	1	1	1	2	8	26	35	36	69
E1A d2-11	dE4orf6/7	AdSyn-CO290	5	21	32	23	49	78	9	10	22	3	3	6	13	27	59	9	11	21
E1A d2-11	E4orf1 dPDZb, dE4orf6/7	AdSyn-CO291	5	7	21	4	22	36	9	31	54	3	2	2	2	4	9	49	28	43
E1A d2-11	dE4orf1, dE4orf6/7	AdSyn-CO292	8	10	24	3	22	36	6	16	44	0	0	1	7	20	34	30	34	47
E1A dLXCXE	wt	AdSyn-CO189	28	32	40	17	46	74	41	65	80	3	3	5	3	8	17	23	37	27
E1A dLXCXE	dE4orf6/7	AdSyn-CO181	39	46	50	78	93	90	98	103	106	3	3	3	20	27	53	32	31	28
E1A dLXCXE	E4orf1 dPDZb, dE4orf6/7	AdSyn-CO285	27	35	46	31	65	81	72	116	106	1	2	3	17	22	38	16	22	57
E1A dLXCXE	dE4orf1, dE4orf6/7	AdSyn-CO286	25	36	56	40	70	81	92	108	107	1	1	2	11	21	44	14	18	45
E1A C124G	wt	AdSyn-CO235	14	21	40	16	39	65	26	60	70	1	1	2	15	28	52	29	39	64
E1A C124G	dE4orf6/7	AdSyn-CO287	26	36	51	38	69	78	76	90	95	1	2	5	16	44	75	16	36	51
E1A C124G	E4orf1 dPDZb, dE4orf6/7	AdSyn-CO288	28	32	33	37	70	83	58	96	102	1	1	2	9	16	49	34	36	52
E1A C124G	dE4orf1, dE4orf6/7	AdSyn-CO289	33	36	49	55	85	95	69	90	105	0	0	1	1	10	38	29	10	25
E1A Y47H, C124G	wt	AdSyn-CO238	5	11	33	15	54	84	46	82	103	1	2	2	2	2	11	30	19	40
E1A Y47H, C124G	dE4orf6/7	AdSyn-CO293	29	36	43	55	84	100	47	61	73	1	1	2	2	4	16	26	13	38
E1A Y47H, C124G	E4orf1 dPDZb, dE4orf6/7	AdSyn-CO294	31	29	34	74	95	98	62	96	98	1	1	2	14	22	50	37	32	44
E1A Y47H, C124G	dE4orf1, dE4orf6/7	AdSyn-CO295	34	37	38	59	89	96	107	103	95	1	1	2	14	28	44	30	14	54
E1A Y47H, C124G, d2-11	wt	AdSyn-CO244	23	38	48	39	81	95	39	61	78	1	1	1	3	10	30	17	21	43
E1A Y47H, C124G, d2-11	dE4orf6/7	AdSyn-CO296	37	53	57	67	92	93	64	76	85	2	1	3	14	27	42	19	11	54
E1A Y47H, C124G, d2-11	E4orf1 dPDZb, dE4orf6/7	AdSyn-CO297	37	35	38	46	67	79	66	94	95	2	4	6	21	43	56	8	17	40
E1A Y47H, C124G, d2-11	dE4orf1, dE4orf6/7	AdSyn-CO298	39	43	49	50	75	88	96	94	101	3	4	6	45	43	48	7	14	53

Figure 24. Heat map of metabolic activity of oncolytic adenovirus-infected cell panel. A panel of oncolytic adenoviruses were tested against normal human astrocytes (NHA), normal small airway epithelial cells (SAEC) and cancer cell lines A549 (lung), MDA MB 231 (TNBC), and U87 (glioma). The metabolic activity of cells after 7 days of virus infection is shown for 3 initial multiplicities of

Chapter acknowledgements

Chapter 3, in part is currently being prepared for submission for the publication of the material. O’Shea, Clodagh; Powers, Colin. The dissertation author was the primary investigator and author of this material.

Chapter 4. Therapeutic application of an oncolytic adenovirus with inducible expanded tropism to infect triple negative breast cancer xenografted cells via EGFR

4.1 Oncolytic AdSyn-CO312 has enhanced breast cancer cell killing when targeted to EGFR

To evaluate the efficacy of retained EGFR-targeting to kill cancer cells with replicating adenovirus, we selected HS578T cells as a model. In our panel of breast cancer cell lines, they are the most poorly infected with wild type adenovirus, but we are able to infect via EGFR when we prepare AdSyn-CO205 with rapamycin. We constructed an EGFR-targeted oncolytic adenovirus (AdSyn-CO312), which bears the EGFRVHH-FKBP gene and FRB*-fiber in combination with a deletion of the LXCXE motif from E1A and deletion of E4orf6/7 described in the previous chapter with AdSyn-CO181. We performed a metabolic activity assay using WST-1 to quantify cell viability after 9 days of infection of HS578T with AdSyn-CO312 at different initial multiplicity of infections (MOI). The metabolic activities were normalized to uninfected cells receiving the same concentration of rapamycin or solvent. When AdSyn-CO312 is grown in the presence of targeting rapamycin or AP21967, it able to kill more cells than in untargeted drug conditions (Fig. 25). This suggests that the increase in cell killing is due to the expanded tropism of AdSyn-CO312 to be able to infect HS578T via EGFR.

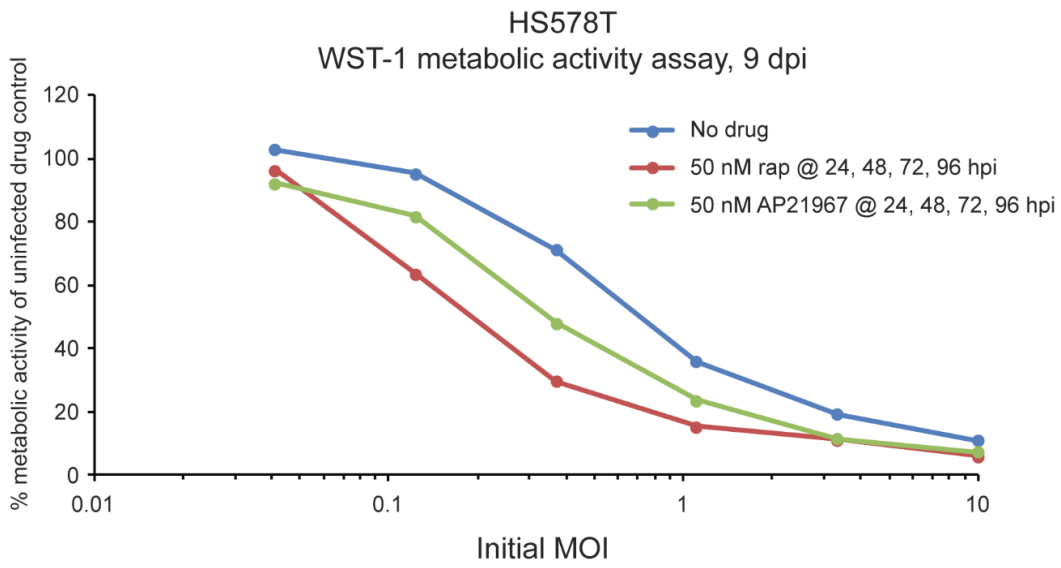

Figure 25. Cell viability of infected HS578T metastatic breast cancer cells after 9 days of infection with AdSyn-CO312. Cells were infected with a range of AdSyn-CO312 MOI. At 24, 48, 72 and 96 hours after infection, fresh rapamycin or AP21967 was added to 50 nM. The metabolic activity was quantified by WST-1 assay, and was normalized to uninfected cells with a matching drug treatment. AdSyn-CO312 bears the oncolytic mutations of E1A ΔLXCXE, ΔE4orf6/7, ΔE3-RIDα/β, ΔE3-14.7k, and expresses the rapamycin- or AP21967-dependent EGFR-targeting genes EGFRVHH-FKBP and FRB*-fiber. There is enhanced killing of cells infected with the EGFR-targeted oncolytic virus that receive either rapamycin or AP21967 versus without the targeting molecule.

4.2 Rapamycin-induced EGFR-targeting of AdSyn-CO335 increases efficacy of oncolytic therapy of HS578T xenografts in mice

To test the efficacy of the targeted delivery of adenovirus progeny via EGFR to treat tumors *in vivo*, we treated subcutaneous HS578T xenografts established on both flanks of nu/nu mice (Fig. 26). When tumors reached 264 ± 16 mm^3 (mean ± SEM), mice were randomized into treatment groups with similar mean-sized tumors. Mice received intratumoral injections of mock (vehicle only), AdSyn-CO335, or AdSyn-CO442. AdSyn-CO335 is an oncolytic virus bearing the features of AdSyn-CO312, and an additional mutation in capsid protein hexon, which eliminates accumulation of adenovirus in the liver (119). AdSyn-CO442 is a control virus which bears the features of AdSyn-CO335, but does not express EGFRVHH-FKBP. Rapamycin (rap) was co-administered every other day during the course of therapy to enable EGFR-targeting of virus progeny.

With mock treatment (n = 8 tumors) and no rap, tumors grew unchecked, with a mean tumor volume of 1300 ± 448 mm^3 at 28 days after the start of mock treatment, after which mice were sacrificed due to large tumor dimensions in agreement with our protocol approved by the Salk Institutional Animal Care and Use Committee. For comparison, data described below are from this time point in the therapy.

We first tested a dose of 8 mg/kg rap every other day in combination with adenovirus administration, but found that the high rap concentration masked the

effect of the virus infection. The 8 mg/kg rap administration alone (no virus infection) was sufficient to slow the tumor growth compared to no treatment ($P = 4.50 \times 10^{-2}$), resulting in a mean tumor volume of 229 ± 49 mm^3. Administration of 2 mg/kg rap alone (n = 8) was not sufficient to block the growth of the tumors (P=0.144).

Oncolytic AdSyn-CO335 alone (n = 11) did not significantly affect the rate of tumor growth compared to no treatment, resulting in a mean tumor volume of 948 ± 207 mm^3. This is likely due to the limitation of HS578T infection by untargeted AdSyn-CO335 progeny. When both AdSyn-CO335 and 2 mg/kg rapamycin were co-administered (n = 11), there was a dramatic and significant reduction in tumor volume when compared to virus alone ($P = 8.54 \times 10^{-4}$) or 2 mg/kg rapamycin ($P = 1.49 \times 10^{-2}$) treatment alone, resulting in a reduced mean tumor volume of 133 ± 22 mm^3. Our data suggests this reduction in tumor volume is dependent on the rapamycin-induced EGFR-targeting of virus progeny, since treatment with 2 mg/kg rapamycin and the control virus AdSyn-CO442 (n = 9) resulted in a mean tumor volume of 401 ± 89 mm^3 which did not bear significant (P = 0.449) difference in mean tumor volume compared to 2 mg/kg rapamycin treatment alone, and resulted in significantly ($P = 4.92 \times 10^{-3}$) larger tumors than the co-administration of 2 mg/kg rapamycin and AdSyn-CO335.

Significant differences between the 2 mg/kg rapamycin treatment and co-administration of 2 mg/kg rapamycin and AdSyn-CO335 were measured as

early as 14 days after the start of treatment ($P = 2.25 \times 10^{-2}$). At this time point, the rapamycin-treated tumors infected with AdSyn-CO442 were measurably outgrowing the AdSyn-CO335-infected tumors ($P = 1.54 \times 10^{-2}$).

Notably, most of the tumors in the groups that received AdSyn-CO335 and rapamycin had a hollow, fluid filled core rather than solid tissue mass.

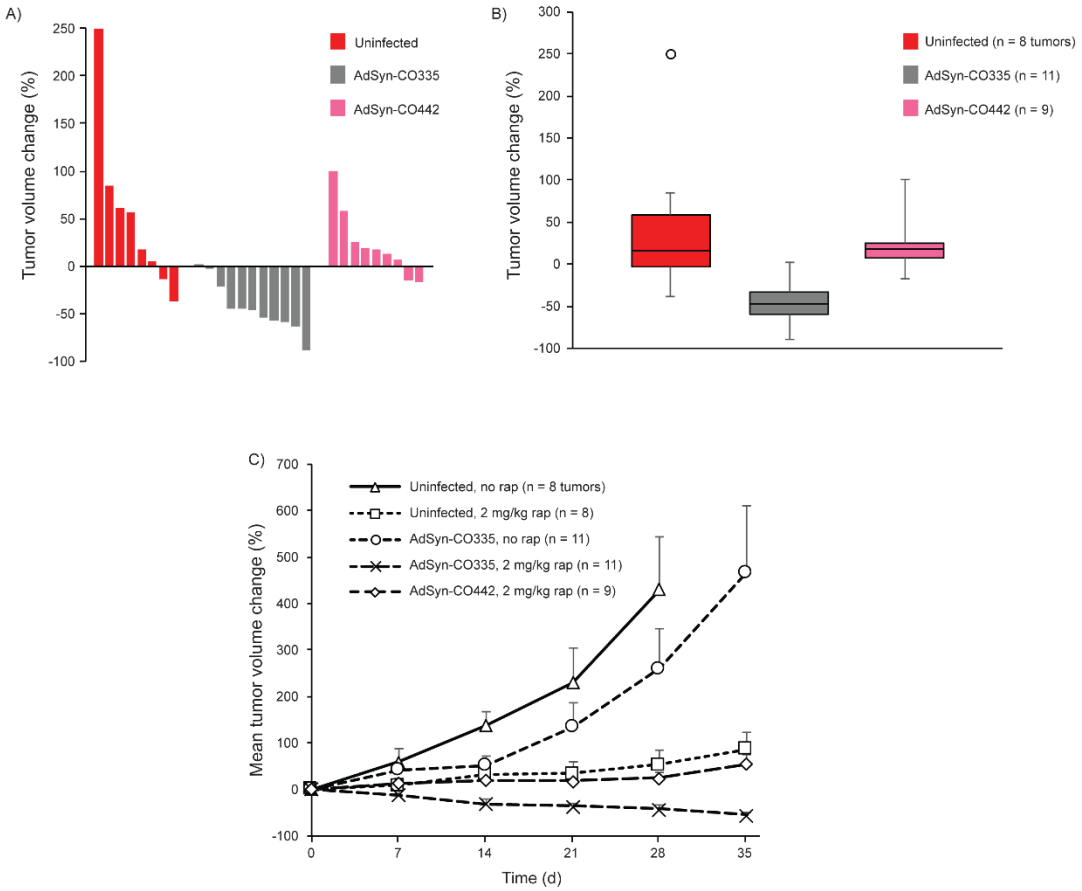

Figure 26. Rapamycin-induced EGFR-targeting of AdSyn-CO335 is more efficacious than rapamycin alone or with untargeted oncolytic adenovirus in HS578T xenograft therapy. A) Waterfall plot showing tumor response after injection of oncolytic adenovirus with 3 weeks of co-administration of rapamycin treatment at 2 mg/kg every other day. Each column represents one individual tumor, with data expressed relative to the pre-treatment tumor volume. B) Box plot showing tumor response after injection of oncolytic adenovirus with 3 weeks of co-administration of rapamycin treatment at 2 mg/kg every other day. Lines depict median response, open circles represent outliers. C) Mean tumor volume change for HS578T xenograft treatment groups. Mice with established tumors received three intratumoral injections every 4 days or vehicle, AdSyn-CO335, or AdSyn-CO442. They subsequently received vehicle or 2 mg/kg rapamycin treatment on each of the days following virus infection, then on every other following day after the final virus injection. Error bars represent standard error of the mean.

4.3 Immunohistochemistry analysis on xenograft tissue sections

4.3.1 Extensive fibrosis revealed by Gomori staining

Upon virus infection, we see large amounts of fibrosis as the tumors are regressing. In damaged tissues, macrophages recruit fibroblasts as “scar tissue” to support a failing structure (reviewed in (120)). This activity of macrophages is not blocked even at high dosages of rapamycin (8 mg/kg) (Fig. 27). Where the rate of cell death exceeded the ability of fibroblasts to infiltrate the tumors, we frequently discovered fluid-filled compartments in the tumors upon resection. At a virus-targeting dose of rapamycin, we don’t anticipate that the drug would compromise immunogenic activity in the tumor microenvironment.

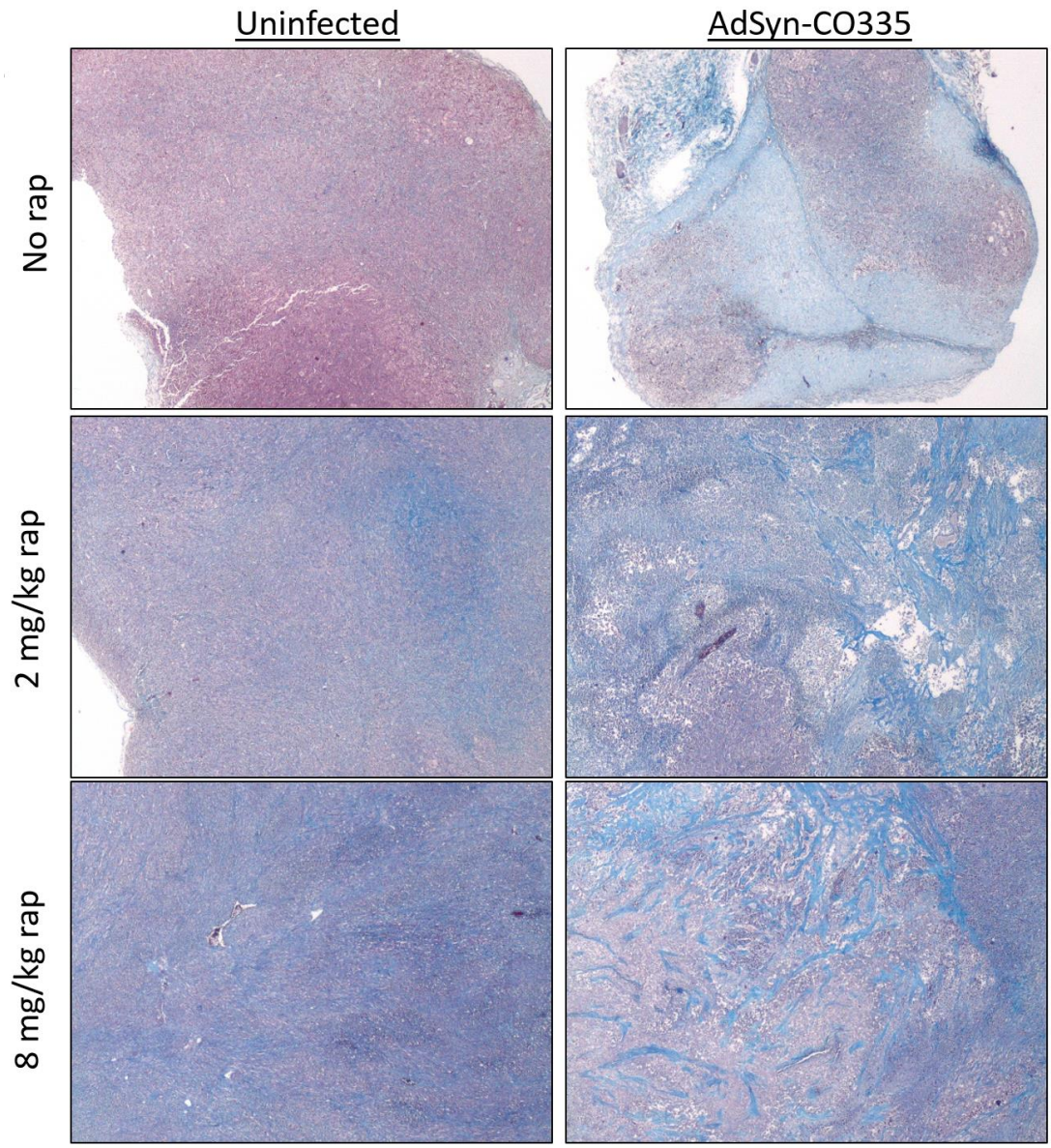

Figure 27: Co-administration of AdSyn-CO335 with rapamycin leads to large fibrotic scars in tumor tissue. Subcutaneous HS578T xenograft tumors in nude mice were treated with intratumoral injection of either vehicle or AdSyn-CO335 on day 1 and 4, and were treated with IP injection of either vehicle, 2, or 8 mg/kg rapamycin on day 2, 5, and 7. Tumors were resected on day 7, 1 h following final rapamycin injection and were fixed in 10% formalin. Fixed tumors were embedded in paraffin wax and sectioned, then stained with Gomori Trichrome. Images shown at 20x magnification. The nuclei of cells are stained in red, while fibrotic tissue is stained in blue. A distinct loss of cohesion and heavy fibrosis is noted in the tumors which were treated with both AdSyn-CO335 and rapamycin.

4.3.2 Non-canonical cell death in addition to apoptosis seen in infected cancer cells

When we stained xenograft tissue sections for cleaved caspase 3, a marker of apoptotic cell death, we saw an increased number of cells staining with AdSyn-CO335 and rapamycin treatment (Fig. 28). Interestingly, we saw a mix of cells undergoing canonical apoptosis, as well as clusters of large, rounded, dying cells that are morphologically representative of cells undergoing viral lysis. We anticipate that both of these forms of cell death are immunogenic, and may have the benefit of stimulating tumor immunogenicity due to the activity of viral lysis.

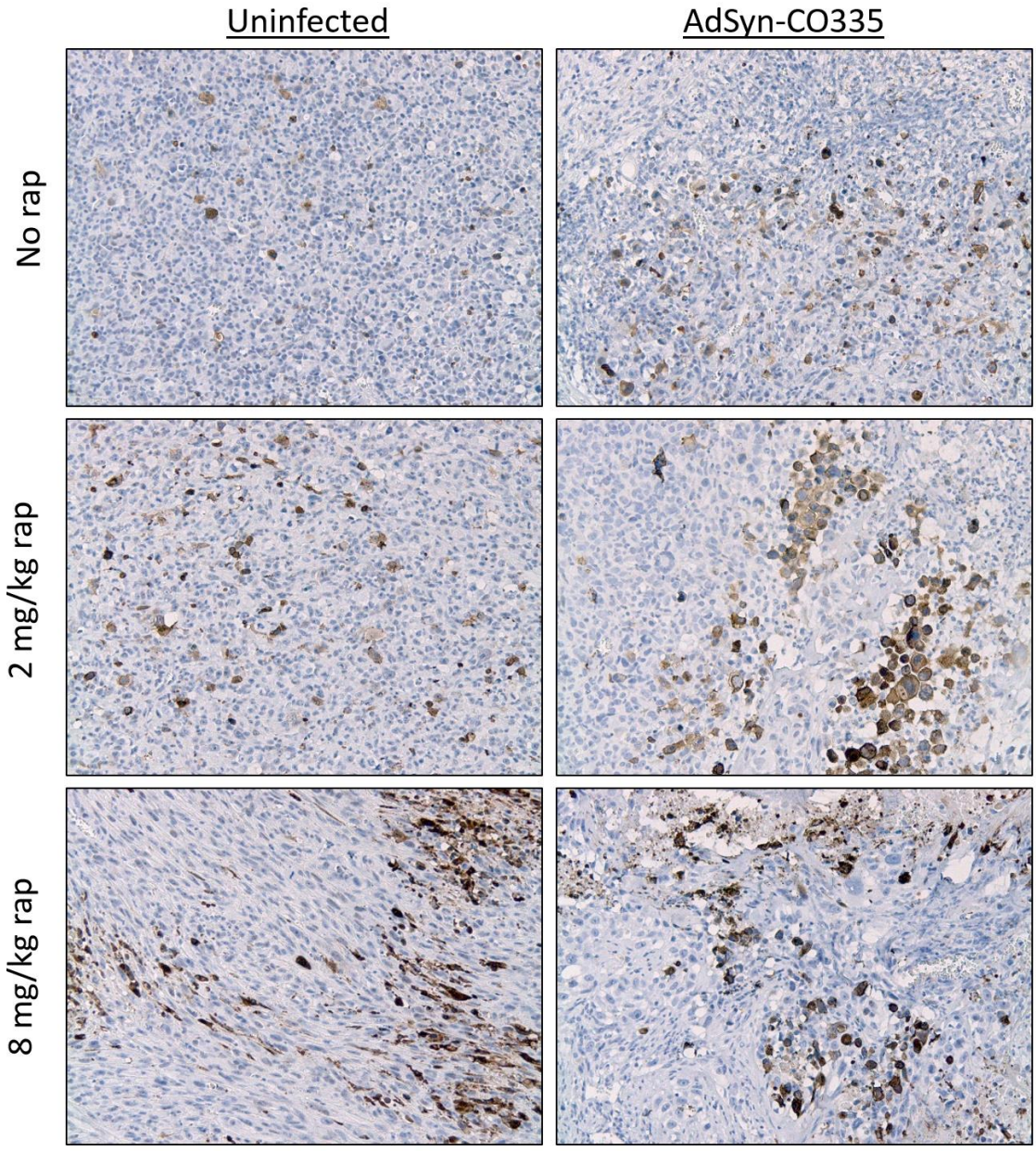

Figure 28: Co-administration of AdSyn-CO335 with rapamycin shows cell clearance beyond canonical apoptosis. Subcutaneous HS578T xenograft tumors in nude mice were treated with intratumoral injection of either vehicle or AdSyn-CO335 on day 1 and 4, and were treated with IP injection of either vehicle, 2, or 8 mg/kg rapamycin on day 2, 5, and 7. Tumors were resected on day 7, 1 h following final rapamycin injection and were fixed in 10% formalin. Fixed tumors were embedded in paraffin wax and sectioned, then stained for cleaved caspase 3. Images shown at 100x magnification.

4.3.3 Effective rapamycin dose does not inhibit S6 phosphorylation

One concern of using rapamycin in a patient are the pleiotropic effects of the drug, including metabolic inhibition via mTOR and its immunosuppressive effects. In cell culture, rapamycin has been shown to potently inhibit mTOR and subsequently its downstream substrate S6K1. We used S6 phosphorylation as a sensitive readout for the activity of rapamycin in xenograft tissue sections. In the low dosage of rapamycin (2 mg/kg) that was able to enhance tumor killing with AdSyn-CO335, the phosphorylation of S6 is not blocked, which suggests that the virus can be targeted without invoking some of the canonical inhibitory effects of rapamycin (Fig. 29).

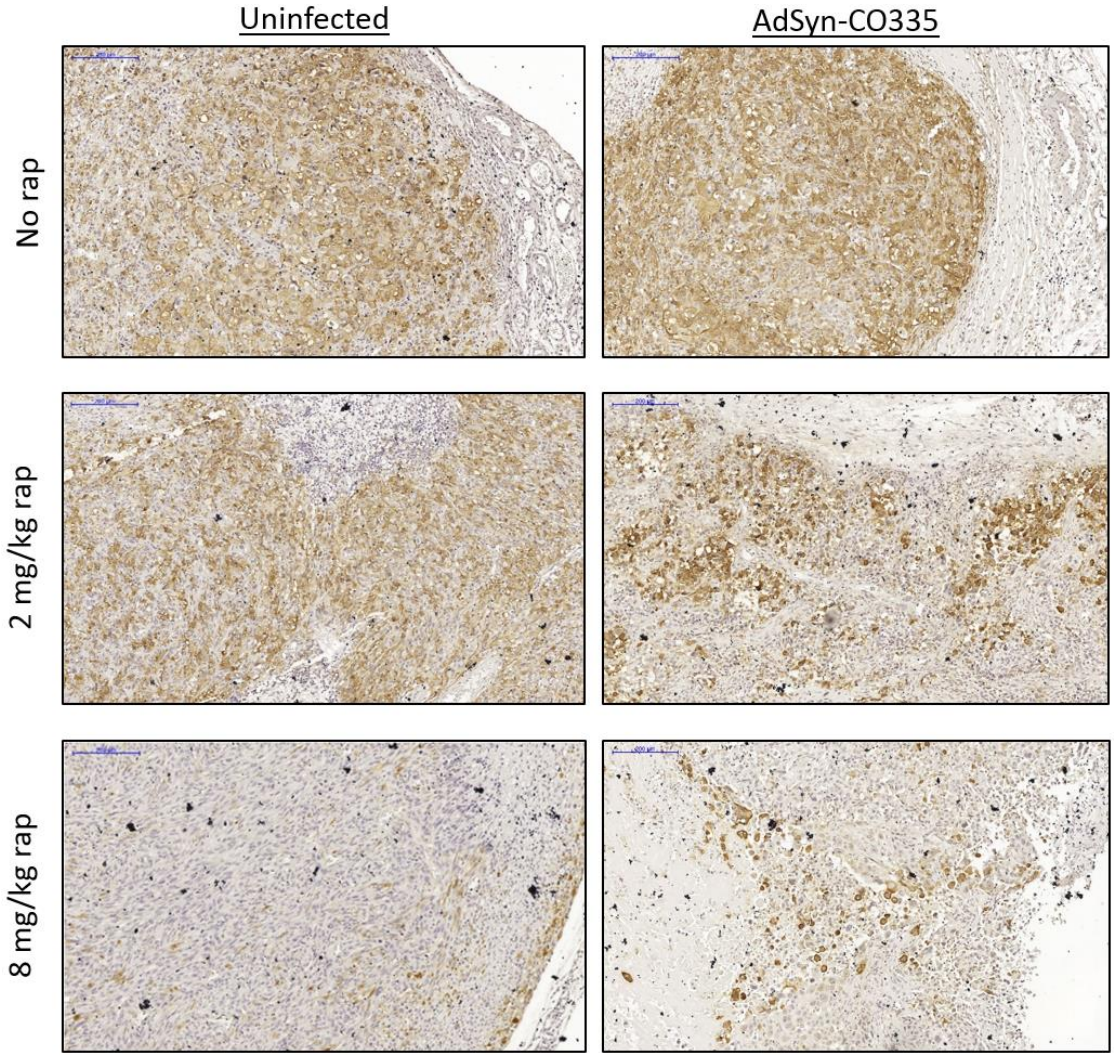

Figure 29. Co-administration of AdSyn-CO335 with rapamycin shows ribosomal S6 phosphorylation is not inhibited by the low, adenovirus targeting dose of rapamycin. Subcutaneous HS578T xenograft tumors in nude mice were treated with intratumoral injection of either vehicle or AdSyn-CO335 on day 1 and 4, and were treated with IP injection of either vehicle, 2, or 8 mg/kg rapamycin on day 2, 5, and 7. Tumors were resected on day 7, 1 h following final rapamycin injection and were fixed in 10% formalin. Fixed tumors were embedded in paraffin wax and sectioned, then stained for phospho-S6. Images shown at 100x magnification.

Chapter acknowledgements

Chapter 4, in part is currently being prepared for submission for the publication of the material. O’Shea, Clodagh; Powers, Colin; Svensson, Rob. The dissertation author was the primary investigator and author of this material.

Chapter 5. Discussion and Future Directions

In an ideal scenario of oncolytic virus therapy for cancer, a patient could receive a systemic injection of a selectively replicating oncolytic virus that could surveil the body for cancer cells. Shortcomings of such an agent are the persistence in the blood, and the ability for the virus to infect the cancer cells, in particular deadly metastatic cancer cells that have undergone epithelial to mesenchymal transition (EMT) and have lost the native virus receptor. Efforts to avoid clearance of oncolytic adenovirus from the blood include capsid swaps to avoid immune recognition, as described in the work by Powers *et al.* and in this work we show application of the liver-detargeting mutation in hexon first described by Alba *et al.* (119). However, as new types of cancer are identified, and as existing tumors develop resistance to current therapies, we must be able to quickly identify and target their weaknesses and lyse them before new resistance pathways arise.

The engineering of specific mutations in the 36 kb adenovirus genome has been challenging until recently (Powers *et al.*), but even with the advent of powerful molecular cloning techniques, adenovirus is a biological machine that can only be manipulated up to a point before beginning to lose its potency. We designed the platform for targeting adenovirus with the goal in mind to preserve the lytic power of this pathogen that has coevolved with humans for millennia to be an efficient cell-killing machine. By adding a chemically-controlled targeting domain on the exterior of the virus particle, we have retained the normal tropism

and structural integrity of the virus particle, and have gained a new guidance system that can target the virus, be it oncolytic or gene delivery vector, to any tissue of choice.

We have demonstrated a proof of principle for a genetically-encoded switch for adenovirus retargeting in cell culture and *in vivo*. If this method is generally applicable, we should be able to target adenovirus to other relevant tumor, vascular, and other cancer-relevant receptors. This potentially enables an unprecedented level of control for targeting adenovirus infection, and should help overcome current limitations in oncolytic adenovirus therapy without compromising patient safety.

Independently of its potential use as an oncolytic virus, adenovirus is a widely used gene delivery vector. Its utility would is greatly enhanced by the ability to target disparate receptors on cells in culture or in animals. A single amino acid mutation in the rapamycin binding site of FRB eliminates its ability to bind rapamycin, but allows it to bind rapamycin-homolog AP12953 and form a heterodimer with FKBP. AP21967 does not inhibit mTOR, so this retargeting molecule would be ideal for retargeting Ad infection in applications where the mTOR pathway is better left unperturbed. We have constructed the virus encoding the FRB mutant inserted into fiber, in combination with the EGFRVHH-FKBP retargeting fusion, and have demonstrated that we can target infection to EGFR with the rapalog AP21967. We anticipate that this platform can be used

to target any other desired receptor target where gene delivery is the primary objective.

In addition, we can target adenovirus tropism independently of genetic incorporation of the targeting molecule, as we demonstrated by the transient transfection of the EGFRVHH-FKBP construct into cells that we infected with AdSyn-CO207. We show that testing of targeting moieties is possible without the cloning of new adenovirus genomes and without the need of further capsid manipulation.

Since the complexity of the targeting domain is independent of adenovirus assembly, the targeting of adenovirus is unlimited in the translated peptide space. For example, in addition to nanobodies, which we employed as a proof of principle in this work, the use of designed akryin repeat proteins (DARPins) have also matured as a method to target adenoviruses. Recently Dreier at al used engineered bispecific trimeric DARPins expressed in E. coli to bridge the adenovirus fiber to targeting HER2, EGFR, and EpCAM (63). We anticipate that like the single-chain antibodies, DARPins could also be ideal FKBP fusion partners for targeting adenovirus infection. We have yet to tap into the great deal of resources available for targeting desirable receptor or cell-surface markers to direct adenovirus tropism.

We have published the strategy of adenovirus targeting using chemically-induced heterodimers in a US patent entitled, “Selective cell targeting using adenovirus and chemical dimers,” PCT/US2013/031002.

The prevalence misregulation of Rb/E2F in almost every human cancer, including breast cancers, has led to this pathway becoming the subject of great therapeutic interest (121). We have identified virus mutations in E1A and E4 that mechanistically converge on this pathway that results in highly selective oncolytic replication, without decreasing the potency of virus replication. We explored further mutations in E1A and E4 mutations that demonstrate that greater selectivity can be achieved, but it may decrease the potency of the oncolytic virus in certain cases. Here we have found a balance where a desired activity has been met without the need for over-engineering adenovirus.

We anticipate that the oncolytic mutations we describe here can serve as the foundation on which we can explore limitless potential modification and arming of the virus to keep it safe and make it a more effective cancer therapeutic. We have published the method of combining these rational mutations for the basis of oncolytic adenoviruses in a US patent entitled, “Oncolytic adenovirus compositions,” PCT/US2014/029587.

We have recently collected a rich RNA-Seq data set to help us more deeply understand the mechanism of the AdSyn-CO181 selectivity. For example, we observed that even in proliferating normal cells (Fig. 24), AdSyn-CO181 replication is blocked. Additionally, we observed that p16 deletion in normal cells partially rescues AdSyn-CO181 replication, consistent with the proposed mechanism of selective oncolytic replication. However, it is known that while phosphorylation of Rb is thought to release E2F (15), during S phase

Rb can be found at E2F target promoters (122), and may play a different role during the normal cell S phase and by the S phase induced by adenovirus infection. Additionally, the recently reported interaction between E1A and the anti-viral cGAS-STRING DNA-sensing pathway through its LXCXE motif (115) may also be another hint as to why the E1A mutation causes such a profound block in oncolytic replication in normal cells. This introduces the intriguing possibility that adenovirus may have evolved this binding motif in E1A as a way to overcome a cellular anti-viral function which resulted in the gain of a secondary function of driving the cell cycle. Using our RNA-Seq data set from normal cells and RNA-Seq data we will generate from infected cancer cells, we hope to more deeply understand how normal cells block replication of AdSyn-CO181 while cancer cells still fully support replication of this oncolytic virus.

Having a better understanding of the mechanism of selectivity of AdSyn-CO181 should also provide rationale for selecting biomarkers that are the most relevant for potent oncolytic replication. For example, during this work we have realized that the E2F-activating function of E4orf6/7 may be phenocopied in a number of cancers by the amplification of TFDP1 and TFDP2, which are not canonically considered to be a part of the cell cycle control pathway. In the cancer genome atlas (TCGA), as examples, we can see that TFDP1 and TFDP2 are upregulated in as much as 3% and 23% in lung squamous cell carcinoma respectively (Fig. 30). The amplifications of TFDP1 and TFDP2 tend to be mutually exclusive with other driving mutations, suggesting that they may be sufficient to drive oncogenesis in some cases. TFDP1 and TFDP2 biomarker

data can inform on when an oncolytic virus like AdSyn-CO181 will be most effective, since the cancer cells have rescued the deletion of E4orf6/7 by a parallel mechanism. Additionally, amplification of these new biomarkers in a patient would also suggest that they would not benefit from a CDK-inhibiting drug like Palbociclib (PD0332991) since it acts upstream of the driving mutation.

This work describes the treatment of a challenging metastatic triple negative breast cancer model HS578T in mouse xenograft tumors, a cell line that is already very poorly infected by wild type adenovirus. We have tested retargeting in this *in vivo* model with the EGFR-targeted oncolytic virus AdSyn-CO335 to show the utility of retargeting in the most relevant context for oncolytic adenovirus therapy. We are currently evaluating relevant toxicology models, exploring the different routes of virus administration, titrating the effective dost of rapamycin, and testing efficacy of AdSyn-CO335 in another metastatic triple negative breast cancer (TNBC) model MDA MB 231. We hope to extend these studies eventually to the clinic to help treat cancers that have not been responsive to available drugs.

In summary, by applying principals of synthetic biology to engineer new functions into viruses, we have demonstrated druggable control of therapeutic oncolytic adenovirus infection with rapamycin or an orthogonal rapalog, designed and constructed enabling platform technology with modular components to design vector targeting to specific receptors, discovered new combination mutations that enhance the replication specificity without

decreasing the potency of an oncolytic adenovirus, specifically targeted a replicating oncolytic virus to cancer cells *in vivo* using nanobodies, and have shown a new approach to treating poor-prognosis triple-negative breast cancer.

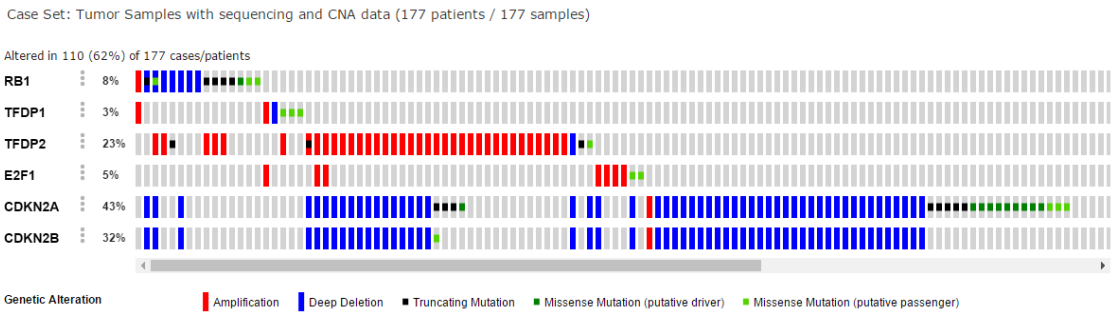

Figure 30. Subset of cell cycle control mutations in lung squamous cell carcinoma in the cancer genome atlas (TCGA) including TFDP1 and TFDP2.

Chapter 6. Experimental Procedures

Cell culture

293 E4 pIX cells (293 E4; Microbix Biosystems Inc.) and human small airway epithelial cells (SAEC; Lonza) were cultured using established methods (97). SAEC were rendered quiescent by growing them to 100% confluency followed by prolonged (8 days) incubation (96). Cancer cell lines MDA MB 231, MDA MB 415, MDA MB 453, and MDA MB 468 were all maintained in DMEM (Cellgro) with 10% FBS (HyClone). BT549 and HS578T cells were maintained in RPMI 1640 (Life Technologies) media with 10% FBS (HyClone).

MDA MB 453 cells were infected with lentivirus, and populations of cells with stable EGFR knockdown were selected with puromycin (2 µg/ml).

Virus growth and purification

Plasmids containing self-excising whole Adenovirus genomes were transfected into 75% confluent 293-E4 cells on 6-well plates using XtremeGene 9 (Roche) according to instructions. 2 µg of DNA and 4 µl of transfection reagent were combined in 100 µl serum free MEM and used to transfect a single well. Plaques were typically visible 5-6 days post transfection, and the cells and supernatant from the well were collected together and snap frozen in dry ice/ethanol. After 3 rounds of quick freeze/thaws, alternating between dry ice/ethanol and 37°C, cell debris was pelleted at 2000 xg for 10 min. Half (typically 1 mL) of the supe was then passaged to a 90% confluent 10 cm dish of 293-E4 cells. Infected cells were typically detached by 48-72 hours post-

infection, and total cells and supernatant collected and snap frozen. After 3 rounds of quick freeze/thaws, cell debris was pelleted at 2000 xg for 10 min and supernatant passaged to 15x 15 cm dishes of 90% confluent 293-E4 cells. Infected cells were typically detached by 48-72 hours post-infection, and total cells and supernatant collected. Cells were pelleted at 300 xg and the supernatant was discarded. The cell pellet was resuspended in 10 mL of TMN buffer (10 mM Tris pH 7.5, 150 mM NaCl, 1 mM $MgCl_2$), frozen/thawed 3x, cell debris pelleted at 2000 xg for 10 min, supernatant removed and spun again at 2500 xg for 10 min, and virus containing supernatant removed. It was then spun twice over layered CsCl gradients. Virus was diluted to 28 mL total by addition of 10 mM Tris pH8 buffer and layered onto a gradient of 10 mL of light CsCl solution (1.2 g/mL density; 22.39 g CsCl + 77.61 mL Tris pH8) underlayed with 10 mL of heavy CsCl solution (1.45 g/mL density; 42.33 g CsCl + 57.77 mL Tris pH8) in an SW32 rotor tube (Beckman). This was spun at 20K rpm for at least 4 h (no more than 16 h) at 4°C. The lowest formed viral band was pulled using an 18 gauge needle, diluted to 4 mL with 10 mM Tris pH8, and layered onto a gradient of 4 mL of light CsCl solution underlayed with 4 mL heavy CsCl solution in an SW41 rotor tube (Beckman). This was spun at 20K rpm for at least 4 h (no more than 16 h) at 4°C. The lowest formed viral band was pulled as before and dialyzed in 3 L of TMN buffer with 10% glycerol for 16-24 h at 4 °C. The virus was then aliquoted and stored at -80 °C.

Virus titration

Ad5 viruses were titered by ELISA as previously described (96). Total virus from media and from cells was harvested, and virus production was measured against a known standard Ad5 by infecting the complementing cell line 293E4 which expresses E1 and E4 proteins in trans. The standard was serially diluted to generate a curve to calculate the number of infectious viruses in our samples. Adenovirus infection was quantified 48 hours after infection *in situ* by ELISA using rabbit polyclonal anti-Adenovirus Type 5 antibody (ab6983, Abcam).

EGFR-specific nanobody (EGFRVHH)

The gene sequence encoding the EGFR-specific nanobody (EGFRVHH) was human codon optimized for expression and synthesized by Blue Heron Biotechnologies based on protein sequences identified by Gainkam et al. (84).

EGFR knockdown with shRNAs

We used the EGFR shRNA B sequence from Engelman *et al.* and cloned it into the pLentiX2 puro backbone with two different hairpin linkers (91). These plasmids were co-transfected with packaging plasmids pRSV.Rev and pMDLg/p-RRE, and envelope plasmid pVSVg into 293T cells using Xtreme Gene 9 transfection reagent. Lentivirus-containing media was collected 48 h post-transfection, and filtered through a sterile 0.45 um filter. Polybrene was added to 8 µg/ml.

Retargeting adenovirus tropism with rapamycin

293E4 cells were seeded on to 6-well plates the day before infection at 1E6 cells/well. The next day cells were counted and infected with MOI 10 virus (typically AdSyn-CO205). 24 hours after infection, media was replaced with growth media containing rapamycin or solvent control. 48 hours after infection, cells and media were collected and frozen at -80 °C. Target cells were seeded on 12-well plates at 1E5 cells/well the day before infection with targeted adenovirus. The next day, frozen aliquots of targeted virus were thawed, and centrifuged at 1000 RPM for 5 minutes to remove cells and cell debris. Media was removed from target cells and replaced with 300 ul fresh growth media. 200 ul of virus-containing supernatant was added to each well and the media was replaced with 1 ml normal growth media after 1 h. 24 h after infection, cells were washed with PBS, and suspended in trypsin. Cells were pelleted by gentle centrifugation at 1000 RPM for 3 minutes, and resuspended in 1% PFA for 5 minutes. Cells were pelleted again and resuspended in 500 uL PBS then quantified for GFP expression by FACS.

CDK4/6 inhibition by PD0332991

A549 (ATCC) lung adenocarcinoma cells were cultured in DMEM (Cellgro) with 10% FBS. SAEC (Lonza) were grown using established methods (97). Cells were grown to confluency in 6-well tissue culture plates. 24 hours before infection, media was replaced containing 1 μM PD 0332991 or with solvent control. A549 wells were each infected with one of the viruses (AdSyn-

CO102, 181, 189, 210) with a multiplicity of infection (MOI) of 10 for total infection. One hour after infection, media was replaced containing 1 μM PD 0332991 or with solvent control. SAEC were infected similarly with an MOI of 30 for total infection. 24 hours after infection, media was replaced with fresh 1 μM PD 0332991 or solvent control. 48 hours after infection, media and cells were harvested from each well, and cells were lysed by flash freezing in liquid nitrogen and stored at – 80° C. Cellular debris was cleared by centrifugation at 1.5K RPM for 5 minutes at 4° C. The plaque forming units (PFU) in the supernatant was titered by ELISA as previously described (96).

Virus infections and transductions

To examine Ad5 virus growth and protein expression, 6-well plates of cells were seeded 24 hrs prior to infection so as to be ~90% confluent. In the case of experiments in SAEC, cells were grown to confluence, and maintained in growth media for 7-10 d to reach senescence before infection. The day of infection, one well of cells was counted and virus diluted to the appropriate MOI in DMEM with 2% FBS. The MOIs of infection for 293-E4 cells, A549, cells were 10, 30 PFU/cell, respectively. Cells were infected in triplicate in a volume of 1mL for 2hrs at 37°C, after which the inoculum was removed, cells washed once in 1mL PBS-/- (no Mg^{2+} or Ca^{2+}), and 2mL of fresh media with 10% serum added. For virus growth, the entire well of cells and supernatant was collected at the indicated time points, frozen/thawed 3 times, debris pelleted at 2000xg for

10min, and supernatant aliquoted and stored at -80°C. Aliquots were thawed and titered via ELISA.

Antibodies and Immunoblotting

Rabbit anti-Adenovirus type 5 (ab6982, Abcam) was used at 1:10000 dilution, mouse anti-β-actin clone AC-15 (Sigma) was used at 1:5000 dilution, rabbit polyclonal anti-EGFR antibody (ab2430, Abcam) was used at a 1:500 dilution, rabbit monoclonal anti-CDKN2A/p16INK4a antibody EP4353Y(3) (ab81278, Abcam) was used at 1:2000 dilution, rabbit polyclonal anti-E2F1 antibody (ab14768, Abcam) was used at 1:1000 dilution, rabbit monoclonal anti-CDK1 antibody [EPR165] (ab133327, Abcam) was used at 1:10000 dilution. Secondary Alexa Fluor conjugated antibodies (Life Technologies) were used at 1:20000 dilution.

To prepare cellular samples for immunoblotting, cells were placed on ice and washed 2x with cold PBS-/-. Cells were then lysed in RIPA buffer (10mM Tris pH7.4, 150mM NaCl, 1mM EDTA, 1% Triton X-100, 1% deoxycholic acid, 1mM NaF, 0.1mM Na_3VO_4, 1mM DTT, 0.1% SDS, and complete mini protease cocktail (Roche)) for 30min on ice. After lysis, cell debris was pelleted at 20,000xg and supernatant removed to a new tube. Protein was quantified with Bio-Rad DC Protein Assay according to manufacturer's instructions and an equal protein amount was run on a Novex 4-20% Tris-Glycine gel (Life Technologies). Proteins were transferred to nitrocellulose, membranes blocked for >1hr in TNT buffer (50mM Tris-Cl pH8, 150mM NaCl, 0.1% Tween-20) with

5% dry milk, probed with primary antibody in TNT buffer with 1% dry milk, washed 1x15min and 4x5min with TNT buffer, probed with secondary antibodies in TNT buffer with 1% dry milk and 0.01% SDS, washed 1x15min and 4x5min with TNT buffer, and imaged using an Odyssey Imager (Li-Cor). To prepare purified viral particles for immunoblot or coomassie, an equal particle number of each virus was diluted in viral lysis buffer to a final concentration of 10mM Tris pH 7.5, 1mM EDTA, and 0.1% SDS. SDS-PAGE loading dye was added and samples run on gels and processed for immunoblot as above.

PCR and self-ligation

Standard PCR conditions were as follows unless otherwise noted: 50µl final volume including 1x Phusion HF Buffer, 200 µM each dNTP, 0.5 µM each primer, 20 ng template, and 1U Phusion High-Fidelity DNA polymerase (NEB). Thermocycler conditions were 98°C for 1min, 35 cycles of 98°C for 10sec, 55°C for 30sec, and 72°C for 20sec/kb, with final extension of 72°C for 5min and hold at 12°C. PCR products were designed to have 22 bp homology for combining with Gibson assembly. Assembled plasmids were transformed into DH10B competent cells, plasmids are screened by restriction digest and sequencing.

Mice and Tumors

HS578T (ATCC-HTB-126; American Type Culture Collection, Manassas, CA) breast cancer cells were cultured as recommended by the supplier. Female 5-week-old athymic mice (J:NU #007850; The Jackson Laboratory, Bar Harbor,

ME) were housed under protocols approved by the Salk Institutional Animal Care and Use Committee. Xenografts were initiated by subcutaneously injecting HS578T cells (5E6 cells suspended in 0.2 ml of BD Matrigel Matrix; BD Biosciences, Bedford, MA) into the left and right flank under anesthesia (Isoflurane).

Two perpendicular tumor diameters (l and w) were measured weekly to follow tumor progression. Tumor volumes were calculated by use of the modified ellipsoid formula where vol = 1/2 ($l * w^2$) (123, 124).

Two months after implantation, 48 mice with 86 tumors with a volume of 270 ± 17 mm^3 (mean ± SEM) were included in the study and randomized into treatment groups with similar mean-sized tumors (n=6 to 8). Not all injections of HS578T successfully established tumors. On days 0, 3, and 6, mice were injected intratumorally with 2E8 PFU of adenovirus diluted in 50 ul PBS. AdSyn-CO335 is an oncolytic adenovirus that expresses a fiber protein with an inserted FRB sequence and expresses FKBP fused to a nanobody which recognizes EGFR (EGFRVHH). AdSyn-CO442 has all the features of AdSyn-CO335, but does not express EGFRVHH. Rapamycin (Lot ASC-127; LC Laboratories, Woburn, MA) diluted in 100 uL 5% Tween 80/5% PEG400 was administered by I.P. injection on days 1, 4, 7, and every other day thereafter at either 2 or 8 mg/kg dosages. Body weight was monitored for toxicity, and tumor sizes were measured while blinded to treatment groups. Mice were sacrificed if tumors were greater than 20 mm in any dimension or showing other signs of significant tumor burden.

Statistical Analysis

Statistical analyses were performed using R Statistical Software 3.2.0 (The R Foundation, Vienna, Austria) with guidance from the NIST/SEMATECH e-Handbook of Statistical Methods (http://www.itl.nist.gov/div898/handbook, 5/28/2015). Outliers were identified using the extreme studentized deviate procedure with 95% confidence interval, assuming normal distribution verified visually by a Q-Q plot. Analysis of variance (ANOVA) was used to test for significant differences between mean tumor volumes of treatment groups at each time point data was collected.

Chapter 7. References

1. Murphree A, Benedict W. Retinoblastoma: clues to human oncogenesis. Science. 1984;223(4640):1028-33. doi: 10.1126/science.6320372.

2. Nevins JR. The Rb/E2F pathway and cancer. Human Molecular Genetics. 2001;10(7):699-703. doi: 10.1093/hmg/10.7.699.

3. Bonelli P, Tuccillo FM, Borrelli A, Schiattarella A, Buonaguro FM. CDK/CCN and CDKI alterations for cancer prognosis and therapeutic predictivity. Biomed Res Int. 2014;2014:361020. Epub 2014/03/08. doi: 10.1155/2014/361020 [doi]. PubMed PMID: 24605326; PubMed Central PMCID: PMC3925518.

4. DeCaprio JA. How the Rb tumor suppressor structure and function was revealed by the study of Adenovirus and SV40. Virology. 2009;384(2):274-84. Epub 2009/01/20. doi: 10.1016/j.virol.2008.12.010. PubMed PMID: 19150725.

5. Dyson N. The regulation of E2F by pRB-family proteins. Genes Dev. 1998;12(15):2245-62. Epub 1998/08/08. PubMed PMID: 9694791.

6. Helin K, Harlow E, Fattaey A. Inhibition of E2F-1 transactivation by direct binding of the retinoblastoma protein. Molecular and Cellular Biology. 1993;13(10):6501-8. doi: 10.1128/mcb.13.10.6501.

7. Flemington EK, Speck SH, Kaelin WG. E2F-1-mediated transactivation is inhibited by complex formation with the retinoblastoma susceptibility gene product. Proceedings of the National Academy of Sciences. 1993;90(15):6914-8.

8. Vandel L, Nicolas E, Vaute O, Ferreira R, Ait-Si-Ali S, Trouche D. Transcriptional Repression by the Retinoblastoma Protein through the Recruitment of a Histone Methyltransferase. Molecular and Cellular Biology. 2001;21(19):6484-94. doi: 10.1128/mcb.21.19.6484-6494.2001.

9. Sellers WR, Rodgers JW, Kaelin WG. A potent transrepression domain in the retinoblastoma protein induces a cell cycle arrest when bound to E2F sites. Proceedings of the National Academy of Sciences. 1995;92(25):11544-8.

10. Luo RX, Postigo AA, Dean DC. Rb interacts with histone deacetylase to repress transcription. Cell. 1998;92(4):463-73. Epub 1998/03/10. doi: S0092-8674(00)80940-X [pii]. PubMed PMID: 9491888.

11. Brehm A, Miska EA, McCance DJ, Reid JL, Bannister AJ, Kouzarides T. Retinoblastoma protein recruits histone deacetylase to repress transcription. Nature. 1998;391(6667):597-601. Epub 1998/02/19. doi: 10.1038/35404 [doi]. PubMed PMID: 9468139.

12. Ferreira R, Magnaghi-Jaulin L, Robin P, Harel-Bellan A, Trouche D. The three members of the pocket proteins family share the ability to repress E2F activity through recruitment of a histone deacetylase. Proceedings of the National Academy of Sciences. 1998;95(18):10493-8.

13. Trouche D, Le Chalony C, Muchardt C, Yaniv M, Kouzarides T. RB and hbrm cooperate to repress the activation functions of E2F1. Proceedings of the National Academy of Sciences. 1997;94(21):11268-73.

14. Zhang HS, Gavin M, Dahiya A, Postigo AA, Ma D, Luo RX, et al. Exit from G1 and S phase of the cell cycle is regulated by repressor complexes containing HDAC-Rb-hSWI/SNF and Rb-hSWI/SNF. Cell. 2000;101(1):79-89. Epub 2000/04/25. doi: 10.1016/s0092-8674(00)80625-x. PubMed PMID: 10778858.

15. Shapiro GI, Park JE, Edwards CD, Mao L, Merlo A, Sidransky D, et al. Multiple Mechanisms of p16INK4A Inactivation in Non-Small Cell Lung Cancer Cell Lines. Cancer Research. 1995;55(24):6200-9.

16. Dimova DK, Dyson NJ. The E2F transcriptional network: old acquaintances with new faces. Oncogene. 2005;24(17):2810-26. Epub 2005/04/20. doi: 10.1038/sj.onc.1208612. PubMed PMID: 15838517.

17. Kovesdi I, Reichel R, Nevins JR. Identification of a cellular transcription factor involved in E1A trans-activation. Cell. 1986;45(2):219-28. Epub 1986/04/25. PubMed PMID: 2938741.

18. Helin K, Wu CL, Fattaey AR, Lees JA, Dynlacht BD, Ngwu C, et al. Heterodimerization of the transcription factors E2F-1 and DP-1 leads to cooperative trans-activation. Genes & Development. 1993;7(10):1850-61. doi: 10.1101/gad.7.10.1850.

19. Chen HZ, Tsai SY, Leone G. Emerging roles of E2Fs in cancer: an exit from cell cycle control. Nat Rev Cancer. 2009;9(11):785-97. Epub 2009/10/24. doi: 10.1038/nrc2696. PubMed PMID: 19851314; PubMed Central PMCID: PMCPMC3616489.

20. Castillo SD, Angulo B, Suarez-Gauthier A, Melchor L, Medina PP, Sanchez-Verde L, et al. Gene amplification of the transcription factor DP1 and CTNND1 in human lung cancer. J Pathol. 2010;222(1):89-98. Epub 2010/06/18. doi: 10.1002/path.2732. PubMed PMID: 20556744.

21. Melchor L, Saucedo-Cuevas LP, Munoz-Repeto I, Rodriguez-Pinilla SM, Honrado E, Campoverde A, et al. Comprehensive characterization of the DNA amplification at 13q34 in human breast cancer reveals TFDP1 and CUL4A as likely candidate target genes. Breast Cancer Res. 2009;11(6):R86. Epub 2009/12/10. doi: 10.1186/bcr2456. PubMed PMID: 19995430; PubMed Central PMCID: PMCPMC2815550.

22. Abba MC, Fabris VT, Hu Y, Kittrell FS, Cai WW, Donehower LA, et al. Identification of novel amplification gene targets in mouse and human breast cancer at a syntenic cluster mapping to mouse ch8A1 and human ch13q34. Cancer Res. 2007;67(9):4104-12. Epub 2007/05/08. doi: 10.1158/0008-5472.can-06-4672. PubMed PMID: 17483321; PubMed Central PMCID: PMCPMC4166497.

23. Pesonen S, Kangasniemi L, Hemminki A. Oncolytic Adenoviruses for the Treatment of Human Cancer: Focus on Translational and Clinical Data. Molecular Pharmaceutics. 2010;8(1):12-28. doi: 10.1021/mp100219n.

24. Jounaidi Y, Doloff JC, Waxman DJ. Conditionally Replicating Adenoviruses for Cancer Treatment. Curr Cancer Drug Targets. 2007;7(3):285-301. PubMed PMID: 17504125; PubMed Central PMCID: PMC3354698.

25. Burke JM, Lamm DL, Meng MV, Nemunaitis JJ, Stephenson JJ, Arseneau JC, et al. A first in human phase 1 study of CG0070, a GM-CSF expressing oncolytic adenovirus, for the treatment of nonmuscle invasive bladder cancer. J Urol. 2012;188(6):2391-7. Epub 2012/10/24. doi: 10.1016/j.juro.2012.07.097. PubMed PMID: 23088985.

26. Chiocca EA, Abbed KM, Tatter S, Louis DN, Hochberg FH, Barker F, et al. A phase I open-label, dose-escalation, multi-institutional trial of injection with an E1B-Attenuated adenovirus, ONYX-015, into the peritumoral region of recurrent malignant gliomas, in the adjuvant setting. Mol Ther. 2004;10(5):958-66. Epub 2004/10/29. doi: 10.1016/j.ymthe.2004.07.021. PubMed PMID: 15509513.

27. Bramante S, Kaufmann JK, Veckman V, Liikanen I, Nettelbeck DM, Hemminki O, et al. Treatment of melanoma with a serotype 5/3 chimeric oncolytic adenovirus coding for GM-CSF: Results in vitro, in rodents and in humans. Int J Cancer. 2015. Epub 2015/03/31. doi: 10.1002/ijc.29536. PubMed PMID: 25821063.

28. Kimball KJ, Preuss MA, Barnes MN, Wang M, Siegal GP, Wan W, et al. A phase I study of a tropism-modified conditionally replicative adenovirus for recurrent malignant gynecologic diseases. Clin Cancer Res.

2010;16(21):5277-87. Epub 2010/10/28. doi: 10.1158/1078-0432.ccr-10-0791. PubMed PMID: 20978148; PubMed Central PMCID: PMCPmc2970766.

29. Cerullo V, Pesonen S, Diaconu I, Escutenaire S, Arstila PT, Ugolini M, et al. Oncolytic adenovirus coding for granulocyte macrophage colony-stimulating factor induces antitumoral immunity in cancer patients. Cancer Res. 2010;70(11):4297-309. Epub 2010/05/21. doi: 10.1158/0008-5472.can-09-3567. PubMed PMID: 20484030.

30. Koski A, Kangasniemi L, Escutenaire S, Pesonen S, Cerullo V, Diaconu I, et al. Treatment of cancer patients with a serotype 5/3 chimeric oncolytic adenovirus expressing GMCSF. Mol Ther. 2010;18(10):1874-84. Epub 2010/07/29. doi: 10.1038/mt.2010.161. PubMed PMID: 20664527; PubMed Central PMCID: PMCPmc2951567.

31. Pesonen S, Nokisalmi P, Escutenaire S, Sarkioja M, Raki M, Cerullo V, et al. Prolonged systemic circulation of chimeric oncolytic adenovirus Ad5/3-Cox2L-D24 in patients with metastatic and refractory solid tumors. Gene Ther. 2010;17(7):892-904. Epub 2010/03/20. doi: 10.1038/gt.2010.17. PubMed PMID: 20237509.

32. Pol J, Kroemer G, Galluzzi L. First oncolytic virus approved for melanoma immunotherapy. Oncoimmunology. 2016;5(1):e1115641. doi: 10.1080/2162402X.2015.1115641. PubMed PMID: 26942095; PubMed Central PMCID: PMCPMC4760283.

33. Flint J, Shenk T. Adenovirus E1A protein paradigm viral transactivator. Annu Rev Genet. 1989;23:141-61. Epub 1989/01/01. doi: 10.1146/annurev.ge.23.120189.001041. PubMed PMID: 2533472.

34. Whyte P, Buchkovich KJ, Horowitz JM, Friend SH, Raybuck M, Weinberg RA, et al. Association between an oncogene and an anti-oncogene: the adenovirus E1A proteins bind to the retinoblastoma gene product. Nature. 1988;334(6178):124-9. Epub 1988/07/14. doi: 10.1038/334124a0. PubMed PMID: 2968522.

35. Bagchi S, Raychaudhuri P, Nevins JR. Adenovirus E1A proteins can dissociate heteromeric complexes involving the E2F transcription factor: A novel mechanism for E1A trans-activation. Cell. 1990;62(4):659-69.

36. Bagchi S, Weinmann R, Raychaudhuri P. The retinoblastoma protein copurifies with E2F-I, an E1A-regulated inhibitor of the transcription factor E2F. Cell. 1991;65(6):1063-72.

37. Kovesdi I, Reichel R, Nevins JR. Role of an adenovirus E2 promoter binding factor in E1A-mediated coordinate gene control. Proc Natl Acad Sci U

S A. 1987;84(8):2180-4. Epub 1987/04/01. PubMed PMID: 2951737; PubMed Central PMCID: PMCPMC304612.

38. Heise C, Hermiston T, Johnson L, Brooks G, Sampson-Johannes A, Williams A, et al. An adenovirus E1A mutant that demonstrates potent and selective systemic anti-tumoral efficacy. Nat Med. 2000;6(10):1134-9. Epub 2000/10/04. doi: 10.1038/80474. PubMed PMID: 11017145.

39. Johnson L, Shen A, Boyle L, Kunich J, Pandey K, Lemmon M, et al. Selectively replicating adenoviruses targeting deregulated E2F activity are potent, systemic antitumor agents. Cancer cell. 2002;1(4):325-37.

40. Cress WD, Nevins JR. Interacting domains of E2F1, DP1, and the adenovirus E4 protein. J Virol. 1994;68(7):4213-9.

41. Schaley J, O'Connor RJ, Taylor LJ, Bar-Sagi D, Hearing P. Induction of the Cellular E2F-1 Promoter by the Adenovirus E4-6/7 Protein. J Virol. 2000;74(5):2084-93. doi: 10.1128/jvi.74.5.2084-2093.2000.

42. Helin K, Harlow E. Heterodimerization of the transcription factors E2F-1 and DP-1 is required for binding to the adenovirus E4 (ORF6/7) protein. J Virol. 1994;68(8):5027-35. Epub 1994/08/01. PubMed PMID: 8035503; PubMed Central PMCID: PMCPMC236445.

43. O'Connor RJ, Hearing P. The E4-6/7 Protein Functionally Compensates for the Loss of E1A Expression in Adenovirus Infection. J Virol. 2000;74(13):5819-24. doi: 10.1128/jvi.74.13.5819-5824.2000.

44. Bandara LR, Lam EW, Sørensen TS, Zamanian M, Girling R, La Thangue NB. DP-1: a cell cycle-regulated and phosphorylated component of transcription factor DRTF1/E2F which is functionally important for recognition by pRb and the adenovirus E4 orf 6/7 protein. EMBO J. 1994;13(13):3104-14. PubMed PMID: 8039504.

45. Tomko RP, Xu R, Philipson L. HCAR and MCAR: The human and mouse cellular receptors for subgroup C adenoviruses and group B coxsackieviruses. Proceedings of the National Academy of Sciences. 1997;94(7):3352-6.

46. Bergelson JM, Cunningham JA, Droguett G, Kurt-Jones EA, Krithivas A, Hong JS, et al. Isolation of a Common Receptor for Coxsackie B Viruses and Adenoviruses 2 and 5. Science. 1997;275(5304):1320-3. doi: 10.1126/science.275.5304.1320.

47. Anders M, Vieth M, Rocken C, Ebert M, Pross M, Gretschel S, et al. Loss of the coxsackie and adenovirus receptor contributes to gastric cancer

progression. Br J Cancer. 2009;100(2):352-9. Epub 2009/01/15. doi: 10.1038/sj.bjc.6604876. PubMed PMID: 19142187; PubMed Central PMCID: PMCPMC2634721.

48. Ruzsics Z, Lemnitzer F, Thirion C. Engineering adenovirus genome by bacterial artificial chromosome (BAC) technology. Methods Mol Biol. 2014;1089:143-58. Epub 2013/10/18. doi: 10.1007/978-1-62703-679-5_11. PubMed PMID: 24132484.

49. Chartier C, Degryse E, Gantzer M, Dieterle A, Pavirani A, Mehtali M. Efficient generation of recombinant adenovirus vectors by homologous recombination in Escherichia coli. J Virol. 1996;70(7):4805-10. Epub 1996/07/01. PubMed PMID: 8676512; PubMed Central PMCID: PMCPMC190422.

50. Reddy PS, Ganesh S, Hawkins L, Idamakanti N. Generation of recombinant adenovirus using the Escherichia coli BJ5183 recombination system. Methods Mol Med. 2007;130:61-8. Epub 2007/04/03. PubMed PMID: 17401164.

51. Tang L, Gong M, Zhang P. In vitro CRISPR-Cas9-mediated efficient Ad5 vector modification. Biochem Biophys Res Commun. 2016;474(2):395-9. Epub 2016/04/30. doi: 10.1016/j.bbrc.2016.04.129. PubMed PMID: 27125457.

52. Dietel M, Häfner N, Jansen L, Dürst M, Runnebaum I. Novel splice variant CAR 4/6 of the coxsackie adenovirus receptor is differentially expressed in cervical carcinogenesis. Journal of Molecular Medicine. 2011;89(6):621-30. doi: 10.1007/s00109-011-0742-6.

53. Matsumoto K, Shariat SF, Ayala GE, Rauen KA, Lerner SP. Loss of coxsackie and adenovirus receptor expression is associated with features of aggressive bladder cancer. Urology. 2005;66(2):441-6.

54. Liu Y, Valadon P, Schnitzer J. Construction of Metabolically Biotinylated Adenovirus with Deleted Fiber Knob as Targeting Vector. Virology Journal. 2010;7(1):316. PubMed PMID: doi:10.1186/1743-422X-7-316.

55. Kim J, Kim PH, Kim SW, Yun CO. Enhancing the therapeutic efficacy of adenovirus in combination with biomaterials. Biomaterials. 2012;33(6):1838-50. doi: 10.1016/j.biomaterials.2011.11.020. PubMed PMID: 22142769; PubMed Central PMCID: PMC3242832.

56. Rein DT, Breidenbach M, Curiel DT. Current developments in adenovirus-based cancer gene therapy. Future Oncology. 2006;2(1):137-43. doi: doi:10.2217/14796694.2.1.137.

57. Nicklin SA, Wu E, Nemerow GR, Baker AH. The influence of adenovirus fiber structure and function on vector development for gene therapy. Mol Ther. 2005;12(3):384-93. Epub 2005/07/05. doi: 10.1016/j.ymthe.2005.05.008. PubMed PMID: 15993650.

58. Belousova N, Krendelchtchikova V, Curiel DT, Krasnykh V. Modulation of adenovirus vector tropism via incorporation of polypeptide ligands into the fiber protein. J Virol. 2002;76(17):8621-31. Epub 2002/08/07. PubMed PMID: 12163581; PubMed Central PMCID: PMCPMC136983.

59. Uusi-Kerttula H, Legut M, Davies J, Jones R, Hudson E, Hanna L, et al. Incorporation of Peptides Targeting EGFR and FGFR1 into the Adenoviral Fiber Knob Domain and Their Evaluation as Targeted Cancer Therapies. Hum Gene Ther. 2015;26(5):320-9. Epub 2015/04/29. doi: 10.1089/hum.2015.015 [doi]. PubMed PMID: 25919378; PubMed Central PMCID: PMC4442602.

60. Zhan Y, Yu B, Wang Z, Zhang Y, Zhang HH, Wu H, et al. A fiber-modified adenovirus co-expressing HSV-TK and Coli.NTR enhances antitumor activities in breast cancer cells. International journal of clinical and experimental pathology. 2014;7(6):2850-60. Epub 2014/07/18. PubMed PMID: 25031704; PubMed Central PMCID: PMCPmc4097267.

61. Grill J, Van Beusechem VW, Van Der Valk P, Dirven CM, Leonhart A, Pherai DS, et al. Combined targeting of adenoviruses to integrins and epidermal growth factor receptors increases gene transfer into primary glioma cells and spheroids. Clin Cancer Res. 2001;7(3):641-50. Epub 2001/04/12. PubMed PMID: 11297260.

62. Kontermann RE. Alternative antibody formats. Curr Opin Mol Ther. 2010;12(2):176-83. Epub 2010/04/08. PubMed PMID: 20373261.

63. Dreier B, Honegger A, Hess C, Nagy-Davidescu G, Mittl PR, Grutter MG, et al. Development of a generic adenovirus delivery system based on structure-guided design of bispecific trimeric DARPin adapters. Proc Natl Acad Sci U S A. 2013;110(10):E869-77. Epub 2013/02/23. doi: 10.1073/pnas.1213653110. PubMed PMID: 23431166; PubMed Central PMCID: PMCPmc3593905.

64. Waehler R, Russell SJ, Curiel DT. Engineering targeted viral vectors for gene therapy. Nat Rev Genet. 2007;8(8):573-87. PubMed PMID: 17607305.

65. Chen J, Zheng XF, Brown EJ, Schreiber SL. Identification of an 11-kDa FKBP12-rapamycin-binding domain within the 289-kDa FKBP12-rapamycin-associated protein and characterization of a critical serine residue. Proc Natl Acad Sci U S A. 1995;92(11):4947-51. PubMed PMID: 7539137.

66. de Wildt RM, Tomlinson IM, Ong JL, Holliger P. Isolation of receptor-ligand pairs by capture of long-lived multivalent interaction complexes. Proc Natl Acad Sci U S A. 2002;99(13):8530-5. PubMed PMID: 12084913.

67. Rivera VM, Clackson T, Natesan S, Pollock R, Amara JF, Keenan T, et al. A humanized system for pharmacologic control of gene expression. Nat Med. 1996;2(9):1028-32. PubMed PMID: 8782462.

68. Clackson T. Dissecting the functions of proteins and pathways using chemically induced dimerization. Chem Biol Drug Des. 2006;67(6):440-2. PubMed PMID: 16882320.

69. Luker KE, Smith MC, Luker GD, Gammon ST, Piwnica-Worms H, Piwnica-Worms D. Kinetics of regulated protein-protein interactions revealed with firefly luciferase complementation imaging in cells and living animals. Proc Natl Acad Sci U S A. 2004;101(33):12288-93. doi: 10.1073/pnas.0404041101. PubMed PMID: 15284440; PubMed Central PMCID: PMCPMC514471.

70. O'Shea C, Klupsch K, Choi S, Bagus B, Soria C, Shen J, et al. Adenoviral proteins mimic nutrient/growth signals to activate the mTOR pathway for viral replication. Embo j. 2005;24(6):1211-21. Epub 2005/03/19. doi: 10.1038/sj.emboj.7600597. PubMed PMID: 15775987; PubMed Central PMCID: PMCPMC556401.

71. Boffa DJ, Luan F, Thomas D, Yang H, Sharma VK, Lagman M, et al. Rapamycin inhibits the growth and metastatic progression of non-small cell lung cancer. Clin Cancer Res. 2004;10(1 Pt 1):293-300. Epub 2004/01/22. PubMed PMID: 14734482.

72. Guba M, von Breitenbuch P, Steinbauer M, Koehl G, Flegel S, Hornung M, et al. Rapamycin inhibits primary and metastatic tumor growth by antiangiogenesis: involvement of vascular endothelial growth factor. Nat Med. 2002;8(2):128-35. doi: 10.1038/nm0202-128. PubMed PMID: 11821896.

73. Xia H, Anderson B, Mao Q, Davidson BL. Recombinant Human Adenovirus: Targeting to the Human Transferrin Receptor Improves Gene Transfer to Brain Microcapillary Endothelium. Journal of Virology. 2000;74(23):11359-66. doi: 10.1128/jvi.74.23.11359-11366.2000.

74. Wickham TJ, Tzeng E, Shears LL, 2nd, Roelvink PW, Li Y, Lee GM, et al. Increased in vitro and in vivo gene transfer by adenovirus vectors containing chimeric fiber proteins. J Virol. 1997;71(11):8221-9. Epub 1997/10/29. PubMed PMID: 9343173; PubMed Central PMCID: PMC192279.

75. Walker RA, Dearing SJ. Expression of epidermal growth factor receptor mRNA and protein in primary breast carcinomas. Breast cancer research and treatment. 1999;53(2):167-76. Epub 1999/05/18. PubMed PMID: 10326794.

76. Bossi P, Resteghini C, Paielli N, Licitra L, Pilotti S, Perrone F. Prognostic and predictive value of EGFR in head and neck squamous cell carcinoma. Oncotarget. 2016. Epub 2016/08/25. doi: 10.18632/oncotarget.11413. PubMed PMID: 27556186.

77. Di Lorenzo G, Tortora G, D'Armiento FP, De Rosa G, Staibano S, Autorino R, et al. Expression of epidermal growth factor receptor correlates with disease relapse and progression to androgen-independence in human prostate cancer. Clin Cancer Res. 2002;8(11):3438-44. Epub 2002/11/14. PubMed PMID: 12429632.

78. Hirsch FR, Varella-Garcia M, Bunn PA, Jr., Di Maria MV, Veve R, Bremmes RM, et al. Epidermal growth factor receptor in non-small-cell lung carcinomas: correlation between gene copy number and protein expression and impact on prognosis. Journal of clinical oncology : official journal of the American Society of Clinical Oncology. 2003;21(20):3798-807. Epub 2003/09/04. doi: 10.1200/jco.2003.11.069. PubMed PMID: 12953099.

79. Uribe P, Gonzalez S. Epidermal growth factor receptor (EGFR) and squamous cell carcinoma of the skin: molecular bases for EGFR-targeted therapy. Pathol Res Pract. 2011;207(6):337-42. Epub 2011/05/03. doi: 10.1016/j.prp.2011.03.002. PubMed PMID: 21531084.

80. Colquhoun AJ, Mellon JK. Epidermal growth factor receptor and bladder cancer. Postgraduate medical journal. 2002;78(924):584-9. Epub 2002/11/05. PubMed PMID: 12415079; PubMed Central PMCID: PMCPmc1742539.

81. Lu Z, Ghosh S, Wang Z, Hunter T. Downregulation of caveolin-1 function by EGF leads to the loss of E-cadherin, increased transcriptional activity of beta-catenin, and enhanced tumor cell invasion. Cancer Cell. 2003;4(6):499-515. PubMed PMID: 14706341.

82. Wang Y, Zhou BP. Epithelial-mesenchymal Transition---A Hallmark of Breast Cancer Metastasis. Cancer Hallm. 2013;1(1):38-49. doi: 10.1166/ch.2013.1004. PubMed PMID: 24611128; PubMed Central PMCID: PMCPMC3944831.

83. Piao Y, Jiang H, Alemany R, Krasnykh V, Marini FC, Xu J, et al. Oncolytic adenovirus retargeted to Delta-EGFR induces selective antiglioma activity. Cancer Gene Ther. 2009;16(3):256-65. Epub 2008/10/18. doi: 10.1038/cgt.2008.75. PubMed PMID: 18927600.

84. Gainkam LO, Huang L, Caveliers V, Keyaerts M, Hernot S, Vaneycken I, et al. Comparison of the biodistribution and tumor targeting of two 99mTc-labeled anti-EGFR nanobodies in mice, using pinhole SPECT/micro-CT. Journal of nuclear medicine : official publication, Society of Nuclear Medicine. 2008;49(5):788-95.

85. Belousova N, Krendelchtchikova V, Curiel DT, Krasnykh V. Modulation of Adenovirus Vector Tropism via Incorporation of Polypeptide Ligands into the Fiber Protein. J Virol. 2002;76(17):8621-31. doi: 10.1128/jvi.76.17.8621-8631.2002.

86. Kaliberov SA, Kaliberova LN, Buggio M, Tremblay JM, Shoemaker CB, Curiel DT. Adenoviral targeting using genetically incorporated camelid single variable domains. Laboratory investigation; a journal of technical methods and pathology. 2014;94(8):893-905. Epub 2014/06/17. doi: 10.1038/labinvest.2014.82. PubMed PMID: 24933423; PubMed Central PMCID: PMCPmc4157633.

87. Fang J, Qian J-J, Yi S, Harding TC, Tu GH, VanRoey M, et al. Stable antibody expression at therapeutic levels using the 2A peptide. Nat Biotech. 2005;23(5):584-90.

88. Kennedy MA, Parks RJ. Adenovirus virion stability and the viral genome: size matters. Mol Ther. 2009;17(10):1664-6. doi: 10.1038/mt.2009.202. PubMed PMID: 19789561; PubMed Central PMCID: PMCPMC2835018.

89. Bauzon M, Castro D, Karr M, Hawkins LK, Hermiston TW. Multigene expression from a replicating adenovirus using native viral promoters. Mol Ther. 2003;7(4):526-34. PubMed PMID: 12727116.

90. Isaacson MK, Feire AL, Compton T. Epidermal growth factor receptor is not required for human cytomegalovirus entry or signaling. J Virol. 2007;81(12):6241-7. doi: 10.1128/JVI.00169-07. PubMed PMID: 17428848; PubMed Central PMCID: PMCPMC1900073.

91. Engelman JA, Mukohara T, Zejnullahu K, Lifshits E, Borrás AM, Gale C-M, et al. Allelic dilution obscures detection of a biologically significant resistance mutation in EGFR-amplified lung cancer. The Journal of Clinical Investigation. 2006;116(10):2695-706.

92. Neve RM, Chin K, Fridlyand J, Yeh J, Baehner FL, Fevr T, et al. A collection of breast cancer cell lines for the study of functionally distinct cancer subtypes. Cancer Cell. 2006;10(6):515-27. Epub 2006/12/13. doi: 10.1016/j.ccr.2006.10.008. PubMed PMID: 17157791; PubMed Central PMCID: PMCPmc2730521.

93. Chin K, DeVries S, Fridlyand J, Spellman PT, Roydasgupta R, Kuo WL, et al. Genomic and transcriptional aberrations linked to breast cancer pathophysiologies. Cancer Cell. 2006;10(6):529-41. Epub 2006/12/13. doi: 10.1016/j.ccr.2006.10.009. PubMed PMID: 17157792.

94. Bayle JH, Grimley JS, Stankunas K, Gestwicki JE, Wandless TJ, Crabtree GR. Rapamycin analogs with differential binding specificity permit orthogonal control of protein activity. Chem Biol. 2006;13(1):99-107. Epub 2006/01/24. doi: 10.1016/j.chembiol.2005.10.017. PubMed PMID: 16426976.

95. Nemunaitis J, Khuri F, Ganly I, Arseneau J, Posner M, Vokes E, et al. Phase II Trial of Intratumoral Administration of ONYX-015, a Replication-Selective Adenovirus, in Patients With Refractory Head and Neck Cancer. Journal of Clinical Oncology. 2001;19(2):289-98.

96. O'Shea CC, Johnson L, Bagus B, Choi S, Nicholas C, Shen A, et al. Late viral RNA export, rather than p53 inactivation, determines ONYX-015 tumor selectivity. Cancer cell. 2004;6(6):611-23.

97. Soria C, Estermann FE, Espantman KC, O'Shea CC. Heterochromatin silencing of p53 target genes by a small viral protein. Nature. 2010;466(7310):1076-81. Epub 2010/08/27. doi: 10.1038/nature09307. PubMed PMID: 20740008; PubMed Central PMCID: PMCPMC2929938.

98. Dubensky Jr TW. (Re-)Engineering tumor cell-selective replicating adenoviruses: A step in the right direction toward systemic therapy for metastatic disease. Cancer cell. 2002;1(4):307-9.

99. Fields BN, Knipe DM, Howley PM. Fields virology. Philadelphia: Wolters Kluwer Health/Lippincott Williams & Wilkins; 2007.

100. Zindy F, Lamas E, Chenivesse X, Sobczak J, Wang J, Fesquet D, et al. Cyclin A is required in S phase in normal epithelial cells. Biochem Biophys Res Commun. 1992;182(3):1144-54. Epub 1992/02/14. PubMed PMID: 1531751.

101. Finn R, Dering J, Conklin D, Kalous O, Cohen D, Desai A, et al. PD 0332991, a selective cyclin D kinase 4/6 inhibitor, preferentially inhibits proliferation of luminal estrogen receptor-positive human breast cancer cell lines in vitro. Breast Cancer Research. 2009;11(5):R77. PubMed PMID: doi:10.1186/bcr2419.

102. Konecny GE, Winterhoff B, Kolarova T, Qi J, Manivong K, Dering J, et al. Expression of p16 and Retinoblastoma Determines Response to CDK4/6 Inhibition in Ovarian Cancer. Clin Cancer Res. 2011;17(6):1591-602. doi:

10.1158/1078-0432.ccr-10-2307. PubMed PMID: 21278246; PubMed Central PMCID: PMC4598646.

103. Rivadeneira DB, Mayhew CN, Thangavel C, Sotillo E, Reed CA, Grana X, et al. Proliferative suppression by CDK4/6 inhibition: complex function of the retinoblastoma pathway in liver tissue and hepatoma cells. Gastroenterology. 2010;138(5):1920-30. Epub 2010/01/27. doi: 10.1053/j.gastro.2010.01.007. PubMed PMID: 20100483; PubMed Central PMCID: PMCPMC2860048.

104. Ingemarsdotter CK, Tookman LA, Browne A, Pirlo K, Cutts R, Chelela C, et al. Paclitaxel resistance increases oncolytic adenovirus efficacy via upregulated CAR expression and dysfunctional cell cycle control. Mol Oncol. 2015;9(4):791-805. doi: 10.1016/j.molonc.2014.12.007. PubMed PMID: 25560085.

105. Wu A, Wu B, Guo J, Luo W, Wu D, Yang H, et al. Elevated expression of CDK4 in lung cancer. J Transl Med. 2011;9:38. Epub 2011/04/12. doi: 10.1186/1479-5876-9-38. PubMed PMID: 21477379; PubMed Central PMCID: PMCPMC3094221.

106. Miller DL, Myers CL, Rickards B, Coller HA, Flint SJ. Adenovirus type 5 exerts genome-wide control over cellular programs governing proliferation, quiescence, and survival. Genome Biol. 2007;8(4):R58. Epub 2007/04/14. doi: 10.1186/gb-2007-8-4-r58. PubMed PMID: 17430596; PubMed Central PMCID: PMCPMC1896011.

107. Zhao H, Dahlo M, Isaksson A, Syvanen AC, Pettersson U. The transcriptome of the adenovirus infected cell. Virology. 2012;424(2):115-28. Epub 2012/01/13. doi: 10.1016/j.virol.2011.12.006. PubMed PMID: 22236370.

108. Zhao H, Granberg F, Pettersson U. How adenovirus strives to control cellular gene expression. Virology. 2007;363(2):357-75. Epub 2007/03/21. doi: 10.1016/j.virol.2007.02.013. PubMed PMID: 17367835.

109. Lukas J, Parry D, Aagaard L, Mann DJ, Bartkova J, Strauss M, et al. Retinoblastoma-protein-dependent cell-cycle inhibition by the tumour suppressor p16. Nature. 1995;375(6531):503-6. Epub 1995/06/08. doi: 10.1038/375503a0. PubMed PMID: 7777060.

110. Serrano M, Hannon GJ, Beach D. A new regulatory motif in cell-cycle control causing specific inhibition of cyclin D/CDK4. Nature. 1993;366(6456):704-7. Epub 1993/12/16. doi: 10.1038/366704a0. PubMed PMID: 8259215.

111. Rocco JW, Sidransky D. p16(MTS-1/CDKN2/INK4a) in cancer progression. Exp Cell Res. 2001;264(1):42-55. Epub 2001/03/10. doi: 10.1006/excr.2000.5149. PubMed PMID: 11237522.

112. Ramalingam S, Annaluru N, Chandrasegaran S. A CRISPR way to engineer the human genome. Genome Biol. 2013;14(2):107. Epub 2013/03/02. doi: 10.1186/gb-2013-14-2-107. PubMed PMID: 23448668; PubMed Central PMCID: PMCPMC3663103.

113. Ran FA, Hsu PD, Lin CY, Gootenberg JS, Konermann S, Trevino AE, et al. Double nicking by RNA-guided CRISPR Cas9 for enhanced genome editing specificity. Cell. 2013;154(6):1380-9. Epub 2013/09/03. doi: 10.1016/j.cell.2013.08.021. PubMed PMID: 23992846; PubMed Central PMCID: PMCPMC3856256.

114. Wang HG, Rikitake Y, Carter MC, Yaciuk P, Abraham SE, Zerler B, et al. Identification of specific adenovirus E1A N-terminal residues critical to the binding of cellular proteins and to the control of cell growth. Journal of Virology. 1993;67(1):476-88.

115. Lau L, Gray EE, Brunette RL, Stetson DB. DNA tumor virus oncogenes antagonize the cGAS-STING DNA-sensing pathway. Science. 2015;350(6260):568-71. Epub 2015/09/26. doi: 10.1126/science.aab3291. PubMed PMID: 26405230.

116. Frisch SM, Mymryk JS. Adenovirus-5 E1A: paradox and paradigm. Nat Rev Mol Cell Biol. 2002;3(6):441-52. Epub 2002/06/04. doi: 10.1038/nrm827. PubMed PMID: 12042766.

117. Hanahan D, Weinberg RA. Hallmarks of cancer: the next generation. Cell. 2011;144(5):646-74. Epub 2011/03/08. doi: 10.1016/j.cell.2011.02.013. PubMed PMID: 21376230.

118. Miyake-Stoner SJ, O'Shea CC. Metabolism goes viral. Cell Metab. 2014;19(4):549-50. Epub 2014/04/08. doi: 10.1016/j.cmet.2014.03.022. PubMed PMID: 24703688; PubMed Central PMCID: PMCPMC4097405.

119. Alba R, Bradshaw AC, Parker AL, Bhella D, Waddington SN, Nicklin SA, et al. Identification of coagulation factor (F)X binding sites on the adenovirus serotype 5 hexon: effect of mutagenesis on FX interactions and gene transfer. Blood. 2009;114(5):965-71. Epub 2009/05/12. doi: 10.1182/blood-2009-03-208835. PubMed PMID: 19429866; PubMed Central PMCID: PMCPMC2721791.

120. Wynn TA, Barron L. Macrophages: Master Regulators of Inflammation and Fibrosis. Semin Liver Dis. 2010;30(3):245-57. doi: 10.1055/s-0030-1255354. PubMed PMID: 20665377; PubMed Central PMCID: PMC2924662.

121. Johnson J, Thijssen B, McDermott U, Garnett M, Wessels LF, Bernards R. Targeting the RB-E2F pathway in breast cancer. Oncogene. 2016;35(37):4829-35. Epub 2016/03/01. doi: 10.1038/onc.2016.32. PubMed PMID: 26923330; PubMed Central PMCID: PMCPMC4950965.

122. Wells J, Yan PS, Cechvala M, Huang T, Farnham PJ. Identification of novel pRb binding sites using CpG microarrays suggests that E2F recruits pRb to specific genomic sites during S phase. Oncogene. 2003;22(10):1445-60. Epub 2003/03/12. doi: 10.1038/sj.onc.1206264. PubMed PMID: 12629508.

123. Euhus DM, Hudd C, LaRegina MC, Johnson FE. Tumor measurement in the nude mouse. J Surg Oncol. 1986;31(4):229-34. Epub 1986/04/01. PubMed PMID: 3724177.

124. Tomayko MM, Reynolds CP. Determination of subcutaneous tumor size in athymic (nude) mice. Cancer Chemother Pharmacol. 1989;24(3):148-54. Epub 1989/01/01. PubMed PMID: 2544306.